

Aus dem Institut für Physiologische Chemie der Medizinischen Fakultät
der Martin-Luther-Universität Halle-Wittenberg
(Direktor: Prof. Dr. Guido Posern)

**The effect of hypoxia on vasculogenesis during early embryonic development of
*Xenopus laevis***

Dissertation

zur Erlangung des akademischen Grades

Doktor rerum medicarum (Dr. rer. medic) für das Fachgebiet

Physiologie und Pathophysiologie

vorgelegt

der Medizinischen Fakultät

der Martin-Luther-Universität Halle-Wittenberg

von Sanjeeva Sudhakar Metikala

geboren am 07.08.1988 in Banaganapalli, Indien

Betreuer: Prof. Dr. Thomas Hollemann

Gutachter:

- 1) Prof. Dr. Dörthe Katschinski, Uni-Göttingen.
- 2) Prof. Dr. Andreas Simm, Klinik für Herz- und Thoraxchirurgie, UK-Halle.

Eröffnungsdatum : 07.10.2014

Verteidigungsdatum : 04.05.2015

Referat

Sauerstoff ist ein wesentliches Element für Lebewesen. Während der Vertebratenentwicklung werden Blutzellen von gemeinsamen Vorläuferzellen gebildet, den Hämangioblasten. Diese Hämangioblasten differenzieren zu Blutzellen und Blutgefäßen, ein Prozess der als Hämatopoese bezeichnet wird. Die Hämatopoese ist ein streng reguliertes genetisches Programm. Sie reagiert zudem auf externe Faktoren, wie beispielsweise umweltbedingten Stress. Während der Entwicklung können Veränderungen in der Sauerstoffversorgung deutliche Einflüsse auf diese Programm haben. Unter hypoxischen Bedingungen reagieren Zellen damit, dass der Zellzyklus zeitweilig angehalten wird, der Energieverbrauch reduziert wird und dass proangiogene Faktoren ausgeschüttet werden. Diese Ereignisse werden durch verschiedene Signale beeinflusst, unter anderem durch Hypoxia inducible factors (HIFs), Transkriptionsfaktoren, die bei der Reaktion der Zellen auf niedrige Sauerstoffkonzentrationen (Hypoxie) eine Schlüsselrolle spielen. Die Stabilität der HIFs wird durch Prolylhydroxylasen (PHDs) reguliert, die als Sauerstoffsensoren fungieren. Während der Embryonalentwicklung ist dieses regulatorische Zusammenspiel bis heute nicht untersucht worden.

In der vorliegenden Arbeit konnte gezeigt werden, dass die Überlebensfähigkeit und die Geschwindigkeit mit der sich Embryonen entwickeln abnimmt, wenn sie unter hypoxischen Bedingungen gehalten werden. Weitergehende Analysen zeigten, dass unter diesen Bedingungen auch die Bildung des Gefäßsystems erheblich beeinträchtigt wird. Die Bildung myelogener Zellen war ebenso betroffen, allerdings konnte keine Beeinträchtigung der Entwicklung erythrogener Zellen gezeigt werden. Experimente mit anti-sense Morpholinos und chemischen Inhibitoren (DMOG), die die Funktion der Prolylhydroxylase 2 reduzierten, führten zu einem ähnlichen Muster bei der Gefäßbildung, wie es auch in Embryonen, die unter hypoxischen Bedingungen gehalten wurden, beobachtet wurde. In beiden Fällen wurde eine verringerte Gefäßbildung beobachtet. Auf die Bildung myelogener Zellen hatte die beschriebene Behandlung der Embryonen nur geringe Auswirkungen und die Bildung erythrogener Zellen war gar nicht beeinträchtigt. Die Reduktion der Funktionen von HIF-1 und von-Hippel-Lindau-Faktor (VHL) führten ebenso zum Verlust vaskulärer Strukturen während der Embryonalentwicklung. Es kann daher geschlossen werden, dass die Bildung des Gefäßsystems während der Embryonalentwicklung nicht durch ein unabhängiges genetisches Programm reguliert wird, sondern vom der Sauerstoffkonzentration in der Umgebung abhängig ist. Die Reduktion der PHD-2-Funktion, ebenso wie hypoxische Bedingungen führten zu einer erheblichen Beeinträchtigung der Gefäßbildung. Im Gegensatz dazu führte die Reduktion der HIF-1-Funktion nur zu vergleichsweise milden Effekten, was möglicherweise dadurch erklärt werden kann, dass PHD-2 nicht nur HIF-1 α , sondern noch weitere Zielproteine reguliert.

Metikala, Sanjeeva Sudhakar: The effect of hypoxia on vasculogenesis during early embryonic development of *Xenopus laevis*. Halle (Saale), Univ., Med. Fak., Diss., 80 Seiten, 2014

Abstract

Oxygen is an essential element for living organisms. During vertebrate development, all the blood cells are formed from a common progenitor called hemangioblasts. These hemangioblasts give rise to blood cells and blood vessels, a process called haematopoiesis. Hematopoiesis is a tightly regulated genetic program. It is sensitive to external factors such as environmental stress. Variations in oxygen availability during development could have notable effects on this genetic program. When cells are subjected to hypoxia, a variety of cellular responses arise leading to temporary arrest in cell cycle, reduction in energy consumption and secretion of survival and proangiogenic factors. These events are coordinated by several pathways including the key modulator of transcriptional response to hypoxic stress, Hypoxia Inducible transcriptional Factors (HIFs). The stability of HIFs is regulated by the PHDs, which are commonly referred to as 'oxygen sensors'. So far, this regulatory system has not been challenged in the developing embryo.

In the current research, I could show that exposing *Xenopus laevis* embryos to hypoxia decreases developmental rate and viability. Analysing the expression of endothelial precursor cells showed that hypoxia affects differentiation of endothelial precursors. Further analysis on the formation of vascular network revealed a strong effect on the formation of vascular structures. Formation of myelogenic cells was also affected but the effect on erythrogenic lineage was not seen. PHD-2 loss-of-function experiments using anti-sense morpholinos and chemical inhibitor (DMOG) resulted in similar pattern of vessel formation as seen in hypoxia embryos. In both cases, decreased formation of vascular structures was observed. Moderate effect was seen on myelogenic progenitor cell formation. No effect was observed on erythrogenic cell formation. Loss-of-function experiments of PHD-1 and PHD-3 did not show any effect on the vessel formation. Suppressing the function of HIF-1 and VHL also resulted in the loss of vascular structures in the embryo. Hence, it can be suggested that hypoxia affects the formation of vascular network *in vivo* and embryonic vasculogenesis and is not an independent process but requires oxygen. Suppressing PHD-2 function also reduces the formation of vascular network, which is a phenotype that was observed in hypoxia. Because the effect of hypoxia and PHD-2 loss-of-function was strong on the formation of vascular network but mild effect was observed in the HIF-1 α loss-of-function studies, it is possible that PHD-2 has targets other than HIF-1 α .

Contents

Contents	I
Abbreviations	V
1 Introduction	1
1.1 Vasculogenesis	1
1.2 Angiogenesis	2
1.3 Hematopoiesis	4
1.4 Neovascularization/neoangiogenesis	6
1.5 Oxygen sensing mechanism	6
1.5.1 Hypoxia inducible transcription factors (HIF)	7
1.5.2 Structure of HIF-1 α	7
1.5.3 Structure of HIF-1 β	8
1.5.4 Prolyl-4-Hydroxylases	9
1.5.5 Regulation of HIF pathway	9
1.6 <i>Xenopus laevis</i> as a model organism to study vascular system	12
1.7 Aim of the thesis	12
2 Materials	13
2.1 The experimental animal - <i>Xenopus laevis</i>	13
2.2 Bacteria	13
2.3 Chemicals	13
2.4 Buffers, solutions and media	15
2.4.1 Embryo preparation	15
2.4.2 Whole-mount <i>in situ</i> hybridization	15
2.4.3 Mini/Maxi preparation of plasmid DNA	16
2.4.4 Gel electrophoresis	16
2.4.5 Immunostaining	16
2.4.6 Media	17
2.5 Antibodies	17

2.6	Enzymes	17
2.7	Kits	18
2.8	Oligonucleotides	18
2.8.1	Oligonucleotides for PCR	18
2.8.2	Antisense Morpholino Oligonucleotides (MO)	18
2.9	Vectors and Constructs	19
2.9.1	Vectors	19
2.9.2	Constructs	19
2.9.3	Cloning	20
2.10	Equipment	20
2.11	Oxygen regulating apparatus	22
3	Methods	22
3.1	Hypoxia Chamber	22
3.1.1	Hypoxia Chamber Setup	23
3.1.2	Oxygen regulator setup	23
3.1.3	The Experiment	23
3.2	Molecular methods	24
3.2.1	Single Oligonucleotide Mutagenesis and cloning Approach (SOMA)	24
3.2.2	Preparation of electro-competent bacteria	25
3.2.3	Electroporation	25
3.2.4	Colony PCR	26
3.2.5	Plasmid mini-preparation	26
3.2.6	Plasmid maxi-preparation	26
3.2.7	<i>In vitro</i> synthesis of sense RNAs	27
3.2.8	<i>In vitro</i> synthesis of anti-sense RNAs	27
3.2.9	Extraction of the total RNA from staged embryos	28
3.2.10	Semi-quantitative polymerase chain reactions (SQ-PCR)	28
3.3	Handling and manipulation of <i>Xenopus</i> embryos	29
3.3.1	Preparation of embryos from <i>Xenopus laevis</i>	29
3.3.2	Microinjection	29

3.4	Analysis Methods	30
3.4.1	Whole-mount <i>in situ</i> hybridization (WMISH)	30
3.4.2	Whole-mount immunostaining of pH3	31
4	Results	32
4.1	Hypoxia decreases embryo viability	33
4.2	Hypoxia decelerates development	33
4.3	Continuous hypoxia affects differentiation and migration of embryonic angioblast precursor cells	34
4.4	Continuous hypoxia hinders embryonic vascular development	36
4.5	Hypoxia affects differentiation of myelogenic lineage	39
4.6	Hypoxia affects differentiation and migration of erythropoietic precursors	42
4.7	Hypoxia limits active division of cells	45
4.8	The general developmental program is unaffected by hypoxia	47
4.9	PHD-2 morpholino acts specifically	49
4.10	PHD-2 loss-of-function reduces vascular network formation	52
4.11	PHD-2 loss-of-function phenotype can be rescued	54
4.12	PHD-2 loss-of-function reduces myeloid progenitor formation	55
4.13	PHD-2 loss-of-function does not affect erythroid precursor differentiation	56
4.14	Loss of PHD-2 alone is sufficient to affect VVN formation	57
4.15	HIF-1 α eoe1 MO acts specifically	59
4.16	Suppression of HIF-1 α function led to reduced vascular structures	60
4.17	VHL eoe2 MO acts specifically	60
4.18	Suppression of VHL function affects vascular structures	61
4.19	Combined loss of HIF-1 α and VHL functions leads to reduced vasculature	62
5	Discussion	63
5.1	Oxygen is essential for proper embryonic morphogenesis and ontogenesis	63
5.2	Not all organs are affected by hypoxia during embryogenesis	65
5.3	Embryonic vasculogenesis is not an independent pre-programmed process but requires oxygen	65

5.4	HIF pathway might not be the solo player during embryonic vasculogenesis	67
5.5	Conclusion	68
6	Bibliography	70
7	Thesen	76
8	Supplementary data	77

Abbreviations

%	Percent
AP	Alkaline phosphatase
Ang1	Angiopoietin-1
APB	Alkaline phosphatase buffer
ARDs	Ankyrin repeat domain
Asn	Asparagine
ATP	Adenosine triphosphate
BCIP	5-Bromo-4-chloro-3-indolyl-phosphate
bHLH-PAS	Basic helix-loop-helix – PER (<i>Drosophila</i> period), AHR (mammalian aryl hydrocarbon receptor, ARNT (aryl hydrocarbon receptor nuclear translocator) and SIM (single-minded)
BMB	Boehringer blocking reagent
BSA	Bovine Serum Albumin
CAD	C-terminal transactivation domain
CDKN	Cyclin-dependent kinase inhibitor gene
cDNA	Complementary DNA
CHAPS	3-(3-cholamidopropyl)dimethylammonio-1-propanesulphate
CITED 2	Cbp/p300-interacting transactivator 2
COUP-TF II	Chicken ovalbumin upstream promoter transcription factor II
CTAD	C-terminal transactivation domain
CXCR4	C-X-C chemokine receptor type 4
DA	Dorsal aorta
ddH ₂ O	Double distilled water
Dig	Digoxigenin
DLAV	Dorsal longitudinal anastomosing vessel
DNA	Deoxyribonucleic acid
DNase	Deoxyribonuclease
e.g.	<i>Exempli gratia</i>
EC	Endothelial cells
EDTA	Ethylenediaminetetraacetic acid
EGFP	Green fluorescent protein
Egln	Egg laying domain nine

eNOS	Endothelial nitric oxide synthase
EPCs	Endothelial progenitor cells
EPO	Erythropoietin
<i>et al.</i>	<i>Et alii</i>
FGF-2	Fibroblast derived growth factor-2
FIH	Factor inhibiting HIFs
h	Hour
hrs	Hours
HCG	Human chorionic gonadotropin
HIFs	Hypoxia-inducible transcription factors
HPASMC	Human pulmonary artery smooth muscle cell
Hpf	Hours post fertilization
Hph	HIF prolyl hydroxylase
HREs	Hypoxia response elements
HS	Horse serum
<i>i.e.</i>	<i>Id est</i>
IPAS	Inhibitory PAS protein
ISV	Inter somitic veins
kb	Kilobase
kDa	Kilo Dalton
l	liter(s)
LB- Amp	Luria-Bertani - Ampicillin
M	Molar (mol/l)
mM	milli Molar
MAB	Maleic acid buffer
MBS	Modified Barth's Saline
MEM	MOPS/EGTA/Magnesium sulfate buffer
MEMFA	MOPS/EGTA/Magnesium sulfate/formaldehyde buffer
min	Minutes
MO	Morpholino
MOPS	4-morpholinopropanosulfonic acid
Msec	Milliseconds
mRNA	Messenger ribonucleic acid
NAD	N-terminal transactivation domain

NADPH	Nicotinamide adenine dinucleotide phosphate
NBT	Nitro blue tetrazolium chloride
NF Stage	Nieuwkoop and Faber stage
NICD	Notch intracellular domain
NLS	Nuclear localization signals
NO	Nitric oxide
NTAD	N-terminal transactivation domain
°C	Degree centigrade
ODC	Ornithine decarboxylase
ODD	Oxygen-dependent degradation domain
OXPHOS	Oxidative phosphorylation
PBS	Phosphate-buffered saline
PC	Personal computer
PCR	Polymerase chain reaction
PCV	Posterior cardinal vein
PDGF	Platelet derived growth factor
PEST-like motifs	Proline, glutamic acid, serine and threonine like motifs
pg	Pico gram
pH	Potential hydrogen
PHDs	Prolyl hydroxylase domain proteins
pH3	Phosphohistone H3
pmol	Pico mol
Pro	Proline
pVHL	Von Hippel-Lindau E3 ubiquitin ligase complex
RNA	Ribonucleic acid
RNase A	Ribonuclease A
ROS	Reactive oxygen species
RT-PCR	Reverse transcriptase-polymerase chain reactions
siRNA	Small interfering RNA
SMC	Smooth muscle cells
SSC	Standard saline citrate buffer
TBE buffer	Tris/boric acid/EDTA buffer
TCA	Tricarboxylic acid cycle
TE buffer	Tris/EDTA buffer

TGF β	Tumour growth factor β
UTR	Un-translated region
VEGF	Vascular endothelial growth factor
VSMC	Vascular smooth muscle cells
WMISH	Whole-mount <i>in situ</i> hybridization
μ	Micro

1 Introduction

Oxygen is the key element for aerobic life on earth. Due to its high energy potential, several organisms depend on it for various intracellular processes. It is an important element for ATP production in mitochondria via oxidative phosphorylation (OXPHOS). For proper cell function, the intracellular oxygen level has to be tightly regulated. Maintaining oxygen homeostasis is important for metabolic processes and to eliminate toxic effects of oxygen free radicals. Hence, oxygen must be delivered to the entire body of an organism. In primitive organisms such as unicellular and few multicellular organisms, sufficient oxygen delivery is achieved by simple diffusion. As organisms become more complex, simple diffusion is inefficient to deliver oxygen to every part of the body. To overcome this obstacle, higher organisms developed circulatory/cardiovascular systems consisting of a heart and a vascular network. Although these two work together to deliver oxygen to all areas, formation of the heart is independent of blood vessel formation (Gilbert, 2000). The heart is formed at the predetermined location and blood vessels form in different locations and finally fuse to the heart during embryogenesis. Although the embryo is not fully developed into an adult, it is crucial that cells in the developing embryo must obtain nourishment, use oxygen and excrete waste products. These functions are carried out by different specified organs in the adult such as intestine, lungs and kidneys respectively. However, embryonic development is simplified by assigning all the three functions to a single system, the vascular system. Hence, it is the first and foremost functional system. Formation of blood vessels is a dynamic process and involves two major steps, vasculogenesis and angiogenesis.

1.1 Vasculogenesis

During vertebrate embryogenesis, formation of blood cells and blood vessels is an interconnected process. Although long debated, the hemangioblast is considered to be the common precursor for both cell types (Shalaby *et al.*, 1997). These cells also emerge from the same site. This is supported by the finding that primitive blood cells and capillary cells express identical proteins on their cell surfaces (Wood *et al.*, 1997; Choi *et al.*, 1998; Liao and Zon, 1999).

Vasculogenesis is the *de novo* aggregation of endothelial structures from mesodermal precursors (Sarah *et al.*, 2009). Initially, a group of cells from the splanchnic mesoderm are specified to become hemangioblasts (Shalaby *et al.*, 1997). Basic Fibroblast Growth Factor (FGF2) signalling facilitates the specification of hemangioblasts from the mesoderm. These hemangioblasts aggregate to form clusters of cells called blood islands. In *Xenopus* embryos, the origin of these cells is found in the ventral region of the embryo. Hence, these blood islands are regarded as ventral blood islands (VBI). Inner mass of the cells from the ventral blood islands become hematopoietic stem cells which are the precursors of all kinds of blood cells and the outer layer of cells become angioblasts which are the precursors of blood vessels. In the next phase of

vasculogenesis, endothelial cells migrate and fuse to form tubes thereby connecting the blood islands resulting in the formation of vascular plexus, a network of capillaries (Flamme *et al.*, 1997; Patan, 2004) (Fig.1). Vascular Endothelial Growth Factor (VEGF) signalling is responsible for the differentiation and multiplication of angioblasts and allows them to coalesce to form tube like structures (Ferrara, 2004; Olsson *et al.*, 2006). VEGF is secreted by mesenchymal cells near blood islands and bind to their corresponding receptors expressed on the hemangioblasts and angioblasts (Millauer *et al.*, 1993). VEGF protein has two major receptors known as Flk1 receptor tyrosine kinase or VEGF R2 and Flt1 receptor tyrosine kinase or VEGF R1. VEGF R2 facilitates the formation of blood islands and differentiated endothelial cells (Ferrara *et al.*, 1996) whereas VEGF R1 drives the organization of endothelial cells to form tubular structures (Fong *et al.*, 1995; Shalaby *et al.*, 1995). The final stage of vasculogenesis is completed by the maturation of blood vessels. This is accomplished by the recruitment of smooth muscle like cells called pericytes which surround endothelial cells. Recruitment of pericytes helps to maintain vessel integrity and quiescence. Angiopoietin-1 (Ang1) signalling plays a major role in recruiting pericytes via its receptor Tie2 (Fig.2). Mutations of either Ang1 or Tie2 in mice resulted in malformation of blood vessels that are deficient in smooth muscle cells (Davis *et al.*, 1996; Suri *et al.*, 1996; Vikkula *et al.*, 1996). Vasculogenesis is followed by angiogenesis.

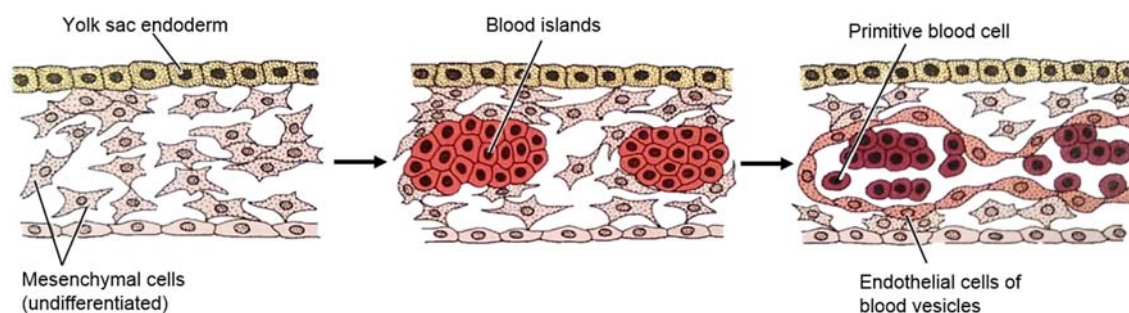


Figure 1: Formation of blood islands: Mesenchymal cells differentiate to form blood islands containing both blood cells and endothelial cells. Outer cells are further differentiated into endothelial cells surrounding the inner primitive blood cells. Once differentiated, they join together via endothelial cell-cell connections forming primitive vascular plexus. Adapted from Gilbert, 2006.

1.2 Angiogenesis

Following the initial phase of embryonic vasculogenesis, the primary capillary networks expand and are remodelled giving rise to differentiated form of blood vessels, arteries and veins. This process is called angiogenesis, which involves endothelial cell sprouting, vessel branching and intussusception from existing blood vessels (Flamme *et al.*, 1997; Patan, 2004). Interestingly, VEGF is also a major signalling molecule in angiogenesis. It promotes endothelial cell differentiation, migration and proliferation, controls endothelial cell-cell junctions and suppresses apoptosis. Regression of blood vessel branches, which is called pruning, involves disassembly of

junctions, followed by cell retraction and also to a variable extent, endothelial cell apoptosis (Baffert *et al.*, 2006; Hughes and Chang-Ling, 2000). VEGF signalling on primitive capillaries loosens cell-cell contacts and degrades extracellular matrix at certain points. These exposed endothelial cells sprout by proliferation ultimately resulting in the formation of a new blood vessel. Growth of existing tubular structures is spearheaded by a specified type of endothelial cell called tip cell and the following cells are referred to as stalk cells (Claxton and Fruttiger, 2004; Hellstorm *et al.*, 2007; Hofmann and Iruela-Arispe, 2007) (Fig.3). The specification of tip-stalk cell phenotype is regulated by Notch/Dll4 signalling (Sainson *et al.*, 2005; Noguera-Troise, 2006; Ridgway *et al.*, 2006; Hellstorm *et al.*, 2007; Leslie *et al.*, 2007; Seikmann and Lawson, 2007; Suchting *et al.*, 2007). Numerous evidence is emerging showing the critical role of Notch/Dll4 signalling during angiogenesis (Phng and Gerhardt, 2009). However, these are not discussed here in detail.

New vessels can also be formed in the primary capillary bed by splitting an existing vessel into two, a process called intussusception angiogenesis (Fig.3). Further, vasculature is specialized into arteries, veins and capillaries. Arteries and veins consist of a single layer of endothelial cells, but arteries are surrounded by multiple layers of smooth muscle cells. These layers provide elasticity and contractility to arteries. In contrast, veins recruit thinner smooth muscle layer with fewer elastic fibres (Rossant and Hiraskima, 2003). Recruitment of pericytes and stabilization of mature

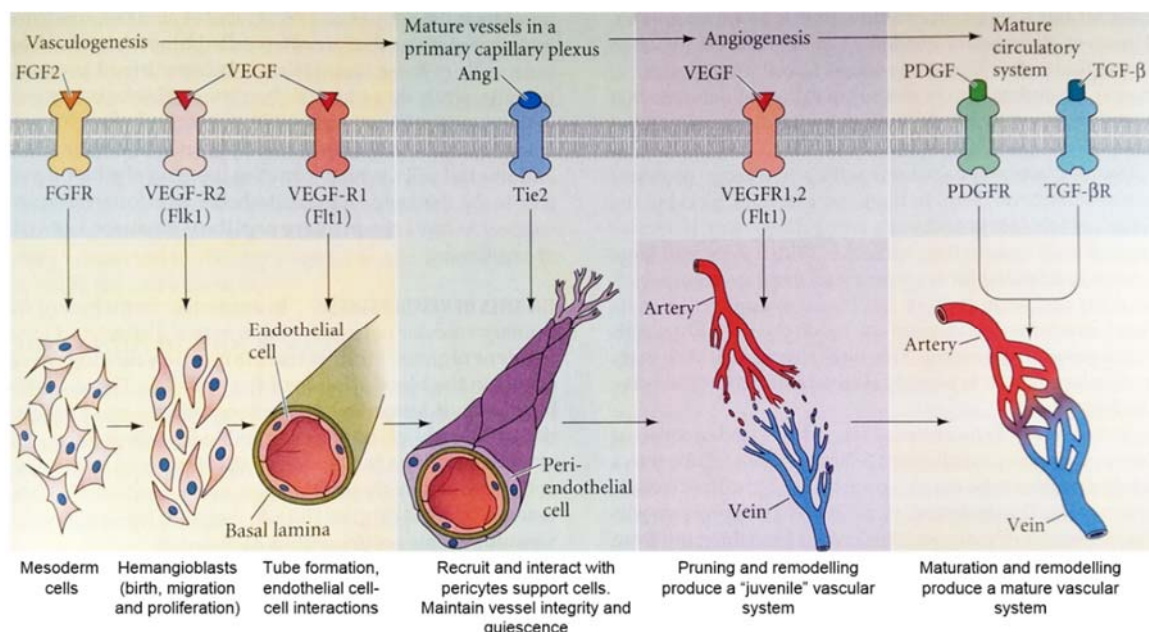


Figure 2: Vasculogenesis and angiogenesis: Vasculogenesis forms basic capillary networks that are later matured to form a functional vascular system via angiogenesis. FGF-2 signalling specifies mesodermal cells to hemangioblasts. These pluripotent cells form primitive vascular tubes with endothelial cell lining driven by VEGF signalling. Further recruiting pericytes gives the tubes their integrity and support via Ang1 signalling. Angiogenesis in turn requires VEGF

ligand for the formation of crude juvenile vascular system which matures and differentiates into functional arteries and veins by PDGF and TGF- β signalling. Adapted from Gilbert, 2006.

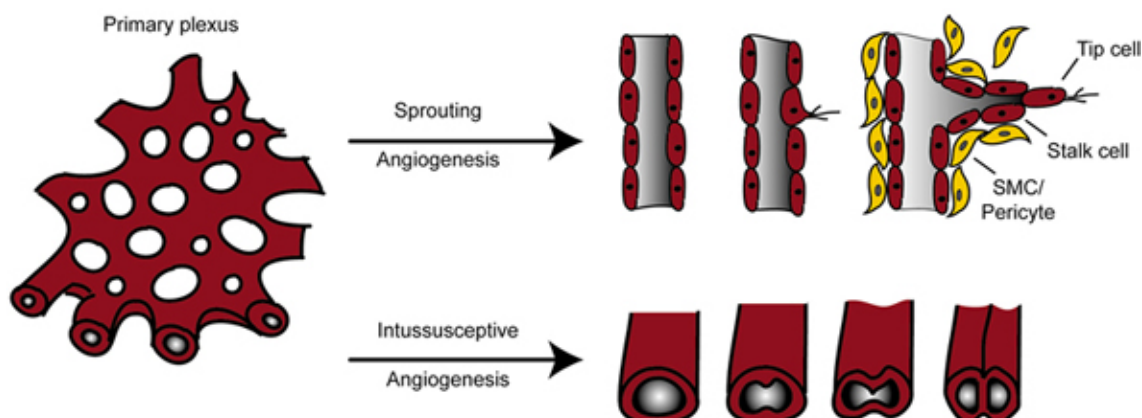


Figure 3: Formation of new vessels: Additional blood vessels are formed from pre-existing vessels mainly by two processes. First via Notch/Dll4 signalling wherein tip cells migrate through the VEGF gradient and stalk cells follow forming a new vessel. In another approach, existing blood vessels divide into two by intussusception forming two vessels side by side. Adapted from Heinke *et al.*, 2012.

vessels is mediated by Platelet-Derived Growth Factor (PDGF) and TGF- β respectively (Lindahl *et al.*, 1997) (Fig.2).

1.3 Hematopoiesis

As mentioned earlier, hemangioblasts give rise to both angioblasts and hematopoietic stem cells. A stem cell is a pluripotent cell that is able to replicate itself as well as give rise to more differentiated cellular progeny. A hematopoietic stem cell (HSC) or often referred to as pluripotent hematopoietic stem cell gives rise to all blood cells and lymphocytes of the body. Two phases of blood development have been discovered during vertebrate life. First is a transient embryonic phase also referred to as primitive phase and second is the definitive phase also known as adult phase. Fundamental difference between these two is the site of blood cell production (Chen and Turpen, 1995). Embryonic hematopoiesis in *Xenopus* takes place in the blood islands in the ventral mesoderm. Hematopoietic stem cells (HSC) arising from these regions are able to produce all blood cell lineages except lymphocytes (Moore and Metcalt, 1970; Rampon and Huber, 2003). Embryonic hematopoiesis is short term, providing the growing embryo with initial blood cells. On the other hand, adult hematopoiesis occurs in the bone marrow (in some instance spleen) and serves the organism by producing all kinds of blood cells that replenish continuously such as red blood cells and cells that last for long time such as leukocytes and lymphocytes.

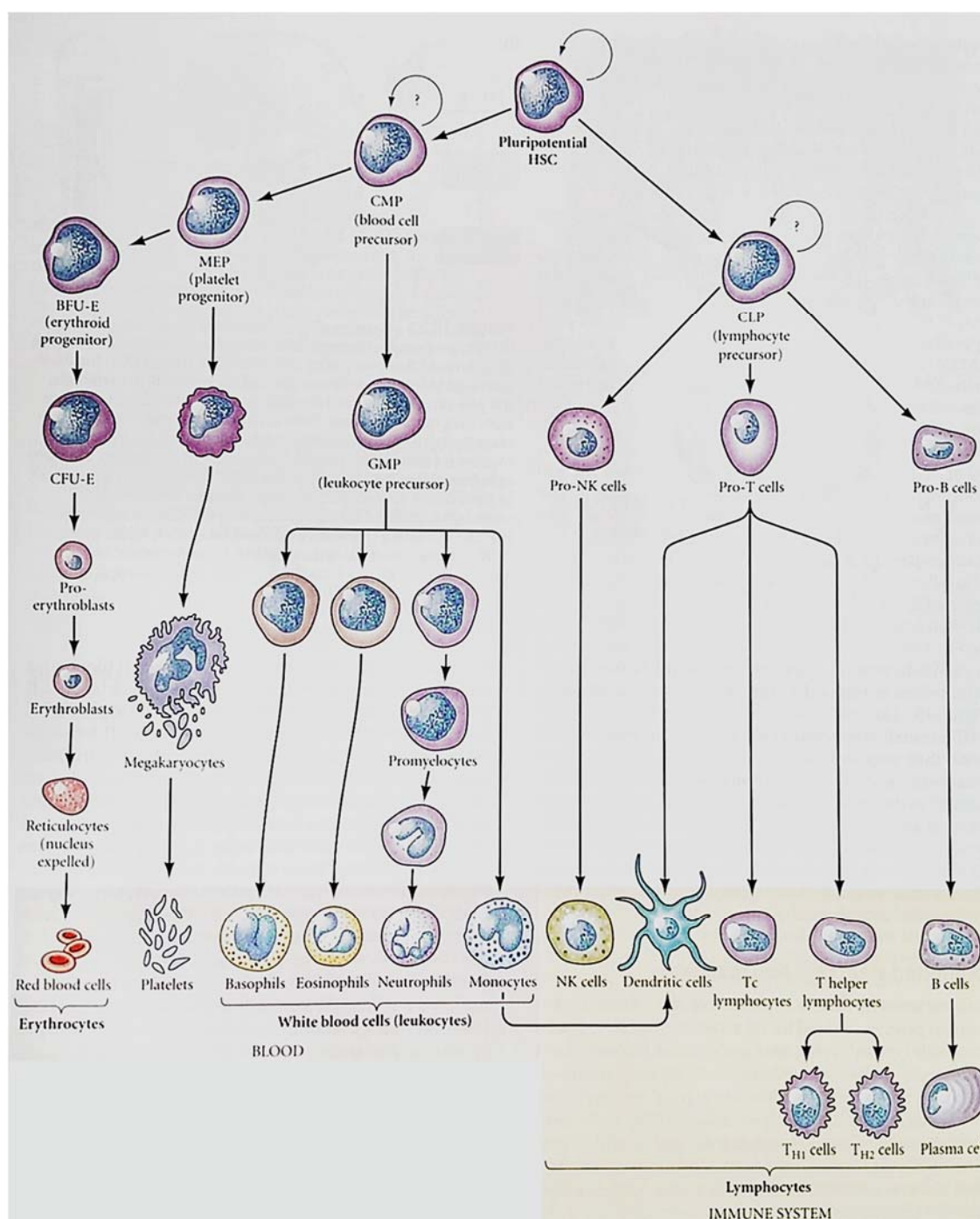


Figure 4: Formation of blood cells: All blood cells are formed from the common precursor cell, the pluripotent hematopoietic stem cell. This cells can give rise to two types of cells called CMP (Common Myeloid Precursor) and CLP (Common Lymphoid Precursor). Erythrocytes, platelets and white blood cells are formed from this common progenitor. T cells, B cells, plasma cells, NK cells and dendritic cells form ultimately from the CLP. Adapted from Gilbert, 2006.

Although there are several models describing the commitment of stem cells and their lineages (Adolfson *et al.*, 2005; Hock and Orkin, 2005), Fig.4 shows the most widely accepted model. Pluripotent hematopoietic stem cells (HSC) could give rise to the common myeloid precursor cell

(CMP) otherwise known as the blood cell precursor as well as the common lymphocyte precursor (CLP) otherwise known as the lymphocyte stem cell. Common myeloid precursor cells (CMP) can differentiate into megakaryocyte/erythroid precursor cells (MEP) and granulocyte/monocyte precursor cells (GMP). Megakaryocyte/erythroid precursor cell (MEP) ultimately differentiates into either red blood cells or megakaryocytes/platelets via several intermediate cell types. On the other hand, granulocyte/monocyte precursor cell (GMP) differentiates into 4 types of leukocytes namely basophils, eosinophils, neutrophils and monocytes. Nevertheless, once they are committed to form a specific cell type, they are able to produce only the same type of cell. For example, committed erythroid progenitor cells (BFU-E) can only form red blood cells/erythrocytes. Furthermore, common lymphocyte precursor (CLP) gives rise to three kinds of cell types. Pro-NK cells differentiate into NK (natural killer) cells, Pro-B cells to B cells and ultimately plasma cells and Pro-T cells into T lymphocytes and T helper lymphocytes as well as dendritic cells (Gilbert, 2006).

1.4 Neovascularization/neoangiogenesis

During adulthood, recruitment of new blood vessels is essential in scenarios such as wound healing and ischemia. The process of formation of functional microvascular networks from pre-existing vessels is called neovascularization or neoangiogenesis. However, besides these physiological functions, neovascularization also occurs during pathological conditions such as tumour formation. During tumour formation, rapid proliferation of cells creates hypoxic condition. For tumour survival, oxygen supply is critical. Tumour cells recruit new blood vessels to fulfil the growing need of oxygen and nutrients via VEGF signalling. It has been shown that hypoxia causes the up-regulation of VEGF expression (Gerhardt *et al.*, 2003). VEGF signalling in turn is associated with formation of new sprouts and blood vessels from the existing endothelial structures (Gerhardt *et al.*, 2003). In cancer microenvironment, hypoxia induces HIF pathway. This has been shown by detecting increased levels of HIF-1 α levels (Semenza, 2003) and VEGF is one of the targets of HIF pathway (Forsythe *et al.*, 1996).

1.5 Oxygen sensing mechanism

Regulation of oxygen level is important for the survival of cells. Hence, it is necessary to monitor varying changes in oxygen concentrations inside the cells. PHDs' (prolyl-4-hydroxylase proteins) are the enzymes which are evolved to sense varying oxygen conditions and regulate the stability of HIFs' (hypoxia inducible transcription factor) via HIF pathway. HIF pathway consists of 4 main factors – an oxygen degradable HIF-1 α , a HIF-1 α dimerizing protein called HIF-1 β or aryl hydrocarbon receptor nuclear translocator (ARNT), an oxygen sensitive prolyl-4-hydroxylase protein named PHD-2 and an E3 ubiquitin ligase called von Hippel-Lindau (pVHL) protein complex.

1.5.1 Hypoxia inducible transcription factors (HIFs)

HIF family consists of five members. So far, three members of α and two members of β subunit of the HIF family are discovered, HIF-1 α , HIF-2 α , HIF-3 α and HIF-1 β and HIF-2 β . HIF-1 α and HIF-1 β are the major components of the HIF pathway and are ubiquitously expressed. On the other hand, expression of other members is tissue specific. HIF α proteins are located in the cytoplasm and HIF β proteins are located in the nucleus (Semenza, 2000). Nevertheless, structure, regulation and function of all HIFs' seems to be similar.

1.5.2 Structure of HIF-1 α

HIF-1 α is a 826 amino acid long protein with a molecular weight of 120 kDa. The N-terminus consists of a basic helix-loop-helix (bHLH) domain from amino acids 17-71, which facilitates DNA binding. A PAS (Per-AHR-ARNT-Sim) domain is present from amino acids 85-298 which encompasses PAS-A from amino acids 85-158, and PAS-B from amino acids 228-298 repeats within (Wang *et al.*, 1995). HIF-1 α activity is regulated by oxygen degradation domain (ODD) which is located from amino acids 401-603. Oxygen degradation domain (ODD) is rich in proline (P), glutamic acid (E), serine (S) and threonine (T) collectively called PEST like motifs which are located from amino acids 499-518 and 581-600 (Rechsteiner and Rogers, 1996) and is responsible for the short half-life of the protein (~10 min), thus making it hard to detect the presence of the protein during normoxia (Chun *et al.*, 2002). Prolines present in the oxygen degradation domain (ODD) at positions pro 402 and pro 564 are hydroxylated during normoxia which targets HIF-1 α to degradation by ubiquitination of amino acids 390-417 and 549-582 respectively by pVHL binding to oxygen degradation domain (ODD) (Ivan *et al.*, 2001). In addition, translocation of HIF-1 α from cytoplasm into nucleus is facilitated by Nuclear Localisation Signals (NLS). It has two NLS, one in the C terminus called C-NLS which is located from amino acids 17-74 and another in the N terminus of the protein called N-NLS and is located from amino acids 718-721. C-NLS plays an important role in the nuclear import of HIF-1 α (Kallio *et al.*, 1998). Two transactivation domains are present namely N-terminus transactivation domain (NAD) which is situated between amino acids 531-575 and C-terminus transactivation domain (CAD) which is situated between amino acids 786-826. Both transactivation domains are located in the C-terminus half of the protein (Pugh *et al.*, 1997) (Fig.5A).

Structure of HIF-2 α is similar to HIF-1 α . However, HIF-2 α is an 870 amino acid long protein. It is also known as endothelial PAS (EPAS1) protein, HIF-like factor (HLF), HIF related factor (HRF) or as member of PAS domain family 2 (MOP2) (Semenza, 2000; Wenger, 2002). On the other hand, HIF-3 α is the shortest of the three. It is 667 amino acid long and lacks CAD domain (Fig.5B and C).

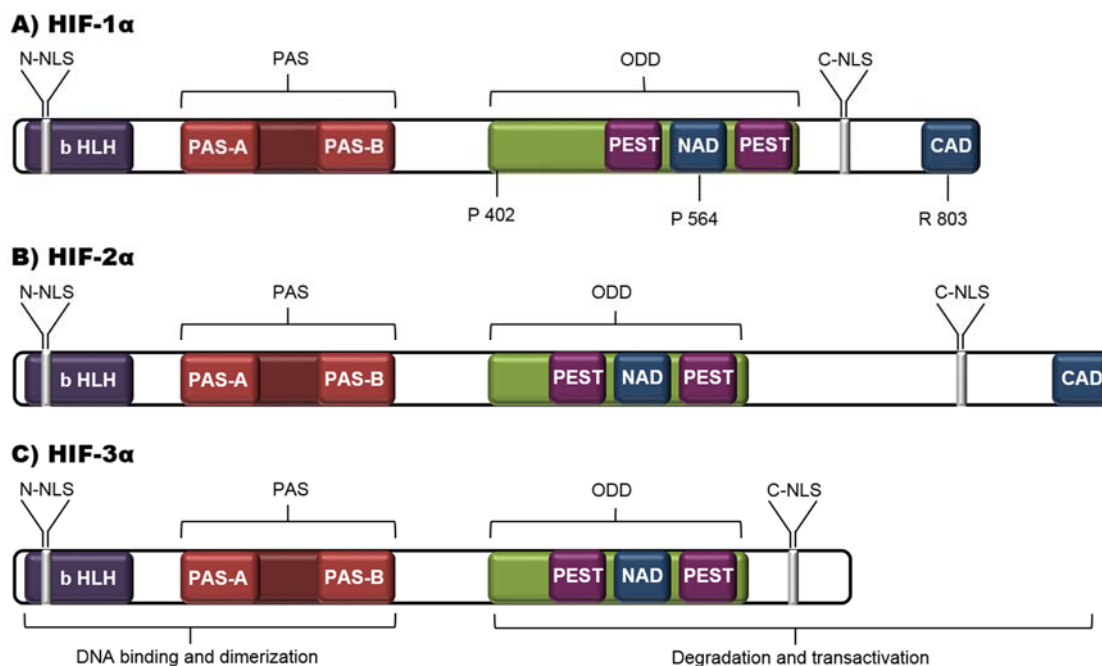


Figure 5: Structure of HIF-1 α , HIF-2 α and HIF-3 α : All the three members of HIF α are similar in their core structure. They contain a bHLH (basic Helix-Loop-Helix) domain for DNA binding, a PAS domain consisting of PAS-A and PAS-B for dimerization with HIF-1 β , an ODD (Oxygen Degradation Domain) which is the stability regulating region and two NLS (Nuclear Localization Signals) N-NLS and C-NLS for exporting the protein into the nucleus. However, only HIF-1 α and HIF-2 α hosts two trans-activating domains (NAD and CAD) whereas HIF-3 α lacks CAD.

1.5.3 Structure of HIF-1 β

HIF-1 β , also known as aryl hydrocarbon nuclear receptor translocator (ARNT), heterodimerizes with aryl hydrocarbon receptor (AHR) to form functional dioxin receptor. Two isoforms have been discovered so far, HIF-1 β and HIF-2 β . HIF-1 β is a 789 amino acid long 94 kDa protein and HIF-2 β is a 774 amino acid long 92 kDa protein. They have a bHLH domain for DNA binding and two PAS domains called PAS-A and B for dimerization with HIF-1 α . Degradation and translocation domains are absent (Fig.6).

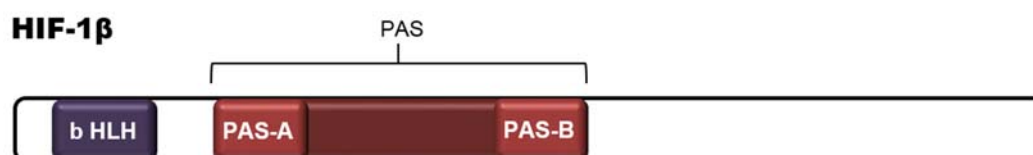


Figure 6: Structure of HIF-1 β : HIF-1 β has a bHLH (basic Helix-Loop-Helix) domain for DNA binding, a PAS domain consisting of PAS-A and PAS-B for dimerization with HIF-1 α . HIF-1 β is a nuclear protein.

1.5.4 Prolyl-4-Hydroxylases

PHD proteins belong to Fe (II) and 2-oxoglutarate dependent oxygenase super family, whose activity is absolutely dependent on oxygen (Kaelin and Ratcliffe, 2008). Flies and worms have a single PHD family member, called Egl9, whereas the genomes of higher metazoans contain three paralogous PHD genes. All three genes were found to be widely expressed with some exceptions (Lieb *et al.*, 2002). PHD-3 mRNA level were high in the heart, whereas PHD-1 mRNA levels were high in murine testis. Transfection studies in human osteosarcoma cells (U2OS) suggested that PHD-1 is exclusively nuclear, PHD-2 is mainly cytoplasmic and PHD-3 is found in both, the cytoplasm and the nucleus (Metzen *et al.*, 2003). PHD-2 and PHD-3 mRNA levels are increased by hypoxia and at least in some cell types, respond to growth factors (Wax *et al.*, 1994; Lipscomb *et al.*, 2001).

PHDs as well as FIH1 (Factors Inhibiting HIF1 α) are dioxygenases, enzymes that use both atoms of molecular oxygen for their activity. One oxygen atom is used for the oxidative decarboxylation of 2-oxoglutarate yielding succinate and CO₂, and the second is incorporated directly into the oxidized amino acid residue of HIF-1 α (Hewitson *et al.*, 2002; McNeill *et al.*, 2002). siRNA studies in human cell lines revealed that PHDs exhibit some degree of specificity regarding the recognition of different HIF α family members. PHD-2 hydroxylates primarily HIF-1 α , PHD-3 targets predominantly HIF-2 α and PHD-1 shows a slightly higher preference for HIF-2 α over HIF-1 α (Appelhoff *et al.*, 2004). Of the three PHD family members, PHD-2 which is also called EglN1 (egg laying domain nine), appears to be the primary HIF prolyl hydroxylase, contributing to the majority of hydroxylase activity in normoxic cells, thereby setting normoxic HIF-1 α levels (Berra *et al.*, 2003; Minamishima *et al.*, 2008; Takeda *et al.*, 2008). PHD-3 (EglN3) is more effective in suppression of HIF-2 α and so might alter the relative abundance of HIF-2 α versus HIF-1 α (Appelhoff *et al.*, 2004).

1.5.5 Regulation of HIF pathway

Under normal oxygen concentrations (normoxia), PHD-2 readily uses the available oxygen to hydroxylate two proline residues (pro 402 and pro 564) present in the oxygen degradation domain (ODD) of HIF-1 α . Both of these sites contain a LXXLAP motif that is highly conserved in metazoans in which Leu 562 strongly facilitates the hydroxylation of Pro 564 (Ivan *et al.*, 2001). Hydroxylation of a single proline residue was shown to be sufficient to target HIF-1 α to an ubiquitin ligase (Maxwell *et al.*, 1999). Once the proline residues are hydroxylated, pVHL binds to HIF-1 α and acts as a substrate recognition component for the E3 ubiquitin ligase protein complex and facilitates recruitment of elongins B and C, cullin 2 and Rbx1 (Semenza, 2001). Finally, HIF-1 α protein is subjected to ubiquitination of its N and C terminus part from amino acids 390-417 and 549-582 respectively via 26s proteasome (Kallio *et al.*, 1999). Inactivation of HIF-1 α is also mediated by the hydroxylation of arginine residue which is located at amino acid

803 in the C-terminus transactivation domain (CAD) by Factors Inhibiting HIF-1 α (FIH1) leading to a steric clash which prevents the recruitment of the co-activators p300 and CBP (Schofield and Ratcliffe, 2004; Kaelin, 2005).

On the other hand, during low oxygen conditions (hypoxia), O₂, which is the substrate for PHD-2 is limited. Therefore, hydroxylation rate of HIF-1 α is reduced, gradually increasing the stability of the translated protein. Stabilized HIF-1 α translocates into nucleus and dimerizes with its partner protein HIF-1 β . The binary complex is then capable of binding to the hypoxia response elements (HRE) and could potentially initiate transcription of about 100-200 genes including genes involved in erythropoiesis, angiogenesis, autophagy and energy metabolism (Kaelin and Ratcliffe, 2008) (Fig.7). Potential target genes that are activated by this pathway are listed in Table 1.

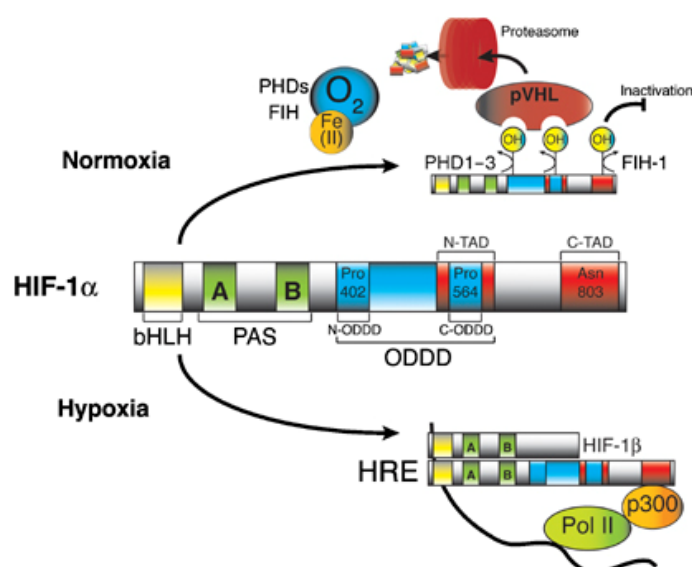


Figure 7: Regulation of HIF pathway: During normoxia, two proline residues present in the oxygen degradation domain (ODD) of HIF-1 α are hydroxylated by PHDs. Fe (II) acts as a catalyst in the reaction. Hydroxylated protein then becomes a target of pVHL ubiquitin ligase. Finally, the protein is degraded by 26s proteasome. Alternatively, hydroxylation of arginine residue in the C-terminus transactivation domain (CAD) region leads to inactivation of the protein. In contrast, hypoxia demotes oxygen availability to PHDs for the hydroxylation reaction leading to stable HIF-1 α protein. Stabilized HIF-1 α translocates to nucleus wherein it dimerizes with HIF-1 β thereby initiating the transcription of several genes to compensate for oxygen scarcity. P300 is necessary for the initiation as a co-factor. Adapted from Gilbert, 2006. Weidemann and Johnson, 2008.

Table 1: HIF-1 α target genes: HIF-1 α activates several hundreds of genes in response to hypoxia. Target genes mainly include increased angiogenesis, erythropoiesis, glucose metabolism and cell cycle controlling factors. List of major genes that are upregulated by HIF-1 α are listed in the table below.

Process		Gene product	Reference
Control of vascular system	Angiogenesis	Vascular endothelial growth factor receptor 1	Forsythe <i>et al.</i> , 1996 Gerber <i>et al.</i> , 1997
		Plasminogen activator inhibitor 1	Kietzmann <i>et al.</i> , 1997
		Transforming growth factor β 3	Caniggia <i>et al.</i> , 2000
	Vasomotor control	Nitric oxide synthase 2	Melillo <i>et al.</i> , 1995
		Endothelin-1	Hu <i>et al.</i> , 1998
		α_{1B} -adrenergic receptor	Eckhart <i>et al.</i> , 1997
	Adrenomedullin	Cormier-Regard <i>et al.</i> , 1998	
Maturation of red blood cells	Erythropoiesis	Erythropoietin	Jiang <i>et al.</i> , 1996
	Iron transport	Transferrin	Rolfs <i>et al.</i> , 1997
		Transferrin receptor	Lok and Ponka, 1999
		Ceruloplasmin	Mukhopadhyay <i>et al.</i> , 2000
Energy metabolism	Glycolysis	Lactate dehydrogenase A	Firth <i>et al.</i> , 1994
		Phosphoglycerate kinase 1	Semenza <i>et al.</i> , 1994
		Aldolase A and C	Iyer <i>et al.</i> , 1998
		Phosphofructo kinase L	Iyer <i>et al.</i> , 1998
		Pyruvate kinase M	Iyer <i>et al.</i> , 1998
		Enolase 1	Iyer <i>et al.</i> , 1998
	Glucose transport	Hexokinase 1 and 2	Iyer <i>et al.</i> , 1998
		Glucose transporter 1	Gleadle and Ratcliffe, 1997
		Glucose transporter 3	O'Rourke <i>et al.</i> , 1996
Multi-functional enzyme	Glyceraldehyde-3-phosphate dehydrogenase	Lu <i>et al.</i> , 2002; Iyer <i>et al.</i> , 1998	
Cell proliferation and viability	Arrest of cell cycle	P21	Carmeliet <i>et al.</i> , 1998
	Apoptosis	Bcl2/E1B 19kDa-interacting protein 3 (BNIP3)	Bruick, 2000
		Nip3-like protein X	Sowter <i>et al.</i> , 2001
	Growth factors	Insulin like growth factor 2	Feldser <i>et al.</i> , 1999
Insulin like growth factor binding protein 1, 2 and 3.		Feldser <i>et al.</i> , 1999	
Others	pH regulation	Carbonic anhydrase 9	Wykoff <i>et al.</i> , 2000
	Nucleotide metabolism	Adenylate kinase 3	O'Rourke <i>et al.</i> , 1996
	Matrix metabolism	Collagen prolyl-4-hydroxylase α 1	Takahashi <i>et al.</i> , 2000
	Catecholamine synthesis	Tyrosine hydroxylase	Norris and Millhorn, 1995
	Feedback regulation	P35srj	Bhattacharya <i>et al.</i> , 1999

1.6 *Xenopus laevis* as a model organism to study vascular system

Xenopus laevis belongs to the order of anura of the class of amphibians. Over a long period of time, *Xenopus laevis* has been one of the widely used model organisms in the field of biology. Its ease in handling and breeding makes it an important model in developmental biology and molecular biology laboratories. Embryos can be subjected to manipulation. For example, microinjection of *in vitro* synthesized RNA/DNA and loss-of-function studies by injecting morpholino oligo nucleotides targeting specific genes. Microinjections can be performed in one cell of a two cell staged embryo leaving the un-injected side as control. *Xenopus laevis* has specific advantages in studying the vascular system i.e., both vasculogenesis and angiogenesis. It has been demonstrated that it possess high degree of similarities within the higher vertebrates than other model organisms such as zebra fish. It exhibits similarities with human embryos (Evans *et al.*, 1912) in having an artery and a vein at each inter somitic vessel whereas zebra fish embryos exhibits a random pattern (Isogai *et al.*, 2001). Posterior cardinal veins are developed as paired vessels which then fuse at tail extending towards anterior region (Ariel *et al.*, 2003) whereas zebra fish exhibits a single medial posterior cardinal vein (Isogai *et al.*, 2001). It exhibits separated atria, lungs, defined heart valves, a mammalian like pattern of tail vasculature, blood islands and a vitelline network (Millard, 1949; Aoyama, 1956; Kau and Trupen, 1983; Cleaver *et al.*, 1999; Kolker *et al.*, 2000; Mohun *et al.*, 2000).

1.7 Aim of the thesis

Embryonic vasculogenesis is a strictly controlled process which leads to the formation of functional cardio vascular system. This is one of the first functional systems formed in the developing embryo. Essential elements, nutrients, signalling molecules such as oxygen and growth factors such as VEGF and TGF- α are delivered to their respective target sites through this system. However, we do not know if vasculogenesis is a genetically pre-programmed system. I therefore asked if embryonic vasculogenesis is an independent process or is dependent on external environmental factor, oxygen. During tumorigenesis, it has been suggested that HIF-1 α levels in the tumour cells increase. High levels of HIF-1 α act as pro-angiogenic factor and promotes recruitment of blood vessels in the hypoxic regions. Therefore, I would like to investigate whether HIF-1 α has a role *in vivo* in vasculogenesis during early vertebrate development. If HIF-1 α plays an important role, is it regulated the same way during embryogenesis or is it differentially regulated?

2 Materials

2.1 The experimental animal - *Xenopus laevis*

The South African clawed frog *Xenopus laevis* is an amphibian of the order *Anura* and has a natural geographic range along the African Rift Valley, south of the Sahara Desert. Pigmented and albino frogs were obtained from a commercial supplier (NASCO, USA) and held in aquaria (water temperature 19 °C).

2.2 Bacteria

E. coli XL1-Blue Stratagene GmbH, Heidelberg

2.3 Chemicals

Acetic acid	Roth [®]
Acetic anhydride	Sigma [®]
Agarose	Roth [®]
Albumin, Bovine Serum (BSA)	Sigma [®]
Blocking reagent	Roche
Boric acid	Roth [®]
5-Bromo-4-chloro-3-indolyl-phosphate (BCIP)	Fermentas
Bromphenol blue sodium salt	Merck
Calcium chloride, dihydrate	AppliChem
CHAPS	Roth [®]
Chloroform	Merck
L-Cysteinhydrochloride	Roth [®]
10 mM dNTP mix	Fermentas
Diethylpyrocarbonate (DEPC)	Sigma [®]
DIG RNA Labeling Mix	Roche
Dimethyl sulfoxide (DMSO)	Roth [®]
Dithiothreitol (DTT)	Sigma [®]
Dimethyloxallyl glycine (DMOG)	Cayman chemical
DNA Ladder, O'GeneRuler™ 1kb	Fermentas
Ethanol (≥99.8%)	Roth [®]
Ethylene-diamine-tetra acetic acid (EDTA)	Sigma [®]
Ethylene glycol-bis(2-amino-ethylether -N,N,N',N')-tetra-acetic acid (EGTA)	Sigma [®]
Ethidium Bromide	Q-Biogene
Ficoll [®] 400	Serva
Formaldehyde	Roth [®]

Formamide	Roth [®]
Glycerol	Roth [®]
Heparin	Roth [®]
HEPES	Roth [®]
Horse Serum (HS)	Gibco [®]
Human chorionic gonadotropin (HCG)	Sigma [®]
Hydrogen chloride	Merck
Hydrogen peroxide (30%)	Roth [®]
Isopropanol	Roth
LB Broth Base	Invitrogene [™]
LB Agar	Invitrogene [™]
Lithium chloride	Roth [®]
Magnesium chloride	Roth [®]
Magnesium sulfate, heptahydrate	Sigma [®]
Maleic acid	Roth [®]
Methanol	Roth [®]
MOPS	Q-Biogene
Nitro blue tetrazolium chloride (NBT)	Fermentas
Nile blue chloride	Fluka [™]
Paraformaldehyde	Roth [®]
Potassium chloride	Roth [®]
Potassium hydrogenphosphate	Roth [®]
Proteinase K	Merck
RNase OUT [™] Ribonuclease Inhibitor	Invitrogene [™]
RNase A	Fermentas
RNase T1	Sigma [®]
Sodium acetate	Roth [®]
Sodium chloride	Roth [®]
Sodium dihydrogenphosphate	Merck
Sodium dodecyl sulfate (SDS)	Roth [®]
Sodium hydroxide	Roth [®]
Torula RNA	Sigma
Triethanolamine	Roth [®]
Tris(hydroxymethyl)-aminomethane (Tris)	Roth [®]
TRIzol [®] Reagent	Invitrogene [™]
Tween-20	Roth [®]
Xylencyanol	Roth [®]

2.4 Buffers, solutions and media

2.4.1 Embryos preparation

Human chorionic gonadotropin (HCG): 10,000 U/vial HCG (Sigma) was suspended in 5 ml ddH₂O to make a stock solution of 2000 U/ml, aliquoted in fractions of 1 ml, stored at -20°C.

10x MBS (Modified Barth's Saline): 440 mM NaCl, 12 mM NaHCO₃, 5 mM KCl, 4.1 mM MgSO₄, 50 mM Hepes in dH₂O, pH adjusted to 7.4 and then supplied with 2.05 mM CaCl₂. The solution was filtered with 0.2 µm filters (Sartorius, Germany) and stored at RT. The stock solution was diluted to 0.1x or 1x MBS.

L-Cystein hydrochloride solution (2%): 2% L-Cystein hydrochloride, pH adjusted to 7.8 – 8.0.

Nile blue solution

1 l phosphate buffer containing 50 mM Na₂HPO₄ and 50 mM NaH₂PO₄ was warmed up to 60°C. 0.01% (w/v) Nile blue chloride was dissolved in it with stirring overnight. After filtration, the Nile blue solution was ready to use.

10x MEM (MOPS/EGTA/Magnesium sulfate buffer)

1 M MOPS, 20 mM EGTA, 10 mM MgSO₄ in dH₂O. The solution was filtrated with 0.2 µm filters and stored at RT.

MEMFA (MOPS/EGTA/Magnesium sulfate/formaldehyde buffer)

3.7% formaldehyde in 1x MEM, prepared before use.

10x PBS (phosphate-buffered saline)

1.37 M NaCl, 27 mM KCl, 80 mM Na₂HPO₄ and 18 mM KH₂PO₄ in dH₂O, pH 7.4. Autoclaved.

2.4.2 Whole-mount *in situ* hybridization

DEPC (Diethylpyrocarbonat) H₂O: 0.1% (v/v) DEPC in ddH₂O was incubated at 37°C for 2 hrs and autoclaved.

PTw: 0.1% Tween-20 in PBS.

PTw/MEMFA: 4% (v/v) formaldehyde in PTw.

Triethanolamine solution: 0.1 M Triethanolamine-hydrochloride in dH₂O, pH adjusted to 7.5.

100x Denhart's solution: 2% BSA, 2% PVP and 2% Ficoll[®] 400 in dH₂O, stored at -20°C.

Torula RNA (10 mg/ml): 10 mg/ml Torula RNA in DEPC H₂O was dissolved at 37°C with shaking overnight. After centrifugation at 6000 rpm for 10 min, the supernatant was aliquoted and stored at -20°C.

20x SSC (standard saline citrate buffer): 3 M NaCl and 0.3 M Na Citrate in dH₂O, pH 7.2-7.4.

Hybridization mix: 50% deionized formamide*, 1 mg/ml Torula-RNA, 10 µg/ml Heparin, 1x Denhardt's, 0.1% Tween-20, 0.1% CHAPS, and 10 mM EDTA in 5x SSC, stored at -20°C.

* To deionize formamide: Add 50g of mixed bead resin (BioRad) to 500 ml formamide, mix on magnetic stirrer for 2 h and filter on Whatman® paper.

NBT solution: 100 mg/mL NBT in 70% DMF, stored at -20°C.

BCIP solution: 50 mg/mL in 100% DMF, stored at -20°C.

Ethanol series: 100%, 75% and 50% (v/v) ethanol in dH₂O respectively; 25% ethanol in PTw.

Methanol series: 100%, 75%, 50% and 25% (v/v) methanol in dH₂O respectively.

5x MAB (maleic acid buffer): 500 mM maleic acid, 750 mM NaCl in dH₂O, pH 7.5, autoclaved.

Boehringer Blocking Reagent (BMB) stock solution: 10% BMB was dissolved 1x MAB at 60°C, autoclaved and stored at -20°C.

MAB/BMB: 2% BMB in 1x MAB.

MAB/BMB/HS: 2% BMB, 20% heat-treated horse serum in 1x MAB.

APB (Alkaline phosphatase buffer): 100 mM Tris-HCl, pH 9.0, 50 mM MgCl₂, 100 mM NaCl and 0.1% Tween-20 in dH₂O.

Color reaction solution: 175 µg/ml NBT and 175 µg/ml BCIP in APB.

TE buffer (Tris/EDTA buffer): 10 mM Tris-HCl (pH 7.5) with 1 mM EDTA.

RNase A stock solution: 10 mg/ml of RNase A dissolved in TE buffer, heated at 100°C for 10 min, and stored at -20°C.

Bleaching solution: 50% (v/v) formamide and 1% H₂O₂ in 5x SSC.

2.4.3 Mini/Maxi preparation of plasmid DNA

Solution A: 50 mM Glucose, 25 mM Tris pH 8.0 and 10 mM EDTA in dH₂O. Stored at 4°C.

Solution B: Prepared fresh every time. 0.2 M NaOH and 1% SDS in dH₂O.

Solution C: 30 ml 5 M KAc pH 5.2 and 5.75 ml glacial acetic acid in 14.25 ml dH₂O. Stored at 4°C.

Lysozyme solution: 10 mg/ml Lysozyme in dH₂O, prepared before use.

2.4.4 Gel electrophoresis

10x TBE buffer (Tris/boric acid/EDTA buffer)

0.89 M Tris, 0.89 M boric acid and 20 mM EDTA in dH₂O.

Glycerol loading buffer: 10 mM EDTA, 30% glycerol (v/v), 0.025% Bromphenol blue and 0.025% Xylencyanol in 10 mM Tris-HCl, pH 7.5.

2.4.5 Immunostaining

4% Paraformaldehyde (PFA): 4% Paraformaldehyde in PBS, stirred and heated to 60-65°C till the solution became clear, pH adjust to 7.2. Aliquots were stored at -20°C.

Permeabilization and blocking solution: 20 mg/ml bovine serum albumin (BSA, Roth[®]) and 0.5% (v/v) Triton X-100 in PBS.

Antibody buffer: 10 mg/ml BSA and 0.05% Triton X-100 in PBS.

PBS-TB: 0.05% (v/v) Tween-20 and 0.2% BMB in PBS.

PBS-TBN: 0.05% (v/v) Tween-20, 0.2% BMB and 0.3 M NaCl in PBS.

2.4.6 Media

Luria-Bertani (LB) medium: 20 g LB Broth Base was dissolved into 1 l dH₂O and autoclaved for 20 min at 121°C, stored at 4°C.

Luria-Bertani (LB)-Ampicillin (Amp) agar plate: 32 g LB Agar was dissolved in 1 l dH₂O and autoclaved for 20 min at 121°C. After the medium was cooled down to around 50°C, ampicillin solution (100 mg/ml in dH₂O) was added with a final concentration of 100 µg/ml and plates were poured in a sterile hood.

Luria-Bertani (LB)-Tetracycline (Tet) agar plate: 32 g LB Agar was dissolved in 1 l dH₂O and autoclaved for 20 min at 121°C. After the medium was cooled down to around 50°C, tetracycline solution (5 mg/ml in 100% Ethanol) was added with a final concentration of 12.5 µg/ml and plates were poured in a sterile hood.

2.5 Antibodies

Anti-Digoxigenin/AP (Roche Diagnostics)

Fab fragment of polyclonal antibodies from sheep specifically recognizing digoxigenin and digoxin, conjugated with alkaline phosphatase.

Anti-Fluorescein/AP (Roche Diagnostics)

Fab fragment of polyclonal antibodies from sheep specifically recognizing free and bound fluorescein, conjugated with alkaline phosphatase.

Anti-phospho-histone H3 (Upstate Biotechnology)

A polyclonal antibody generated from rabbit with synthetic phospho-peptide derived from the sequence of human Histone H3 as the immunogen.

2.6 Enzymes

Restriction enzymes with supplied buffers	NEB [®]
RNase A	Sigma-Aldrich [®]
RNase T1	Sigma-Aldrich [®]
Proteinase K	Merck
T4 DNA-Ligase (3 U/µl) with supplied buffer	Fermentas
SP6 RNA-Polymerase (50 U/µl) with supplied buffer	Stratagene
T3 RNA-Polymerase (50 U/µl) with supplied buffer	Stratagene

T7 RNA-Polymerase (50 U/μl) with supplied buffer	Stratagene
<i>Taq</i> DNA-Polymerase (5 U/μl) with supplied buffer	Fermentas
<i>Phusion</i> DNA-Polymerase (2.5 U/μl) with supplied buffer	Fermentas
Deoxyribonuclease I (DNaseI, RNase-free) (1 U/μl)	Fermentas

2.7 Kits

The following kits were used in this study, according to manufacturers' instructions:

mMESSAGE mMACHINE [®] SP6	Ambion [®]
QIAGEN [®] PCR Purification Kit	Qiagen [®]
QIAEX [®] Gel Extraction Kit	Qiagen [®]

2.8 Oligonucleotides

2.8.1 Oligonucleotides for PCR

Oligonucleotides were ordered from Sigma-Aldrich and dissolved in ddH₂O to get a 100 μM stock solution. In the following sequences, f represents forward and r represents reverse primer.

For SQ-PCR of MO specificity constructs

ODC-1-f	5'-GCCATTGTGAAGACTCTCTCCATTC-3'
ODC-1-r	5'-TTCGGGTGATTCCTTGCCAC-3'
XI-HIF-1α eoe1-f	5'-AGATCTGACCTTGCCAACGA-3'
XI-HIF-1α eoe1-r	5'-CTCCTTACTCCTCCGACACC-3'
XI-VHL eoe2-f	5'-GTGCCAGCCCAATTGTAAA-3'
XI-VHL eoe2-r	5'-CTTCCCAGAAACGGATTGCC-3'

For MO specificity constructs

PHD-2 WT + GFP:	5'- GGATCCCATCGATTCCAATTCATAATTGGGAGACA GCAGACAGACATAATGTCTAAAGGTGAAGAATTATTCAC-3'
PHD-2 MUT + GFP:	5'- GGATCCCATCGATTCCAATTCATAGTTAGGCGATAG AAGGCAAACGTAATGTCTAAAGGTGAAGAATTATTCAC -3'

2.8.2 Antisense Morpholino Oligonucleotides (MO): Morpholino Oligonucleotides were obtained from Gene Tools (USA) and dissolved in RNase-free H₂O to make the stock concentration of 1 mM.

Standard MO (Control MO)	5'-CCTCTTACCTCAGTTACAATTTATA-3'
XI-PHD-1 specific MO (XI-PHD-1-MO)	5'-TCCCTGCTGATGCCCTCTATCCATC-3'
XI-PHD-2 specific MO (XI-PHD-2-MO)	5'-ATGTCTGTCTGCTGTCTCCCAATTA-3'
XI-PHD-3 specific MO (XI-PHD-3-MO)	5'-ACTCAGGATCTCTGACAGAGACAGC-3'

XI-HIF-1 α specific MO (XI-HIF-1 α eoe1-MO)5'-GGCGGAGCACTCACCTTTTCTTCTC-3'
XI-VHL specific MO (XI-VHL eoe2-MO) 5'-GCTTACCTGGCAGTGAGATATTTAC-3'

2.9 Vectors and Constructs

2.9.1 Vectors

pCS2+ (Mental Health Research Institute, University of Michigan)

This multipurpose expression vector contains a strong enhancer/promoter (simian CMV IE94) followed by a multiple cloning site I (MCS I) and the SV40 late poly-adenylation site. The SP6 promoter allows *in vitro* RNA synthesis of sequence cloned into MCS II. The second MCS provides several possible sites to linearize the vector for SP6 RNA transcription. This vector was used in generation of constructs for *in vitro* synthesis of sense mRNA.

pCS2+MT

This one is similar to pCS2+ with additional myc tag. This vector also contains a strong enhancer/promoter (simian CMV IE94) followed by a multiple cloning site and the SV40 late poly-adenylation site. The SP6 promoter allows *in vitro* RNA synthesis of sequence cloned into MCS. The MCS provides several possible sites to linearize the vector for SP6 RNA transcription. This vector was used in generation of constructs for *in vitro* synthesis of sense mRNA.

pTP218

pTP218 contains the green fluorescent protein (GFP) gene, an ampicillin resistance (Amp^R) gene, a URA3 gene as well as yeast centromere (CEN) and an autonomous replication site (ARS) for plasmid amplification and selection in *Saccharomyces cerevisiae*. It contains a CMV promoter, an MCS followed by a SV40 poly-adenylation site.

pBluescript II SK

This vector contains an ampicillin selection cassette. It is one of the widely used plasmids for cloning. The PCR fragments with overhanging restriction sites could be directly cloned into pBluescript II SK vector. It contains T7 and T3 RNA polymerase promoters flanking a multiple cloning region. This vector was used to construct plasmids generating anti-sense RNA probes.

2.9.2 Constructs

The sense (+) and antisense (-) probes generated from the following indicated constructs are all specific for *Xenopus* transcripts (Table 2).

2.9.3 Cloning

For cloning the desired genes, PCRs were carried out in a 50 µl reaction mix containing 5 µl 10x buffer (supplied with enzyme), 1-2 ng DNA template, 0.25 µM each of forward and reverse primers, 0.5 mM each of dNTPs and 1 µl Phusion DNA polymerase. The thermocycler program was performed with activating the enzyme and denaturing the DNA template at 95°C for 2 min, followed by 26 cycles of DNA denaturation at 95°C for 45 sec, annealing at 55-60°C for 45 sec and extension at 72°C for 1-3 min according to the length of the PCR product (1kb/30 sec as recommended by the manufacturer), and the final extension at 72°C for 10 min.

Table 2: Constructs. The table shows constructs that were used to make antisense (-) probes for whole mount *in situ* hybridization and synthetic sense (+) mRNAs' for microinjections.

Construct	Vector	Insert (length)	Restriction digestion	Transcription -al promoter	Probe
Ami_SK	pBSKII	Partial	<i>EcoRI</i>	T7	-
pCS2+_ER71	pCS2+	Partial	<i>EcoRI</i>	T7	-
pCS2+_mpo	pCS2+	Partial	<i>EcoRI</i>	T7	-
pCMV-sport6_lmo-2	pCMV-sport6	Partial	<i>EcoRI</i>	T7	-
pSPT_β-globin	pSPT	Partial	<i>PstI</i>	T7	-
pCS2+_Muscle Actin	pCS2+	Full	<i>BamHI</i>	T3	-
pBST-KS_n-tubulin	pBST-KS	Partial	<i>BamHI</i>	T3	-
pTP218_PHD-2 WT + GFP	pTP218	Partial	<i>KpnI</i>	SP6	+
pTP218_PHD-2 MUT + GFP	pTP218	Partial	<i>KpnI</i>	SP6	+
pCS2+MT_PHD-2	pCS2+MT	Full	<i>NotI</i>	SP6	+

2.10 Equipments

Microliter pipettes

Pipetman P2, P10, P20, P200, P1000

Gilson® S.A.S., France

PCR Thermocycler

Tpersonal Thermocycler

Biometra, Germany

TGRADIENT Thermocycler

Biometra, Germany

Centrifuge

Biofuge pico

Heraeus, Germany

SIGMA 2K15	Sigma Laborzentrifugen, Germany
Sorvall RC-5B	Thermo Scientific, USA
Spectrophotometer	
NanoDrop [®] Spectrophotometer ND-100	peQlab Biotechnology, Germany
Sterile Hood	
KS12	Thermo Scientific, USA
Incubator/Thermoblock/Waterbath	
Incubator: Function line	Heraeus Instruments, Germany
Incubator shaker: innova TM 4300	New Brunswick [™] Scientific, USA
Incubator shaker: innova TM 4230	New Brunswick [™] Scientific, USA
Water bath DIN 40050-IP20	Memert, Germany
Thermomixer: Thermomixer 5437	eppendorf, Germany
Thermomixer: HTMR-131	HLC-Haep Labor Consult, Germany
Shaker	
Rocky 100	Labortechnik Fröbel, EU
RM5V-30 CAT.	M. Zipperer, Germany
Electrophoresis	
Electrophoresis power supply E844	Consort, Belgium
Power Pack P25	Biometra, Germany
Bio-Rad Gel Doc 2000	Bio-Rad Laboratories, USA
Microinjection	
Microinjector: PV820 Pneumatic Picopump	Helmut Saur, Germany
Needle-puller: PN-30	Narishige, Japan
Microscope	
Zeiss Stemi 2000	Carl Zeiss, Germany
Olympus SZX12	Olympus Microscopy, Japan
Leica DMR	Leica Microsystem, Germany
Nikon Eclipse E600	Nikon, Japan
UV supply for Microscope	
ebq 100 LEJ	Leistungselektronik, Germany
Camera	

iNTAS MS 500	iNTAS, Germany
Vosskühler CCD-1300QLN	Vosskühler, Germany
Computer	
Personal Computer	Sony VAIO, Japan
Software	
BLAST (http://www.ncbi.nlm.nih.gov/BLAST/)	National Institute for Health, USA (Altschul <i>et al.</i> , 1997)
Microsoft® Office 2013, Windows 7	Microsoft, USA
Photoshop CS5.1	Adobe Systems®, USA
Primer3 (http://frodo.wi.mit.edu/)	Whitehead Institute for Biomedical Research, USA (Rozen and Skaletsky, 2000)
QCapture Pro 5.1	QImaging, USA
Image J (Analyze plugin)	NCBI, USA

2.11 Oxygen regulating apparatus

4-channel oxygen regulator system 230V	Loligo® Systems, Denmark
DAQ-M-Analog data acquisition device	
AMP DAQ4-Analog to digital convertor	
Oxygen sensors	
Relay system	
Stirrers	IKA®, RW 11 basic, Germany
Thermostat	Humeau laboratories, France

3 Methods

3.1 Hypoxia Chamber

Information regarding the setting up of hypoxia chamber is available from previous records in which zebra fish was raised (Cao *et al.*, 2010; Rouhi *et al.*, 2010). However, many modifications and pilot experiments had to be done to get best possible conditions and regulation of all the four chambers at the same time because of the differences such as i) Only one chamber was used in the previous experiments whereas four chambers are used here which facilitates simultaneous estimation of the effects of different oxygen concentrations on the development of embryos, ii) Zebra fish embryos (48 hpf) were used in the previous experiments to study tumour metastasis (Rouhi *et al.*, 2010) whereas frog embryos at two cell stage (~1.5 hpf) were used here.

3.1.1 Hypoxia Chamber Setup

Hypoxic conditions were created using plastic aquaria chambers. The aquaria are 3 litre plastic tanks (22*15*13 cm). Chambers were thoroughly cleaned and filled with 0.1x MBS buffer filling up 80% volume. A small glass beaker (5*5*5 cm) was placed on one side of the chamber. The purpose of it was to avoid floating of the embryos out of the petri dishes and thus causing damage due to the swirling effect caused by the stirrer. A petri dish was placed on the glass beaker wherein embryos will be placed. Oxygen electrode was introduced near to the glass beaker. On the other end of the chamber, an air stone which is connected to gas tubing was placed. This is important to avoid any hindrance to the mixing stirrer and oxygen measuring probe. A stirrer was fixed approximately at the centre of the chamber with the end of the stirrer reaching the bottom. This also helps to reduce the currents produced by it from reaching the embryos. Once all the components were fixed in the chamber (including the embryos), the chamber was closed using plastic lids. Because of the fact that the purged nitrogen gas introduces pressure and the need for continuous exchange of atmospheric air, a 1-2 cm opening was added to the lid design near the stirrer entry. This setup was repeated with three other chambers. All the chambers including control chamber were placed on a cooling plate which was set to 20°C (Fig.8 and Supplementary Fig.1).

3.1.2 Oxygen regulator setup

The oxygen regulator was a 4-channel oxygen regulator system from Loligo[®] Systems, which can be connected to a PC for continuous monitoring of the experiment. The system consists of an analog data acquisition device (DAQ-M), an analog to digital convertor (AMP DAQ 4), a relay system (solenoid valves) (4X), galvanic cell oxygen probes (4X), tubing and PC software. Before starting the actual experiment, oxygen probes were calibrated according to the manufacturer's instructions.

3.1.3 The Experiment

Eggs were obtained as mentioned in section 3.3.1 Preparation of embryos from *Xenopus laevis*. Embryos were collected at the 2-cell stage. 100 embryos each were placed in five 10 cm petri dishes and the dishes were placed immediately in the chambers (4 in the hypoxia chambers and 1 in the control chamber) on the glass beaker without lids. Required oxygen levels were then selected on the PC interface. Once the values are selected, nitrogen gas is used to regulate the oxygen in the chambers and the readings were recorded every second in an excel file format. A stirrer was also placed in the control chamber to rule out the stirring effect between controls and experimental embryos. By opening a small area of the chamber lid, actual dissolved oxygen concentration was measured in all the chambers using a "Mettler Toledo OptiOx" oxygen measuring device at regular intervals to see the actual dissolved oxygen and to check the

reproducibility of the device. At the same time, 5-10 embryos were taken out of the chamber in a new dish and the respective stages were determined under the microscope and quickly placed back. All the information was documented. When embryos reached desired stages, such as NF stage 30, few embryos were collected, fixed in MEMFA, dehydrated with ethanol and stored at -20°C . The rest were left to grow till further stages and the procedure is repeated until collecting the rest of the embryos at stage 37/38. Further analysis was performed as required.

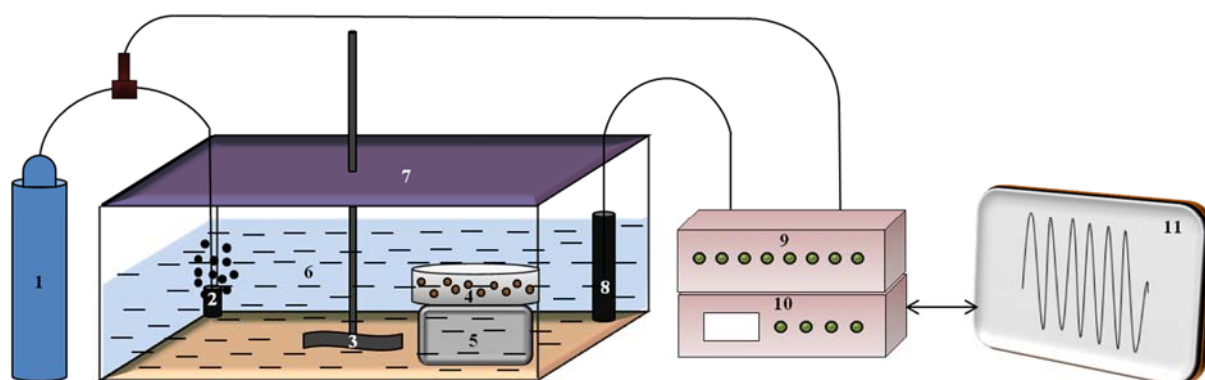


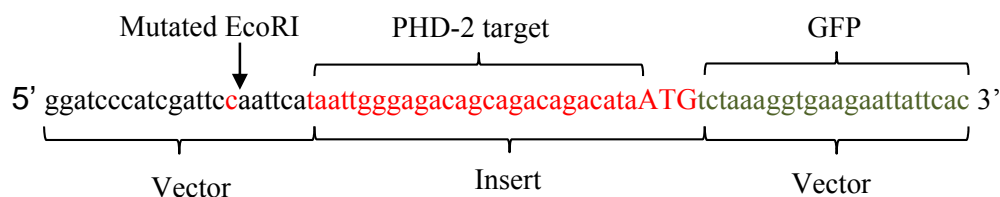
Figure 8: Schematic of hypoxia chamber setup: 1 – Nitrogen gas, 2 – Air stone, 3 – Stirrer, 4 – Embryos, 5 – Glass beaker, 6 – 0.1x MBS buffer, 7 – Lid, 8 – Oxygen probe, 9 & 10 – OXY REG device, 11 – Computer interface.

3.2 Molecular methods

3.2.1 Single Oligonucleotide Mutagenesis and cloning Approach (SOMA)

For determining PHD-2 morpholino specificity, the SOMA method was employed (Pfaffmann *et al.*, 2013). A construct was made, in which the PHD-2 MO target sequence was inserted at the 5'- end of the GFP sequence contained in the vector pTP 218. For the construction a 74 bp long primer was designed consisting of a mutated EcoRI sequence (GAATTC - CAATTC), PHD-2 WT sequence complimentary to PHD-2 MO (red) and a start codon (ATG) after PHD-2 MO target sequence for the translation of following GFP sequence (green).

Primers were phosphorylated at the 5' end. In a 50 μl reaction, 2 μl 100 μM primers, 5 μl 10x T4 polynucleotide kinase buffer, 0.5 μl 100 mM ATP and 1 μl T4 polynucleotide kinase were added to 41.5 μl dH₂O. The reaction mixture was incubated at 37°C for 1 h. To stop the reaction, the mixture was incubated at 65°C for 15 min.



A PCR reaction was carried out in a final volume of 50 μ l. To 23.5 μ l dH₂O, 2.5 μ l phosphorylated primer (100 μ M), 10 μ l NAD⁺ (5 mM), 10 μ l 5x HF buffer, 1 μ l Phusion polymerase, 1 μ l Taq DNA ligase, 1 μ l dNTP mix (10 mM) and 1 μ l template (100 ng) were added, mixed. For the PCR reaction the following cycle conditions were used. Initial denaturation of the DNA template at 95°C for 1 min, followed by 30 cycles of DNA denaturation at 95°C for 1 min, annealing at 55°C for 1 min and extension at 72°C for 4 min, and a final extension at 72°C for 10 min. The template DNA in the PCR mixture was digested for 2 h at 37°C by the addition of 3 μ l DpnI (Fast digest; Fermentas) and 5 μ l 10x Fast digest buffer. Finally, the PCR product was transformed into *E.coli* and colonies were selected on ampicillin containing LB agar plate. For the mutated PHD-2 construct, a primer containing multiple point mutations was designed

3.2.2 Preparation of electro-competent bacteria

A single colony of *E. coli* XL-1 Blue was picked from a LB plate containing tetracycline, inoculated in 3 ml LB medium without antibiotics, and cultured overnight at 37°C with a rotary speed of 220 rpm. This 3 ml bacteria culture was then added to 300 ml LB medium without antibiotics in a 1 l flask, and cultured at 37°C with a rotary speed of 220 rpm for about 3 hrs until the OD 600 reached approximately 0.5. The culture was cooled on ice. Meanwhile, the centrifuge cups, pipets and 1.5 ml eppendorf tubes required for the preparation were all pre-cooled at 4°C. The bacteria were transferred to a pre-cooled centrifuge cup and precipitated by centrifugation at 6,000 rpm for 15 min at 4°C. The supernatant was discarded. The pellet was gently re-suspended in ice cold 10% glycerol (autoclaved) and collected again by centrifugation at 6,000 rpm for 20 min. The washing step with the chilled 10% glycerol was repeated three more times and the pellet was finally re-suspended in 2 ml 10% glycerol. The bacteria were aliquoted in 50 μ l per eppendorf tube on ice and immediately frozen in liquid Nitrogen. Aliquots were stored at -80°C.

3.2.3 Electroporation

2 μ l ligated plasmid was added to 50 μ l electro-competent bacteria (thawed on ice) and gently mixed by tapping. After incubation on ice for 5 min, the cell-DNA mixture was transferred to a chilled 1 mm electroporation cuvette (Equibio, UK) and transferred to an electroporator (Electro Square Porator™ ECM830, BTX). The sample was pulsed once (500 V for 8 msec) and added 600 μ l chilled LB medium to it. After being gently mixed by pipetting, the bacteria were kept on

ice. This 650 μ l bacteria was transferred to a 1.5 ml eppendorf tube and incubated at 37°C for 30 min. A 50 μ l aliquot and the rest were spread on two LB-Amp plates respectively, and incubated overnight at 37°C.

3.2.4 Colony PCR

A single colony was picked with an autoclaved toothpick from a LB-Amp plate and scratched on a fresh LB-Amp plate. The rest of the bacteria on the toothpick were rinsed in 10 μ l ddH₂O. This 10 μ l bacteria suspension was heated at 95°C for 10 min to lyse the bacteria, and 8 μ l of it was used as the template for the colony PCR. A standard 25 μ l colony PCR reaction contained 8 μ l of the template, 1.5 mM MgCl₂, 2.5 μ l *Taq* polymerase buffer (supplied with enzyme, without MgCl₂), 1 μ M each of a forward primer and a reverse primer, 0.1 mM dNTPs and 0.1 μ l *Taq* polymerase (5 u/ μ l, Fermentas). The PCR reaction was run using a thermocycle program with activating the enzyme and denaturing the DNA template at 95°C for 2min, followed by 26 to 30 cycles of DNA denaturation at 95°C for 45 sec, annealing at 55-58°C for 45 sec and extension at 72°C for 45 sec to 2 min according to the length of the PCR product (1kb/1min as recommended by the manufacturer), and the final extension at 72°C for 10 min. The PCR products were analysed on a 1% agarose gel along with 1kb DNA Ladder (Fermentas).

3.2.5 Plasmid mini-preparation

Bacteria were grown in 3 ml LB medium containing appropriate antibiotics overnight at 37°C. 1.5 ml of the bacterial culture was collected in an eppendorf tube and centrifuged at full speed for 30 sec in a bench top centrifuge. The supernatant was removed. The pellet was fully re-suspended in 100 μ l of solution A and incubated on ice for 5 min. 200 μ l of solution B was added, mixed and incubated on ice for 5 min and finally 150 μ l of solution C was added and mixed. After incubation on ice for 5 min, the bacterial lysate was centrifuged at full speed for 10 min at RT. 400 μ l supernatant was put in a fresh 1.5 ml eppendorf tube and plasmid DNA was precipitated by adding 1 ml absolute ethanol. After 5 min incubation at RT, plasmid DNA was pelleted by centrifugation for 3 min at full speed. Ethanol was discarded and the pellet was washed with 500 μ l 70% ethanol. After discarding ethanol, the pellet was air dried and dissolved in 50 μ l TE buffer (pH 7.5) containing RNase A (50 μ g RNase A per ml TE). 1 μ l was taken for restriction analysis (Sambrook *et.al.*, 1989).

3.2.6 Plasmid maxi-preparation

When using the plasmid DNA for quantitatively and qualitatively demanding applications such as *in vitro* transcription, plasmid was extracted using maxi-preparation protocol.

Bacteria were grown in 200 ml LB medium containing appropriate antibiotics overnight at 37°C in a shaker. All the bacterial culture was collected in a 200 ml centrifuge tube and centrifuged at 5000 rpm (Sorvall) for 10 min. The supernatant was discarded and the pellet was re-suspended in 50 ml of solution A and transferred into 50 ml falcon tube. Bacteria was lysed by adding 50 µl Lysozyme (10 mg/ml), mixed and incubated on ice for 10 min. To this, 20 ml of fresh solution B was added, mixed and incubated on ice for 10 min and finally 15 ml of cold solution C was added and mixed. After incubation on ice for 10 min, the bacterial lysate was centrifuged at 5000 rpm for 15 min at 4°C. The lysate was filtered into a fresh 50 ml falcon tube. To the filtered supernatant, 20 ml isopropanol was added, mixed, incubated for 15 min at RT and centrifuged at 5000 rpm for 10 min at 4°C. The supernatant was discarded, the pellet was dissolved in 4 ml dH₂O plus 4 ml 5 M LiCl and incubated on ice for 20 min. The extract was then spun for 10 min at 4000 rpm at 4°C and the supernatant was transferred to a 30ml Corex tube. Plasmid DNA was precipitated by adding 18 ml absolute ethanol and incubated at -20°C for 1 h. Plasmid DNA was pelleted by centrifugation for 10 min at 9000 rpm, 4°C. The supernatant was discarded, the pellet was dissolved in 500 µl TE buffer (pH 7.5) and transferred to a 1.5 ml eppendorf tube. 10 µl RNase A (10 mg/ml) was added and incubated at 60°C for 30 min. Then 10 µl Proteinase K (10 mg/ml) was added and incubated at 37°C for 1 h. The plasmid DNA was extracted using phenol/chloroform. To the extract, 50 µl 3 M sodium acetate (pH 5.2) and 1 ml 100% EtOH was added and incubated overnight at -20°C. On the next day, it was spun at highest speed for 10 min at 4°C and the pellet was washed with 70% EtOH. The pellet was then air dried and dissolved in 200 µl 1x TE (pH 7.5) containing RNase A (50 µg RNase A per ml TE). 1 µl was taken for restriction analysis (Sambrook *et.al.*, 1989).

3.2.7 *In vitro* synthesis of sense RNAs

To prepare synthetic capped RNA, the SP6 mMessage-mMachine™ Kit (Ambion) was used according to the manufacturer's protocol. A 20 µl reaction contains 1-1.5 µg linearized plasmid template, 2 µl 10x reaction buffer, 10 µl 2x NTPs, 2 µl enzyme mix. Transcription was carried out at 37°C for 2.5 hrs. The DNA template was removed by addition of 2 U DNaseI followed by incubation at 37°C for 30 min. The mRNA was purified with the RNeasy Mini Kit (Qiagen) according to the manufacturer's protocol and eluted with 20 µl RNase-free H₂O. The concentration of synthesized RNA was determined using the NanoDrop® Spectrophotometer ND-1000 (peQlab, Germany), and the quality was examined on a 1% agarose gel. The synthesized RNA was stored in aliquots at -20°C.

3.2.8 *In vitro* synthesis of anti-sense RNAs

The preparation of digoxigenin/fluorescein labelled antisense RNA was carried out in a 20 µl reaction mixture containing 1-1.5 µg linearized template plasmid, 4 µl 5x Transcription buffer

(Fermentas), 2 μ l 0.1 M DTT, 0.5 μ l RNase OUT (Invitrogen), 1 μ l RNA polymerase (Fermentas), and 4 μ l Digoxigenin/fluorescein mix (a mix of 10 mM ATP, 10 mM GTP, 10 mM CTP, 6.5 mM UTP, and 3.5 mM Dig-11-UTP/fluorescein, Roche). The reaction mixture was incubated at 37°C for 2.5 hrs, and the DNA template was removed by addition of 2 μ l DNaseI (Fermentas) and the following incubation at 37°C for 30 min. Antisense RNA probes were purified by adding 300 μ l 96% ethanol, 33 μ l 7.5M ammonium acetate and 100 μ l ddH₂O to the mixture. The mixture was incubated for 30 min or overnight at -80°C and centrifuged at 4°C at 15000 rpm for 15 min. The pellet was rehydrated in 100 μ l ddH₂O. The concentration was measured using “Nanodrop”. The purified RNA probe was diluted in hybridization mix at a concentration of 1 μ g/ml and stored at -20°C.

3.2.9 Extraction of the total RNA from staged embryos

10 embryos were collected in a 1.5 ml eppendorf tube and immersed with 500 μ l Trizol. Embryos were then completely homogenized by sequentially passing 10 or more times each through needles with 0.9, 0.7, and 0.4 mm diameter fitted to an RNase-free syringe. To the embryo lysate, 100 μ l chloroform was added and the two-phase mix was vortexed briefly. The lysate was then centrifuged at 10000 rpm at 4°C for 5 min. The upper phase was transferred to a new tube and re-extracted with an equal volume of chloroform, vortexed, spun at 10000 rpm at 4°C for 2 min. The supernatant was transferred to a new tube, mixed with 500 μ l isopropanol, vortexed briefly. The precipitated RNA was isolated by centrifugation at 10000 rpm at 4°C for 5 min. The RNA pellet was washed with 500 μ l 70% ethanol and air-dried. The pellet was re-suspended in RNase free H₂O (50-100 μ l).

3.2.10 Semi-quantitative polymerase chain reactions (SQ-PCR)

The first strand cDNA was synthesized with the Super Script™ II Reverse Transcriptase Kit (Invitrogen) according to the manufacturer’s protocol. 500 ng of total RNA from staged embryos was mixed with 2.5 μ l random hexamer primer (0.2 μ g/ μ l), 2.5 μ l dNTP mix (10 μ M) and filled with H₂O to a volume of 30.5 μ l. After gently mixing and a brief centrifugation step, the mixture was incubated at 65°C for 5 min. Then the mixture was chilled on ice. To the mixture were further added 10 μ l 5x transcription buffer, 5 μ l 0.1M DTT and 2 μ l Ribonuclease Inhibitor (20 u/ μ l). The mixture was gently mixed and incubated at 25°C for 2 min. Finally, 2 μ l Reverse Transcriptase (200 u/ μ l) was added and mixed. This reaction mixture with a final volume of 50 μ l was incubated at 25°C for 10 min followed by 42°C for 50 min and in the end heating to 70°C for 10 min to stop the reaction. A standard 20 μ l PCR reaction contained 1 μ l cDNA obtained from RT reaction, 2 μ l of 10x reaction buffer, 1 μ l of 10 μ M dNTP mix, 0.5 μ l of specific primer mixture (forward and reverse primers, 7.5 μ M for each), 0.3 μ l Taq polymerase (5 u/ μ l, Fermentas), and 14.7 μ l ddH₂O. The PCR program used was as follows:

pre-denaturation at 95 °C for 10 min, 26 cycles (for ODC-1) or 28 cycles (for HIF-1 α eoe1 and VHL eoe2) of denaturation at 94°C for 1 min, annealing at 58°C (for HIF-1 α eoe1) or 56°C (ODC-1) or 50°C (VHL eoe2) for 30 sec and extension at 72 °C for 1 min, followed by final extension at 72 °C for 10 min. 10 μ l of the reaction mix was taken out for analysis. The PCR products were separated on a 1 % agarose gel and photographed with Bio-Rad Gel Doc 2000 (Bio-Rad, USA).

3.3 Handling and manipulation of *Xenopus* embryos

3.3.1 Preparation of embryos from *Xenopus laevis*

One day before egg collection, female albino or pigmented *Xenopus laevis* frogs were primed with 50-100 U of human chorionic gonadotropin (HCG). For induction of full ovulation, 500-1000 U HCG were injected into the dorsal lymph sac of frogs 10 hr prior to egg collection. Eggs were fertilized *in vitro* with minced testes in 0.1x MBS, the protective gel around the embryo was removed with of 2% cysteine hydrochloride (2% L-cystein hydrochloride, pH 7.8-8.0), and cultured in 0.1x MBS. Albino embryos were stained with Nile Blue solution after dejellying. The developmental stage of the embryos was determined according to Nieuwkoop and Faber (Nieuwkoop and Faber, 1967).

3.3.2 Microinjection

Microinjection needles were prepared using borosilicate glass capillaries (Harvard apparatus, UK) on the Narishige PN-30 needle puller (Narishige, Japan). The needles were back-filled using microloaders (Eppendorf). Prior to microinjection, embryos were transferred to 1x MBS and then arranged on a glass slide with a little buffer left. The injection was performed with a pneumatic PicoPump PV820 injector (Helmut Saur Laborbedarf, Germany) on a cooling plate. A volume of 5 nl containing a mixture of the desired synthetic RNAs or morpholino oligonucleotides (MOs) with synthetic EGFP RNA was injected in an animal pole region of the blastomere of embryos at the 2/4-cell stage. After injection, embryos were cultivated in 1x MBS in Petri dishes for 1 hr and then in 0.1x MBS till the embryos reached the desired stages. Embryos were fixed in MEMFA for 30 min - 1h and washed three times for 10 min in PBS. For whole-mount *in situ* hybridization assay, embryos were sufficiently dehydrated with absolute ethanol and stored at -20°C. For pH3 immunostaining (see below), embryos were dehydrated with methanol and stored in Dent's fix (20% DMSO in methanol) at -20°C for at least 24 hrs prior to use.

3.4 Analysis Methods

3.4.1 Whole-mount *in situ* hybridization (WMISH)

The whole-mount *in situ* hybridization was performed according to a three days procedure as described previously (Sive *et al.*, 2000).

Day 1:

Embryos were rehydrated through an ethanol series (75%, 50% in dH₂O and 25% in PTw) for 5 min in each step, followed by intensive washing 4 times with PTw for 5 min. Embryos were then digested with 10 µg/ml Proteinase K (Sigma) in PTw at RT for 10-20 min according to the stage of the embryos. Subsequently, embryos were washed twice with 0.1 M triethanolamine (pH 7.5) for 5 min and acetylated twice by sequentially adding of 12.5 µl acetic anhydrite into the 5 ml embryos incubation tube fully-filled with 0.1 M triethanolamine (pH 7.5) and incubating at RT for 5 min after each addition. After the embryos were washed twice with PTw for 5 min, the embryos were re-fixed with PFA at RT for 20 min. Afterwards, embryos were washed 5 times with PTw for 5 min and rinsed with 1ml mixture of equal volumes of PTw and hybridization mix. After pre-incubation in 500 µl hybridization mix at 65°C for 10 min, the embryos were pre-hybridized in 1 ml hybridization mix at 60°C for 6 hr. Embryos were then hybridized overnight in 1 ml hybridization solution containing the appropriate amount of antisense probe at 60°C.

Day 2:

The probe/hybridization mix was recovered and stored at -20°C for reuse. Embryos were suspended 1 ml hybridization mix and incubated at 60°C for 5 min, washed 3 times in 2x SSC at 60°C for 20 min each time. Non-specifically bound antisense probe was digested by an RNase Mix of 20 µg/ml RNase A and 10 U/ml RNase T1 in 2x SSC at 37°C for 60 min. Embryos were washed once with 2x SSC for 10 min at RT and then washed twice with 0.2x SSC at 60°C for 30 min. The procedure afterwards was performed at RT except specified. After washing twice with 1x MAB for 15 min, embryos were blocked in MAB/BMB for 20 min and then in MAB/BMB/HS for 60 min. Embryos were incubated in MAB/BMB/HS containing 1:3000 diluted anti-Digoxigenin/AP (Roche) (for normal WMISH) / anti-Fluorescent/AP (Roche) (for double WMISH) for 4 hrs. After incubation, embryos were washed 3 times with 1x MAB for 30 min and then overnight at 4°C.

Day 3 (only for double WMISH):

Embryos were washed 2 times with MAB for 30 min and then washed once with dH₂O for 2 min. Embryos were then equilibrated twice in 0.1 M Tris-HCl (pH 8.2) and transferred to staining solution (1 Fast Red tablet/2 ml 0.1 M Tris-HCl pH 8.2) . Staining was carried out at RT in dark. Embryos were then washed once in 0.1 M Tris-HCl (pH 8.2) for 15 min, twice in 1x MAB + 100 mM EDTA for 15 min each. To stop the staining reaction, embryos were incubated in 1x MAB + 100mM EDTA for 10 min at 65°C. Later, embryos were washed once

in 1x MAB and blocked in 1x MAB/BMB for 1 h at RT. Embryos were incubated in MAB/BMB/HS containing 1:3000 diluted anti-Digoxigenin/AP (Roche) for 4 hrs. After incubation, embryos were washed 3 times with MAB for 30 min and then overnight at 4°C.

Day 3/4:

Embryos were washed 2 times with MAB for 30 min and then equilibrated twice in APB for 10 min. After the embryos were transferred to a pre-cooled colour reaction solution (APB containing NBT and BCIP), embryos were incubated on ice in the dark until sufficient staining was reached. Staining reaction was stopped by directly changing the staining solution to 1x MAB for 3-4 times. Embryos were rehydrated through a methanol series (75%, 50% and 25% methanol) for 5 min in each step if necessary to reduce background staining and stored in MEMFA at 4°C.

3.4.2 Whole-mount immunostaining of pH3

Whole-mount pH3 assay was performed according to the protocol as described (Dent *et al.*, 1989) with minor modification. After fixation in MEMFA, embryos were dehydrated through a methanol series (25%, 50%, 75% methanol in dH₂O and 100% methanol) and then transferred to Dent's solution (20% DMSO in methanol, v/v). After Dent's solution was changed twice, embryos were stored at -20°C at least overnight before the procedure was continued. Embryos were rehydrated through a methanol series (100%, 75%, 50% methanol in dH₂O and 25% methanol in PBS, 5 min for each step) followed by washing 3 times with PBS for 5 min. Unspecific binding was blocked by incubation of embryos with 20% horse serum in PBS at RT for 4 hrs. Embryos were incubated overnight with 1 to 200 diluted anti-phosphohistone H3 (anti-pH3, Upstate Biotechnology, USA) in PBS containing 20% horse serum and 5% DMSO at 4°C. On the following day, the antibody solution was recovered, and after the addition of 0.02% Azide it was stored at 4°C for reuse. To remove unbound antibody, embryos underwent intensive washing steps: twice with PBS-TB for 2 hrs, once with PBS-TBN for 2 hrs, 3 times with PBS-TB for 5 min, and then were kept in PBS-TB overnight at 4°C.

The secondary antibody (anti-rabbit/AP, Sigma-Aldrich) was applied at a 1:1000 dilution in PBS containing 20% serum and 5% DMSO. After incubation with the secondary antibody for 5 hrs at RT, embryos were intensively washed twice with PBS-TB for 30 min, once with PBS-TBN for 30 min, 3 times with PBS-TB for 5 min and then kept in PBS-TB overnight at 4°C. The colour reaction was performed as in the whole-mount *in situ* hybridization assay. After equilibrated twice with APB, embryos were incubated in a NBT/BCIP colour reaction solution at 4°C in dark. It took 2 days to reach an intensive staining. The colour reaction was stopped by transferring embryos to 100% methanol, and methanol was changed a few times until the background colour could not be washed off anymore. Embryos were then rehydrated through a methanol series of 75%, 50% and 25% methanol in dH₂O and were stored in MEMFA at 4°C.

4 Results

To investigate the effect of hypoxia on vasculogenesis in *Xenopus laevis*, hypoxic conditions were created using the OXYREG device (see material and methods) and embryos were grown in these hypoxia chambers. Optimizing the operating conditions and setup of hypoxia chambers was done during my master thesis. Using the optimal conditions, Embryos were raised in 8%, 6% and 4% dissolved oxygen concentrations. Embryo viability and developmental profiles were also determined. In brief, results showed reduced embryo viability in all hypoxia conditions compared to controls (Table 3). Developmental time was also increased in embryos raised in hypoxia (Fig.9). As I was interested to study the effect of hypoxia on the formation of a vascular network during embryogenesis, embryos grown under hypoxic conditions were analysed via whole mount *in situ* hybridization against Ami, which is a vascular differentiation marker. Embryos grown in hypoxia showed reduced expression of Ami than normoxia grown embryos (Fig.11 from 8% oxygen to 4% oxygen grown embryos). To quantify the effect of hypoxia on formation of the vascular network, total number of blood vessel branching points were counted. A comparison of the number of branching points in embryos grown under hypoxic and normoxic conditions showed a statistically significant difference in the formation of vascular network (Fig.12 from 8% oxygen to 4% oxygen grown embryos). As embryos grown in hypoxia showed reduced formation of vascular network, the role of PHD-2 (Prolyl-4-hydroxylase-2) was analysed during my master thesis. Performing PHD-2 loss-of-function experiments using morpholino oligonucleotides also interestingly showed reduced formation of blood vessels (Fig.23A and B). As described in the introduction, the general model shows that hypoxic conditions and PHD-2 loss-of-function experiments lead to stabilization of HIF-1 α thereby increasing blood vessel formation. Hence, one would expect an increase in the formation of blood vessels during hypoxia and PHD-2 loss-of-function experiments. However, during my master thesis, the opposite effect was observed, i.e. decreased vessel formation in embryos grown in hypoxia during embryonic development. Therefore, I wanted to investigate the effect of hypoxia during embryonic vasculogenesis and its effect on general embryonic developmental program. Subsequently, I also wanted to investigate the role of HIF pathway during embryonic vasculogenesis. To have an overview about the whole data, results obtained during my master thesis are presented in the following sections wherever necessary together with the data that is obtained in the current study. Data used from my master thesis is as follows

- 1) Embryo viability and development profile of embryos grown in 8%, 6% and 4% oxygen (Table 3 and Fig.9),
- 2) Whole mount *in situ* hybridization against vascular marker Ami and statistical analysis of vascular network of embryos grown in 8%, 6% and 4% oxygen (Fig.11 and Fig.12 from embryos grown in 8%, 6% and 4% oxygen),

- 3) PHD-2 loss-of-function experiments, whole mount *in situ* hybridization against vascular marker *Ami* and statistical analysis of vascular network (Fig.23A and B).

4.1 Hypoxia decreases embryo viability

To investigate the effect of hypoxia on growth and development, embryos were raised in various dissolved oxygen concentrations such as 35% O₂, 25% O₂, 15% O₂, 8% O₂, 6% O₂ and 4% O₂. A control chamber with normal dissolved oxygen was also included. 100 embryos at NF st-2 were placed in each chamber initially. The experiment was started and respective oxygen levels were tightly regulated. Embryos were checked for viability twice a day and dead embryos were sorted out. Embryos were collected at three different stages namely NF st-30, 33 and 37 for further analysis.

At oxygen concentrations between 35% - 15% O₂, embryos developed normally and reduced viability could not be observed. The effect is seen from 8% O₂. Oxygen levels below this point had significant effect on the embryo viability. With reduced concentrations of available oxygen, the viability of the embryos was reduced in a concentration dependant manner. Embryos died at various stages of development. Majority of the embryos did not survive when less oxygen was available at higher stages of their development such as neurula and tailbud stages. Number of embryos that died at various developmental stages are shown in Table 3.

Table 3: Embryo viability: Table shows number of embryos survived at different oxygen conditions. Initially, 100 embryos were placed in each chamber. Embryos were periodically examined for viability. Dead embryos were sorted out at various developmental stages. A higher number of embryos was found to be dead in very low oxygen conditions (6% to 4% O₂). Deaths were more during tailbud stages.

		Controls	35% O ₂	25% O ₂	15% O ₂	8% O ₂	6% O ₂	4% O ₂
Collected	NF st-30	30	30	30	30	30	25	25
	NF st-33	30	30	30	30	30	25	25
	NF st-37	39	39	39	38	35	24	17
Survived		99	99	99	98	95	74	67
Dead	Gastrulation	1	1	1	0	1	5	8
	Neurulation	0	0	0	1	1	9	12
	Tailbud	0	0	0	1	3	12	13
Total		100	100	100	100	100	100	100

4.2 Hypoxia decelerates development

Embryos were exposed to hypoxia starting at NF st-2 (two cell stage). Once the embryos were exposed to hypoxia, their developmental profile was carefully determined and documented. Developmental profiles of the embryos grown in hypoxia chambers were compared to controls. Embryos raised in oxygen levels from 35 - 15% had developmental profile similar to controls.

Development of embryos in 8% O₂ was slowed after they reached tailbud stages. This delay in development was seen from earlier developmental stages with further decreasing oxygen content. Development was unusually slow in 4% O₂. For example, control embryos reached NF st-33 in 51 hours, whereas embryos grown in 4% O₂ reached the same stage in 81 hours. Control embryos reached NF st-37 in 62 hours, whereas embryos grown in 4% O₂ required more than twice the time i.e. 125 hours. Detailed development profiles of embryos grown in various oxygen conditions are shown in the Supplementary Table 1. A graph was plotted showing development profiles of embryos grown in various oxygen conditions (Fig.9). Embryos cultured in 35% - 15% O₂ had similar development profiles as controls (data not shown).

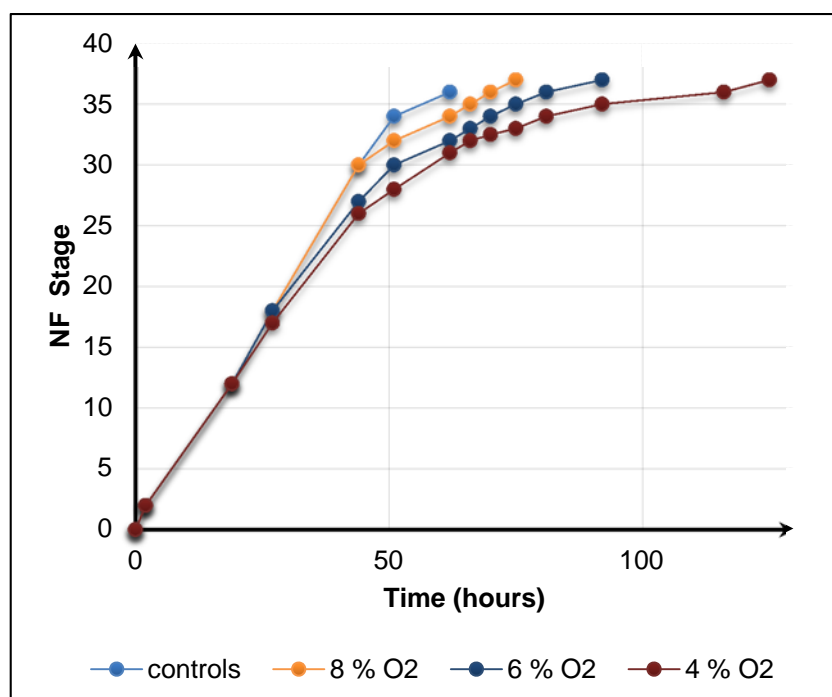


Figure 9: Developmental profile: Graph shows the differential time taken by the embryos raised in various hypoxia chambers against control embryos. Embryos grown in 35 to 15% O₂ had similar developmental profiles compared to controls (data not shown). Effects on development was seen from 8% O₂. Further reduction of oxygen had severe implications on developmental speed. More time was needed by the embryos in 6% and 4% O₂ for their development respectively. All embryos were raised at 20°C.

4.3 Continuous hypoxia affects differentiation and migration of embryonic angioblast precursor cells

As I was interested to see the effect of hypoxia on embryonic vasculogenesis, formation and differentiation of vascular precursor cells and vascular structures was visualized in embryos grown in normoxia and hypoxia. It was shown previously, that ER71 is expressed in the progenitor cells as well as differentiated structures of the vascular system (Neuhaus *et al.*, 2010).

Hence, whole mount *in situ* hybridization (WMISH) was performed against angioblast precursor cells using embryos from different oxygen conditions to see the expression pattern of ER71 in embryos grown in hypoxia. In control embryos, expression of ER71 at NF st-30 could be seen in vitelline veins (VV), posterior cardinal vein (PCV), branchial arches (BA), ventral precursors (VP) and posterior precursors (PP). During this stage, expression of ER71 was seen at the lateral side of the embryo showing the migratory pattern of these cells from ventral blood island (VBI) region to the dorsal and anterior regions of the embryo. At higher developmental stages (NF st-37), less expression of ER71 was seen only in the posterior precursor (PP) area. Therefore, comparison is optimal at NF st-30. In the embryos grown in hypoxia, expression of ER71 was reduced.

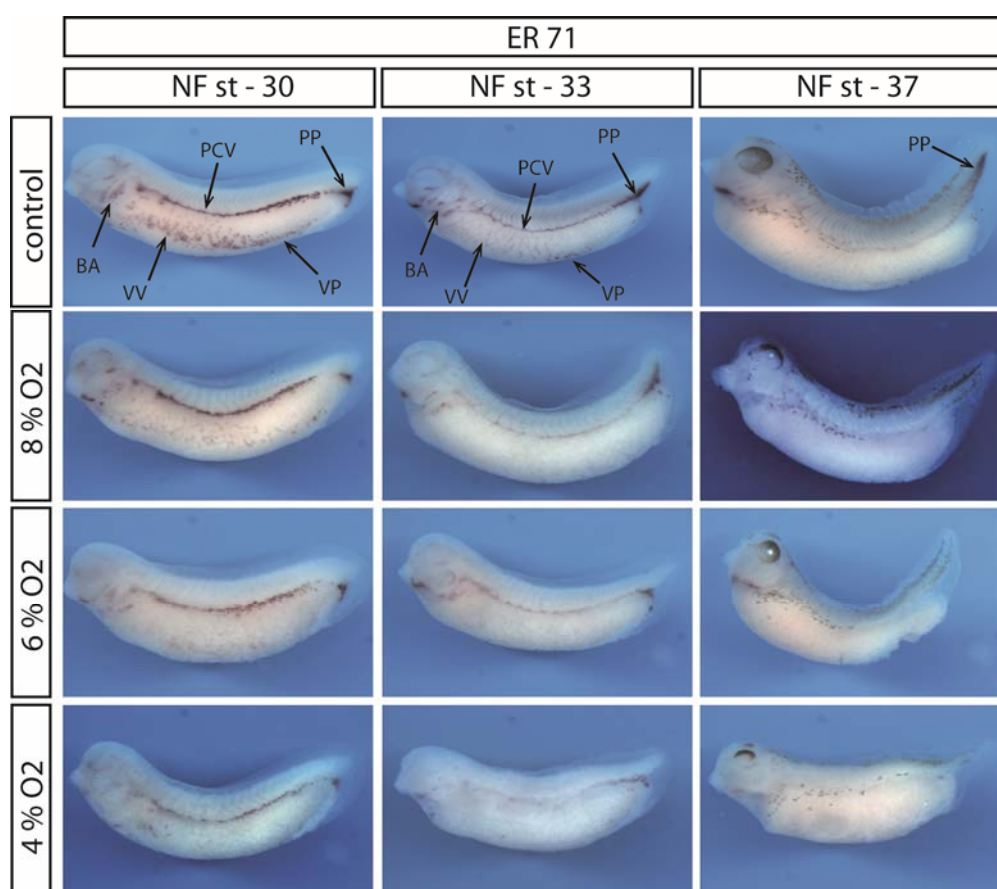


Figure 10: Spatial expression of ER71 in embryos grown in hypoxia. Figure shows WMISH of hypoxia and normoxia grown embryos against ER71. Embryos from all the chambers were analysed at three different stages namely NF st-30, 33 and 37. ER 71 expression was seen in great detail at NF st-30 showing various precursor cells. Notable loss of vitelline veins (VV) and posterior cardinal vein (PCV) could be observed in embryos grown in hypoxia. Complete loss of branchial arches (BA), ventral precursors (VP) and posterior precursors (PP) was seen in very less oxygen conditions such as 4% O₂.

Significant effect was observed in the vitelline veins (VV) precursors. In embryos raised in 4% O₂, the structures expressing ER71 was drastically reduced. Very few cells could be seen. In contrast, expression of ER71 in the branchial arches (BA), ventral precursors (VP) and posterior precursors (PP) was completely absent. However, expression of precursors of posterior cardinal vein (PCV) was strongly reduced. Embryos raised in oxygen conditions other than 4% also showed reduced expression of ER71 when compared to normoxia grown embryos. At higher stages (NF st-37) of development, loss of posterior precursors (PP) was observed even at oxygen levels such as 8% O₂ (Fig.10). In the embryos from all hypoxia conditions examined, more than 90% showed reduced expression of ER71. Supplementary Table 2 shows the total number of embryos which showed reduced ER71 expression in embryos raised in hypoxic conditions.

4.4 Continuous hypoxia hinders embryonic vascular development

As hypoxia had significant effect on the formation of endothelial progenitor cells, I wanted to study the effect of hypoxia on the formation of vascular network. Ami is a differentiation marker that is expressed in the vascular system during development. Embryos were exposed to different hypoxic conditions starting at NF st-2 until NF st-37. It was previously shown that, expression of vascular marker Ami was seen by RT-PCR starting at NF st-16. Whole mount *in situ* hybridization against Ami showed that the expression was confined to heart anlage until NF st-28. From NF st-30, formation of vascular vitelline network (VVN) with blood vessels and branches was seen in the anterior ventral region of the embryo. Further, this primitive vascular vitelline network (VVN) became highly branched and occupied major portion of the embryo in the lateral side by NF st-37 (Inui and Asashima, 2006). Hence, embryos from hypoxia chambers were collected at three different stages as follows, NF st-30, NF st-33 and NF st-37 to analyse the VVN.

In my experiments, control embryos at NF st-30 showed vascular vitelline network (VVN) in the anterior ventral region with few blood vessels and branches. Embryos grown in 35% to 15% O₂ had vascular vitelline network (VVN) similar to that of control embryos. In contrast, embryos grown in 8% O₂ and below revealed significant differences in the formation of vascular vitelline network (VVN). Embryos in 8% O₂ showed a lower number of blood vessels. This difference in the reduction of blood vessels was increased as available oxygen was decreased. The effect was significant in embryos raised in 4% O₂. In this case, embryos showed abnormally low numbers of blood vessels with very few branches. The difference was even stronger at NF st-33 embryos. Embryos raised in low oxygen from 8% to 4% O₂ showed fewer blood vessels as well as branches. In addition, inter-somitic vessel (ISV) formation could be seen in control embryos and embryos grown in hypoxia from 35% to 8% O₂. However, these vessels could not be seen in the embryos raised in 6% to 4% O₂. At NF st-37, in controls, 35% and 15% oxygen raised embryos, vascular vitelline network (VVN) was seen covering the major portion of the ventral side of the embryos with more blood vessels and was highly branched. VVN occupancy and branching were reduced

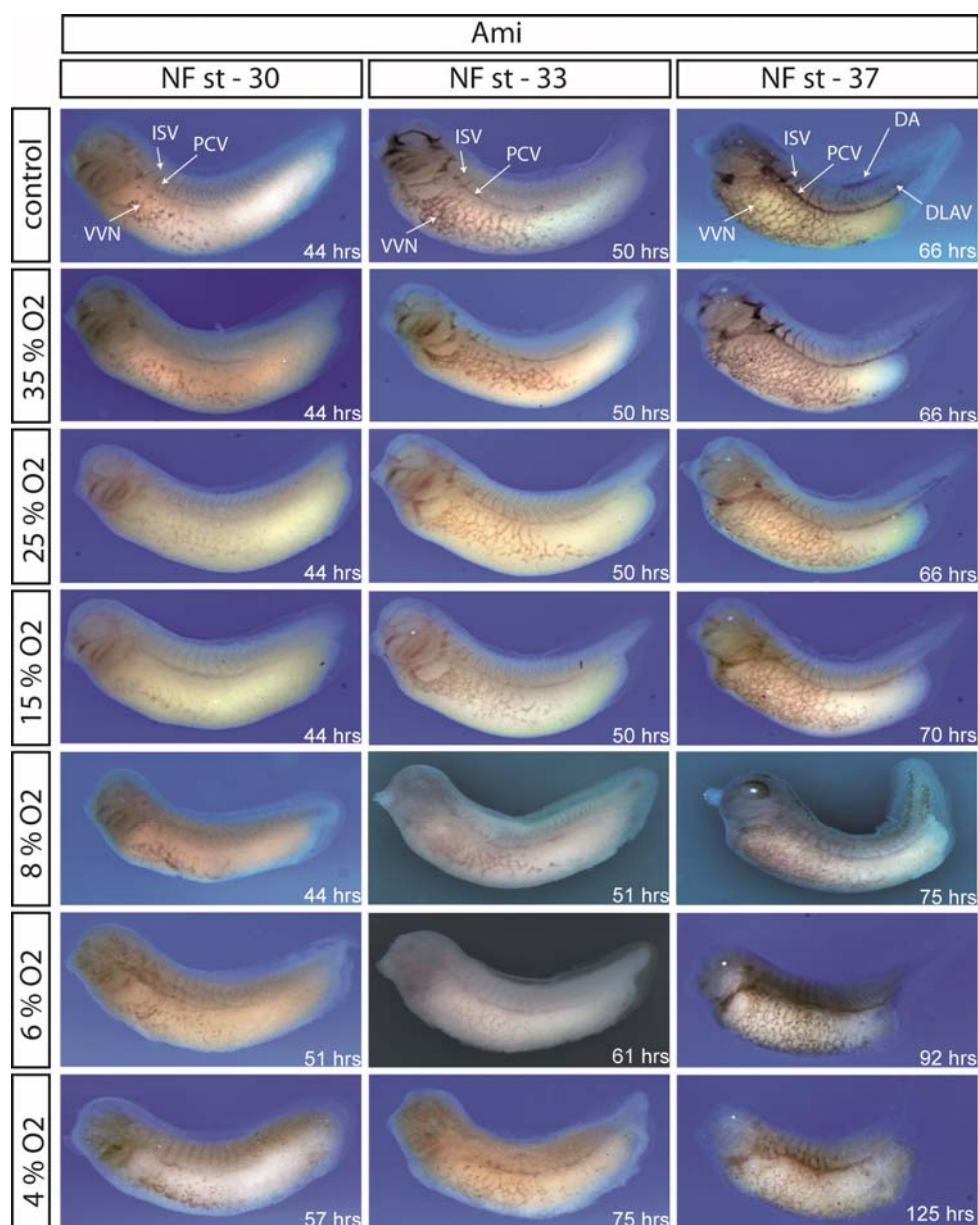


Figure 11: Spatial expression of Ami in embryos grown in hypoxia: Figure shows WMISH of embryos against vascular marker, Ami. Embryos from all chambers were analysed at three different stages namely NF st-30, 33 and 37. Although Ami expression could be seen in the vascular system at NF st-30, it is more pronounced at later stages of development (NF st-37). At NF st-37, details of the vascular system such as vascular vitelline network (VVN), inter-somatic veins (ISV), posterior cardinal vein (PCV), dorsal aorta (DA) and dorsal longitudinal anastomosing vessel (DLAV) could be observed. Loss of formation of VVN could be seen in embryos grown in hypoxia starting from 8% O₂. In these embryos, VVN was formed with reduced numbers of blood vessels and branches. However, Ami expression could be observed in inter-somatic vessels (ISV), posterior cardinal vein (PCV) and dorsal longitudinal anastomosing vessel (DLAV). In contrast, the dorsal aorta (DA) was completely lost regardless of the oxygen content compared to embryos grown in normoxia. Respective developmental time is displayed on each image.

in embryos from 8% to 4% O₂. Formation of the dorsal aorta (DA) and the dorsal longitudinal anastomosing vessel (DLAV) was seen in control embryos. These vessels, though, could not be seen in embryos grown in hypoxia irrespective of the oxygen content at which they were raised. However, inter-somitic vessels (ISV) appear in 6% and 4% O₂ grown embryos (Fig.11).

Difference in the formation of vascular vitelline network (VVN) between embryos grown in normoxia and hypoxia could also be shown by quantifying the vascular vitelline network (VVN). The numbers of branching points, a junction where two or more blood vessels meet at the lateral side of the embryo were determined for this purpose. Five embryos were used for each condition to quantify the vascular vitelline network (VVN). Standard deviation was determined and t-test was performed. Embryos raised from 35% - 15% O₂ had branching points comparable to control embryos. However, as shown in whole mount *in situ* hybridizations, vascular vitelline network (VVN) branches were found to be reduced from 8% O₂. This effect was considerably strong when the available oxygen was reduced further. For example, at NF st-37, embryos grown in normoxia had on average 151 branching points per embryo whereas, embryos grown in 8% O₂ had 112. Furthermore, embryos grown in 4% O₂ had only 50 branching points showing a 66% reduction in the formation of vascular vitelline network (VVN). The significance of these statistics was proved applying a t-test (Fig.12).

Controls and embryos raised in 35%, 25% and 15% oxygen showed reduced expression of Ami in approximately less than or equal to 10% of total embryos in each stage examined. In embryos raised in 8%, 6% and 4% oxygen, more than 90% of all examined embryos showed reduced expression of Ami in each condition. Supplementary Table 3 shows the total number of embryos which showed reduced Ami expression in embryos raised in hypoxic conditions.

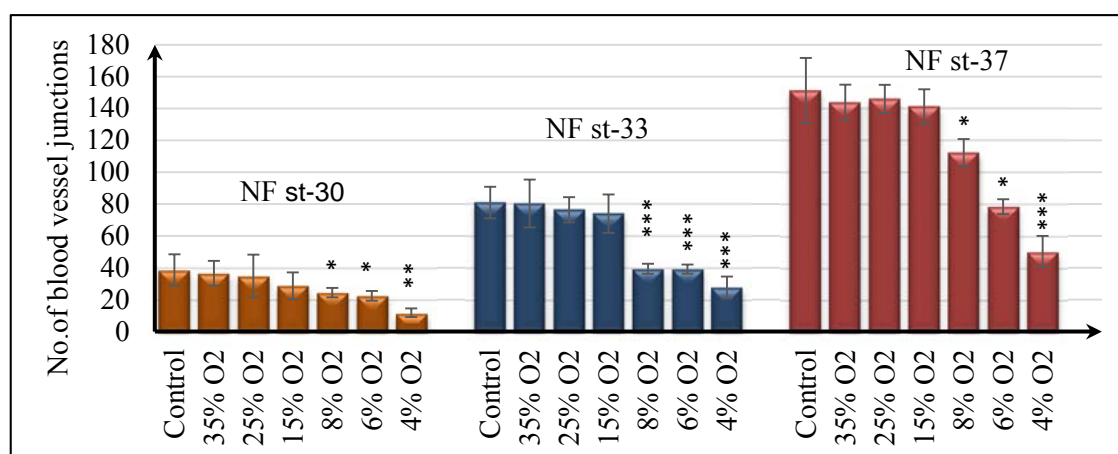


Figure 12: VVN quantification: Bar graph shows the quantification of branching points of the vascular vitelline network (VVN) in embryos grown in hypoxia. Total number of branching points were counted on the lateral side of the embryo. Embryos from all chambers were analysed and quantified at three different stages namely NF st-30, 33 and 37. At any given stage, the total number of branching points was reduced in embryos grown in hypoxia. Mild effects were seen in

35% - 15% O₂. A noticeable reduction in branching was seen until 8% O₂. However, very low oxygen such as 4% O₂ had severe effects on vascular vitelline network (VVN) branching. For example, at NF st-37, controls showed about 151 blood vessel junctions per embryo per side whereas embryos raised in 4% O₂ showed only 50 vascular vitelline network (VVN) junctions. A threefold reduction in branching pattern. Five embryos were used in each case. Averages were calculated and standard deviations were derived. The significance of the results, when I compared embryos grown in hypoxia with control embryos, were determined using a t-test. * shows that the difference in the observations are significant. * corresponds to p-value between 0.05 – 0.005, ** corresponds to p-value between 0.005 – 0.0005 and *** corresponds to p-value <0.0005.

4.5 Hypoxia affects differentiation of myelogenic lineage

Above results suggest that the differentiation of endothelial cells and the formation of a primitive vascular network is hindered by hypoxia. Furthermore, I wanted to investigate if hypoxia also affects hematopoiesis. I performed whole mount *in situ* hybridizations against myelogenic progenitor for embryonic leukocytes, mpo (myeloperoxidase) (Smith *et al.*, 2002) using embryos from 8%, 6% and 4% hypoxia chambers. In embryos grown in normoxia, cells expressing mpo could be seen all over the embryo. During early tailbud stages (NF st-30), these cells originate from the ventral blood island (VBI) region. This can be observed in the ventral view in Fig.13. Cells then migrate from ventral region to the dorsal region of the embryo. At higher stages of development (NF st-37), precursor cells are distributed uniformly throughout the embryo. The number of myelogenic precursor cells was reduced in the ventral blood island (VBI) region of embryos grown in 8% and 6% O₂. The effect became stronger with decreasing available oxygen. A very low number of cells originating in the ventral blood island (VBI) region was seen in embryos raised at 4% O₂. However, the migratory capacity of the remaining cells was not restricted. This suggests that the origin of the precursor cells was strongly affected but not the migration (Fig.13).

Less than 5% of control embryos showed reduced mpo expressing cells. In the embryos from all hypoxia conditions examined, more than 90% showed reduced expression of mpo expressing cells. Supplementary Table 4 shows the total number of embryos which showed reduced mpo expressing cells in embryos raised in hypoxic conditions.

To show the difference in the number of mpo positive cells statistically, the total number of progenitor cells was counted on one side of the embryo. Five embryos were used for each condition and the mean of these values was calculated. Standard deviation points were also calculated and a two tailed t-test was performed confirming the significance of the difference.

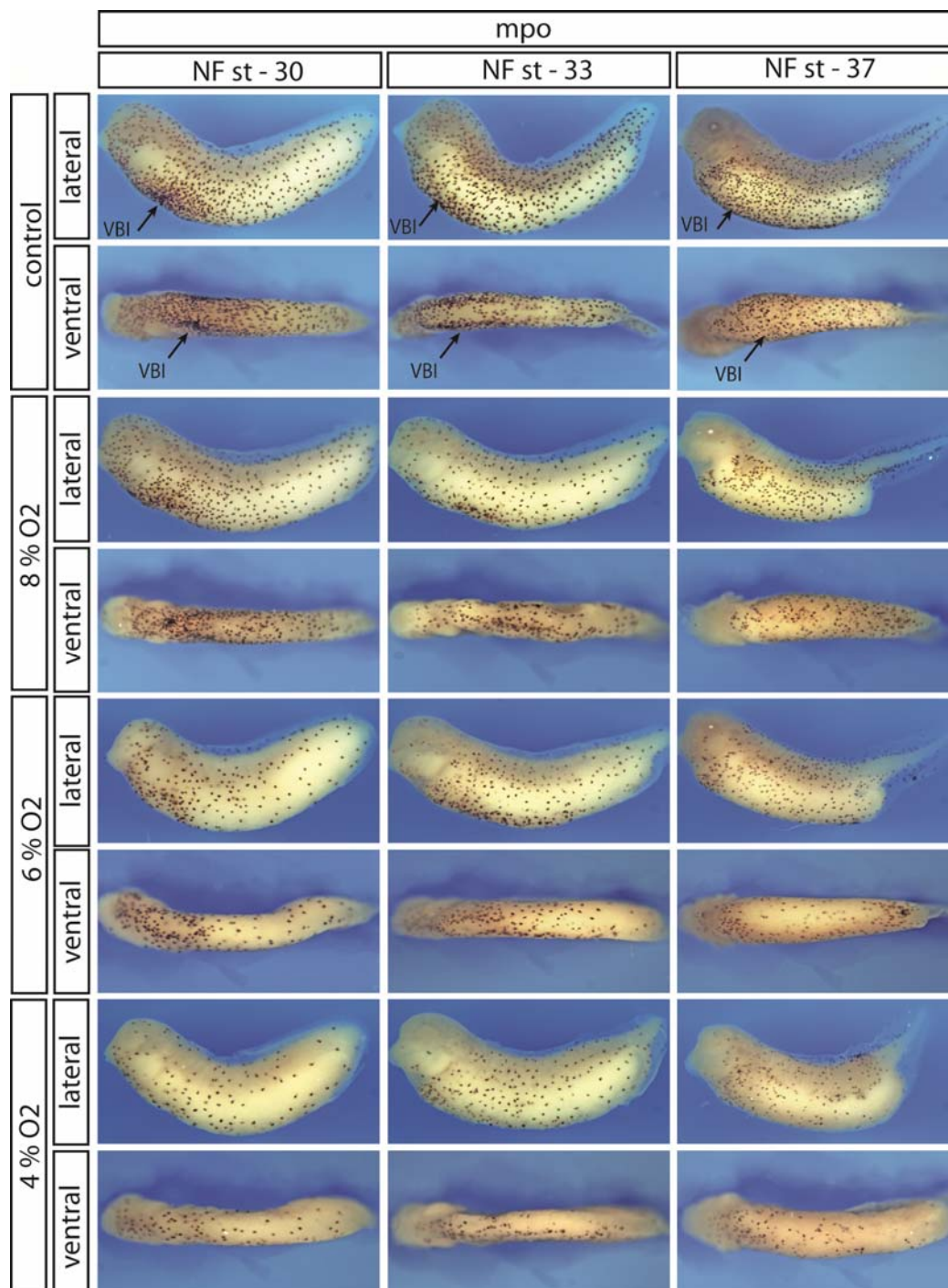


Figure 13: Spatial expression of mpo in embryos grown in hypoxia: Images show myeloid progenitors in embryos grown in normoxia and various embryos grown in hypoxia. mpo expression could be observed in the entire embryo. In embryos grown in normoxia, myeloid precursors were concentrated in the ventral blood island region (VBI). Precursors migrating from VBI were distributed all along the embryo including head, notochord and tail regions. On the other hand, in embryos grown in hypoxia, precursor cells concentrated in the ventral blood island (VBI) region were less in 8%, 6% and 4% O₂. Although very few cells were present altogether, mpo expressing cells were observed throughout the embryo.

Fewer cells could be seen in embryos grown in hypoxia compared to embryos grown in normoxia at every developmental stage examined. Difference in the total number of cells expressing mpo was higher when embryos were raised in lower oxygen content. Significant difference could be seen from 8% O₂. At NF st-30, controls had on average, 466 mpo positive cells. These numbers decreased drastically with increasing hypoxic conditions. In 4% O₂ grown embryos, only 173 mpo expressing cells were present caused by a 2.7 fold reduction in mpo progenitor proliferation. At NF st-37, 825 mpo expressing cells could be counted on one side of embryos grown in normoxia. Even 8% O₂ had a significant effect on the proliferation of mpo progenitors. It showed only 485 cells per embryo/side. The difference is severe in 4% O₂. In 4% O₂, only 259 mpo cells could be observed, making a twofold reduction (Fig.14). Hence, it can be suggested that hypoxia affects proliferation of myelogenic precursors.

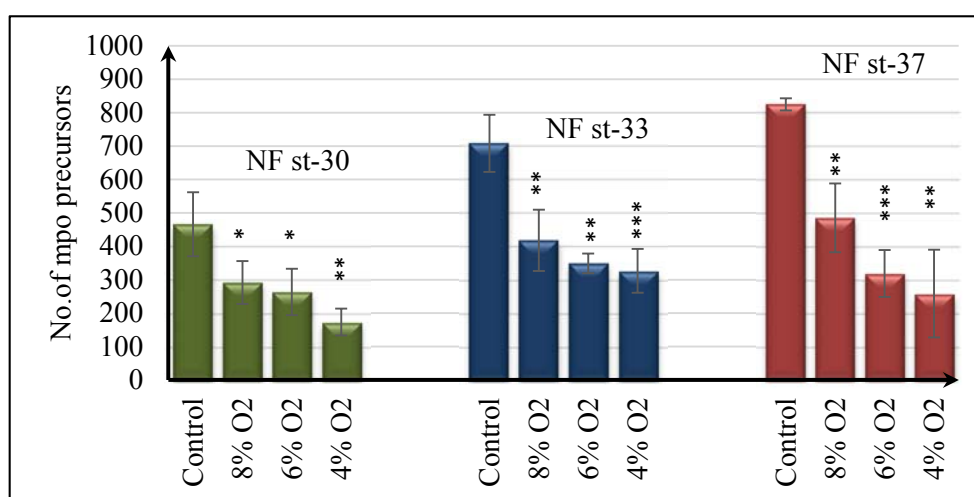


Figure 14: Quantification of mpo progenitor cells: Bar graph shows the quantification of mpo progenitor cells in embryos grown in hypoxia. Total number of progenitor cells were determined on the lateral side of the embryo. Embryos from all chambers were analysed at three different stages namely NF st-30, 33 and 37. At any given stage, the total number of mpo precursors was drastically reduced in embryos grown in hypoxia. 4% O₂ had severe effect on the proliferation of mpo progenitor cells. For example, at NF st-37, controls showed about 825 cells per embryo per side whereas embryos grown in 4% O₂ showed only 259 mpo cells. A twofold reduction in differentiation was observed. Five embryos were used in each case. Averages were calculated and standard deviations were derived. Significance of the results from embryos grown in hypoxia were determined against embryos grown in normoxia using t-test. The significance of the results, when I compared embryos grown in hypoxia with control embryos, were determined using a t-test. * shows that the difference in the observations are significant. * corresponds to p-value between 0.05 – 0.005, ** corresponds to p-value between 0.005 – 0.0005 and *** corresponds to p-value <0.0005.

4.6 Hypoxia affects differentiation and migration of erythropoietic precursors

As seen in the previous sections, hypoxia affected the formation of vascular network, and myelogenic precursors. Hence, I wanted to see the effect of hypoxia on the erythropoiesis. Whole mount *in situ* hybridizations were performed on erythropoietic precursors to examine the effect of hypoxia on these precursors. Two different erythropoietic markers were chosen for this investigation namely lmo-2 and β -globin. lmo-2 is a precursor marker for erythropoietic lineage and β -globin is a marker for mature erythrocytes. Hence, these two were chosen to observe the effect of hypoxic conditions on erythropoiesis.

Expression of lmo-2 can be seen in the anterior and posterior ventral blood island (VBI) area, in the posterior cardinal vein (PCV), in the tail region at NF st-30 and in branchial arches (BA) at NF st-33 and 37 in embryos grown normoxia. In embryos grown in hypoxia, lmo-2 expression remained undistinguishable in the ventral blood island (VBI) region, posterior cardinal vein (PCV) and tail region. The expression pattern was the same at NF st-33. However, expression in branchial arches (BA) was lost in embryos grown in hypoxia. A significant effect was observed at higher stages of development. At NF st-37, reduced lmo-2 expression was observed in the ventral blood island (VBI) area and complete loss of expression in the branchial arches (BA) region of embryos grown in 4% O₂ (Fig.15).

At NF st-30, expression of β -globin was undistinguishable over wide range of oxygen levels. Even at 4% O₂ at NF st-30, no noticeable effects on the differentiation of β -globin could be observed. The expression can be clearly seen in ventral view. Difference in β -globin expression was not noticeable even at NF st-33. At NF st-37, differences in β -globin expression was noticeable in embryos grown under low oxygen conditions. Loss of β -globin expression was observed in the ventral blood island (VBI) region at any observed hypoxic condition. At this stage, β -globin expression could be seen in the anterior head region, in the posterior cardinal vein (PCV) and in the tail region in the embryos grown in normoxia. In low oxygen conditions like 6% and 4% O₂, structures expressing β -globin were distributed or drastically reduced in the head area and completely absent in the posterior cardinal vein (PCV) and tail region (Fig.16). Hence, it can be suggested that hypoxia affects the differentiation of erythropoietic precursors. The effect could be observed at higher stages of development (NF st-37).

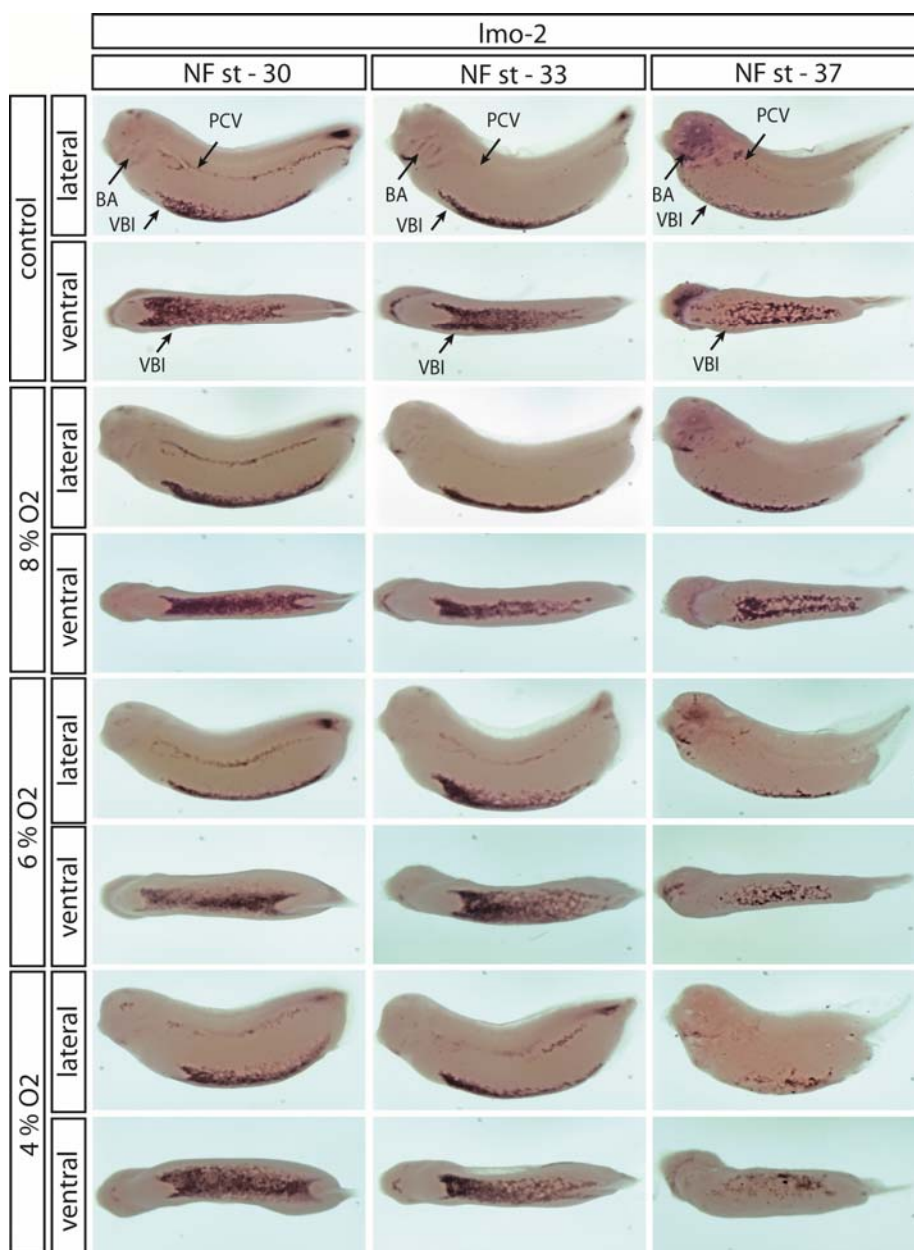


Figure 15: Spatial expression of lmo-2 in embryos grown in hypoxia: Images show structures expressing lmo-2 in various embryos grown in hypoxia. In embryos grown in normoxia, strong expression of lmo-2 was seen in the ventral blood island (VBI) region (see ventral view) as well as in the posterior cardinal vein (PCV), tail region at NF st-30 and 33 and branchial arches (BA) at NF st-33 and 37. Strong expression was observed in the head region of the embryo at NF st-37. In embryos grown in hypoxia, lmo-2 expression was undistinguishable in most of the hypoxic conditions examined such as 8%, 6% and 4% O₂ in ventral blood island (VBI), posterior cardinal vein (PCV) and tail regions at NF st-30 and 33. At NF st-37, significant effect was observed in the expression of lmo-2. Loss of structures expressing lmo-2 were reduced in the ventral blood island (VBI) region as well as in the branchial arches (BA) and head region.

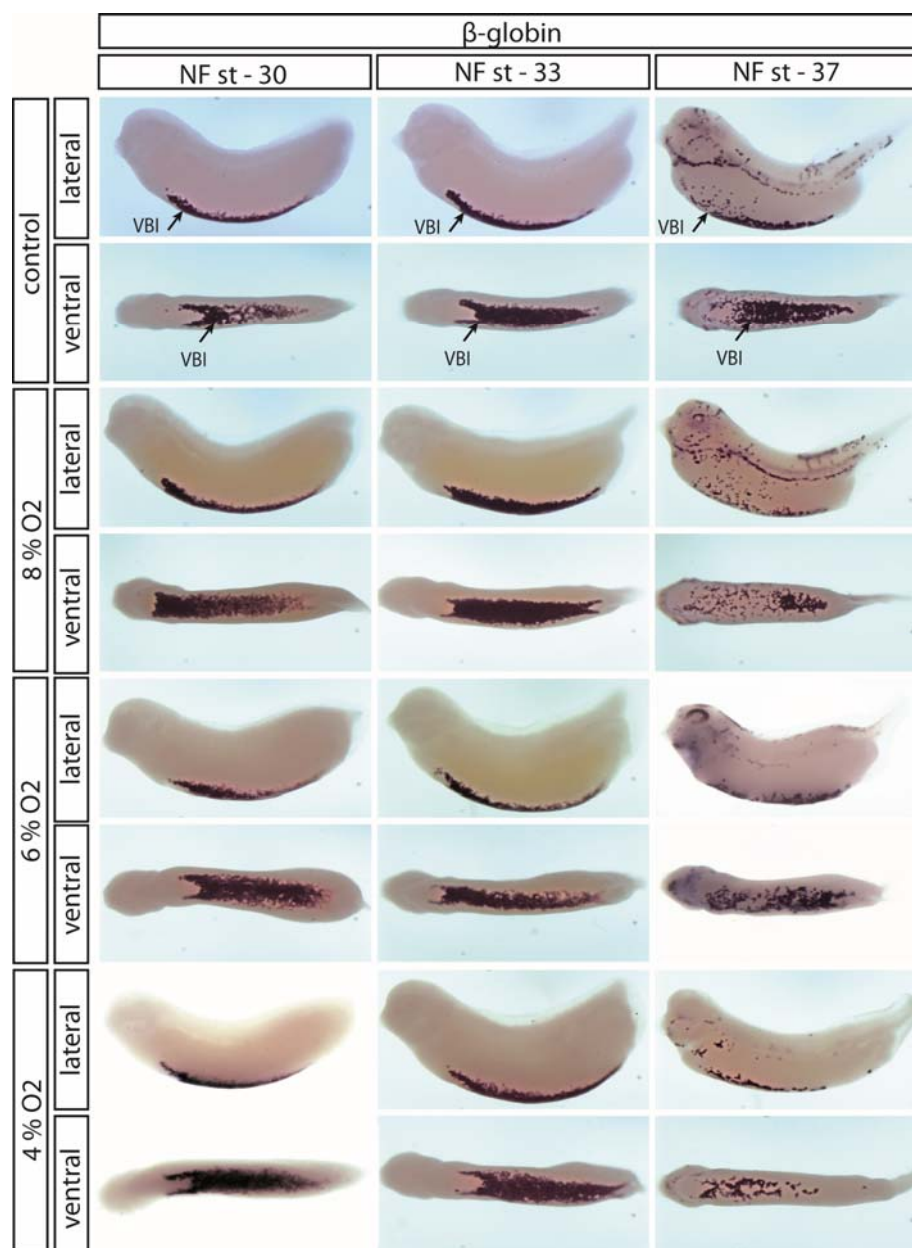


Figure 16: Spatial expression of β -globin in embryos grown in hypoxia: Images show structures expressing β -globin in various embryos grown in hypoxia. In embryos grown in normoxia, expression of β -globin was seen in the ventral blood island (VBI) region. The expression is clearly seen in a ventral view. At NF st-37, precursor cells were found in the head and tail regions of the embryo which migrated from ventral blood island (VBI) region. In embryos grown in hypoxia, β -globin expression was constant in most of the hypoxic conditions observed like 8% 6% and 4% O₂ at NF st-30 and 33. However, at NF st-37, significant effect was observed in differentiation as well as migration of precursor cells as reduced and absence of expression could be seen in other parts of the embryo, except in the ventral blood island (VBI) region.

Controls showed reduced expression of lmo-2 and β -globin in less than 5% of total embryos in each stage examined. In embryos raised in 8%, 6% and 4% oxygen, majority of the embryos showed almost normal expression at NF st-30 and 33. However, many embryos showed reduced

expression of lmo-2 and β -globin at NF st-37. Supplementary Table 5 and 6 show the total number of embryos which showed reduced lmo-2 and β -globin expression in embryos raised in hypoxic conditions.

4.7 Hypoxia limits active division of cells

Embryos grown in hypoxic conditions developed slower than embryos grown under normoxic conditions (see section 4.2). To analyse whether hypoxia affects cell division, the number of actively dividing cells in hypoxia raised embryos was analysed via proliferation assay also called pH3 assay (Phospho-Histone H3). In control embryos, dividing cells were observed throughout the embryo. More cells were concentrated in the head region. In contrast to this, in embryos grown in hypoxia, less dividing cells were observed. In embryos grown in 8% O₂, although cells were distributed all along the embryo, fewer cells were found throughout the embryo. At lower oxygen concentrations such as 6% and 4% O₂, lower numbers of actively dividing cells were present in the embryo showing empty spaces where no actively dividing cells could be seen. At 4% O₂, only very few cells showed active cell division (Fig.17).

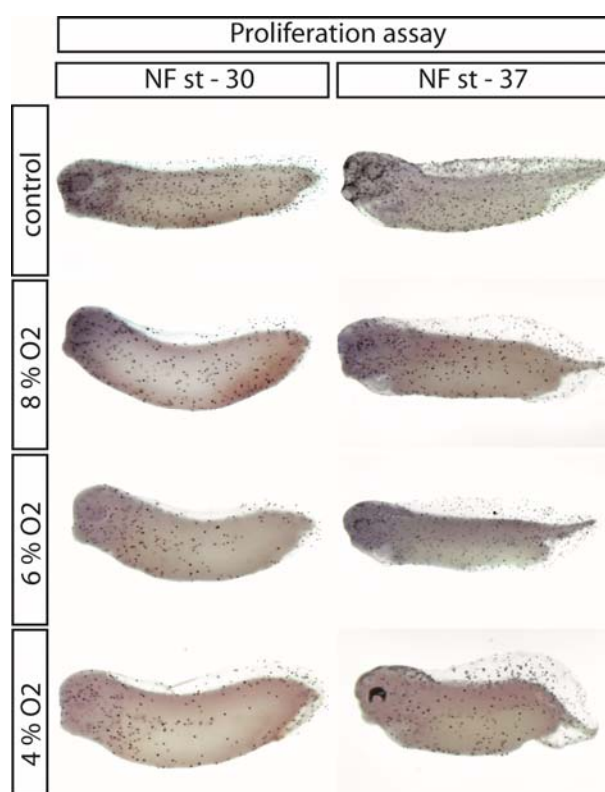


Figure 17: Proliferation (pH3) assay of embryos grown in hypoxia: pH3 assay was performed on embryos grown in hypoxia to visualize actively dividing cells in the embryos during development. Control embryos showed more number of cells distributed in the embryo. In hypoxia raised embryos, dividing cells were reduced significantly. In conditions with very less oxygen such as 4% and 2%, severe effect was found on cell division. Very few cells were found in these cases dispersed in the embryos.

The number of actively dividing cells was quantified in embryos obtained from each condition. Total number of cells were counted on one side of the embryo. Five embryos were for each condition. Averages were calculated and standard deviation values were derived. Significance of the results was tested using t-test. On average, at NF st-30, wild type embryos showed 802 dividing cells. In contrast, embryos grown in hypoxia displayed much lower numbers of dividing cells. In embryos grown in 8% O₂ 394 dividing cells could be detected and in embryos grown in 6% O₂ 374 dividing cells could be detected. At very low levels of available oxygen, very few cells were found as observed in embryos grown in 4% O₂ (285). Embryos grown in 4% O₂ showed approximately three times less actively dividing cells compared to embryos grown in normoxia (Fig.18).

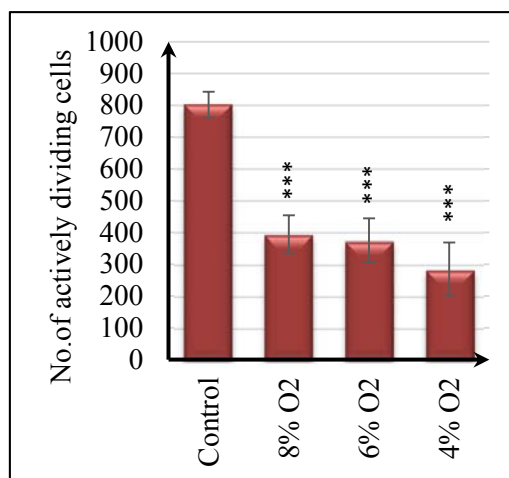


Figure 18: Quantification of proliferating cells in embryos grown in hypoxia: Actively dividing cells were quantified in embryos raised in various oxygen conditions. Embryos grown in normoxia showed more number of cells (802) that were dividing. Hypoxia had significantly affected the cell division in the embryos. Embryos grown in hypoxia displayed very few proliferating cells. Average number of proliferating cells in embryos grown in hypoxia are, 8% O₂ - 394, 6% O₂ - 374 and 4% O₂ - 285. Proliferation was severely affected in 4% O₂ wherein only approximately two fifths of the total number of proliferating cells were observed compared to embryos grown in normoxia. t-test show that the quantitative differences were statistically significant. Proliferating cells were quantified using NF st-30 embryos. The significance of the results when I compared embryos grown in hypoxia with control embryos were determined using a t-test. * shows that the difference in the observations are significant. * corresponds to p-value between 0.05 – 0.005, ** corresponds to p-value between 0.005 – 0.0005 and *** corresponds to p-value <0.0005.

In the embryos from all hypoxia conditions examined, 100% showed reduced number of dividing cells when compared to control embryos. Supplementary Table 7 shows the total number of embryos which showed reduced number of dividing cells in embryos raised in hypoxic conditions.

4.8 The general developmental program is unaffected by hypoxia

The analysis of development of the vascular system under hypoxic condition showed that hypoxia affects the differentiation and migration of vascular structures as shown by the expression of ER71 and Ami thereby hindering the formation of a complete vascular network. However, influences of hypoxia on hematopoietic differentiation was limited. Effect on the differentiation of myelogenic (mpo) precursor cells was substantial but the effect was weak on the differentiation of erythropoietic (β -globin and lmo-2) precursors. In this context, it is interesting to examine if hypoxia also affects the expression of mesodermal and neural developmental markers. Hence, mesodermal and neural developmental markers in contrast to vascular marker were examined in the double WMISH of embryos grown in normoxia and hypoxia.

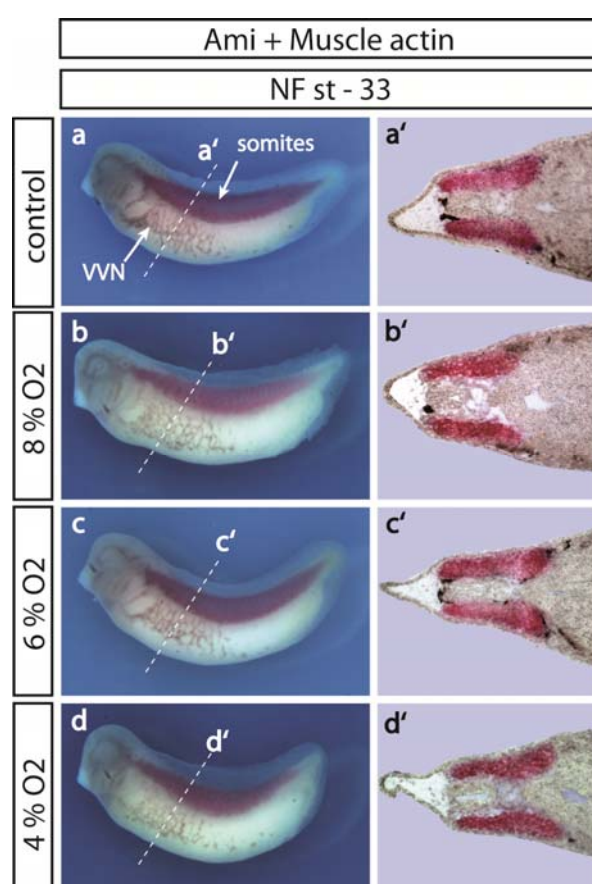


Figure 19: Spatial expression of Ami and muscle actin in embryos grown in hypoxia: Expression of vascular marker Ami (digoxigenin tagged) was analysed simultaneously with mesodermal marker muscle actin (fluorescein tagged) in embryos grown in hypoxia via WMISH. Ami expression was reduced when available oxygen was low as seen in the previous experiments. Fewer blood vessel branches were found in embryos grown in hypoxia compared to controls. Expression of muscle actin was not affected regardless of the hypoxic conditions they were raised in. Expression of muscle actin is observed in the somites in the sections of the embryos.

To show the difference in the expression of different genes simultaneously in the same embryo, WMISH was performed to detect the vascular marker Ami together with the mesodermal marker muscle actin and Ami together with the neural marker n-tubulin. WMISH against vascular marker Ami was performed using digoxigenin labelled probe and mesodermal marker muscle actin and neural marker n-tubulin with fluorescein tagged probes using embryos grown in normoxia and 8%, 6% and 4% O₂ at NF st-33. Muscle actin is expressed in the somitic mesoderm, whereas n-tubulin is expressed from fore brain region and extends to the neural tube, running along the length of the embryo. Images are shown in Fig.19 and Fig.20. In Fig.19, spatial expression pattern of Ami and muscle actin can be seen. Expression of Ami was consistent with the previous results as it was reduced with reducing available oxygen from 8% O₂ to 4%O₂. Expression of muscle actin was found to be mostly unchanged in all embryos. Embryos grown in various conditions were sectioned to observe the expression of muscle actin in the embryos. Sections of the embryos are shown in Fig.19 a', b', c' and d'. Expression of muscle actin in the somites was almost undistinguishable in embryos raised in normoxia and 8%, 6% and 4% oxygen.

At 8% and 6% oxygen, 100% and 97% embryos showed similar expression of muscle actin and reduced expression of Ami when compared to controls respectively. At 4% oxygen, 83% of total embryos examined showed similar expression of muscle actin and reduced expression of Ami when compared to controls. Supplementary Table 8 shows the total number of embryos which showed normal expression of muscle actin and reduced expression of Ami in embryos raised in 8%, 6% and 4% hypoxia.

Expression of Ami with n-tubulin was visualised in Fig.20. Steady with the previous results, Ami expression was found decreasing as the available oxygen was decreased. Embryos grown in various conditions were sectioned to observe the expression of n-tubulin in the embryos. Sections of the embryos are shown in Fig.20 a' & a'', b' & b'', c' & c'' and d' & d''. Expression of n-tubulin in the rhombencephalon, brachial nerves and neural tube was similar in embryos raised in 8%, 6% and 4% oxygen when compared to control embryo. This shows that hypoxia does not affect the formation of somites and neural tube during early embryonic development.

89% of control embryos showed normal n-tubulin expression and normal Ami expression. At 8% and 6% oxygen, 86% and 78% embryos showed similar expression of n-tubulin and reduced expression of Ami when compared to controls respectively. At 4% oxygen, 75% of total embryos examined showed similar expression of n-tubulin and reduced expression of Ami when compared to controls. Supplementary Table 9 shows the total number of embryos which showed normal expression of n-tubulin and reduced expression of Ami in embryos raised in hypoxia.

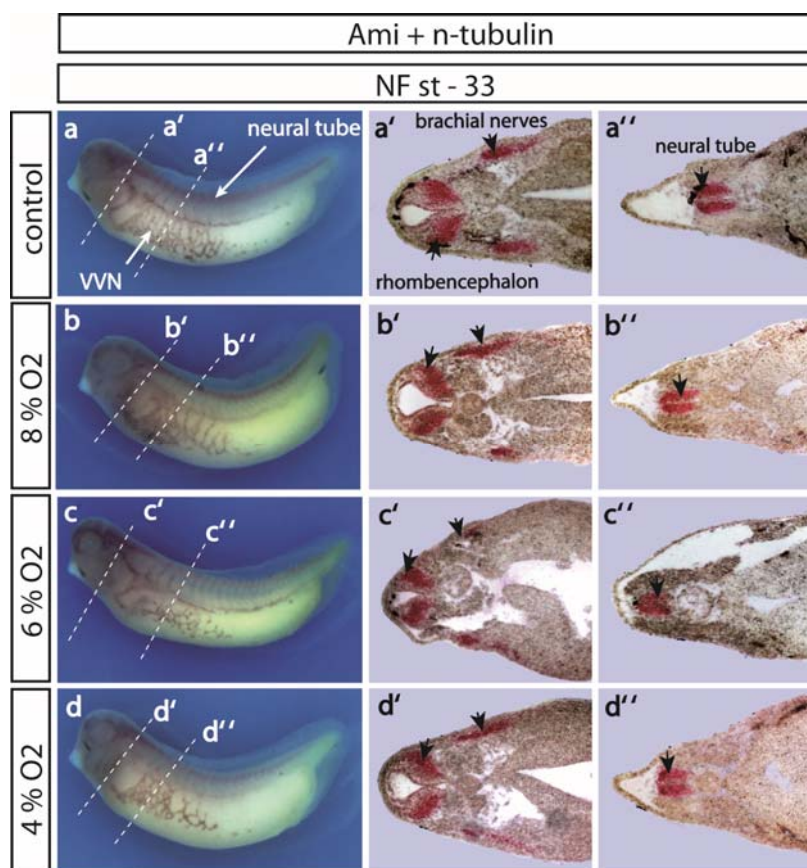


Figure 20: Spatial expression of Ami and n-tubulin in embryos grown in hypoxia: Expression of vascular marker Ami (digoxigenin tagged) was analysed simultaneously with neural marker n-tubulin (fluorescein tagged) in embryos grown in hypoxia via WMISH. Ami expression was reduced when available oxygen was low. Fewer blood vessel branches were found in embryos grown in hypoxia compared to controls. Expression of n-tubulin was not affected regardless of the hypoxic conditions they were raised. Expression of n-tubulin could be observed in brachial nerves, rhombencephalon and neural tube in the sections of the embryos.

4.9 PHD-2 morpholino acts specifically

It was previously shown that PHD-2 function is dependent on the oxygen availability in the cell (Kaelin and Ratcliffe, 2008). During hypoxia, PHD-2 activity is limited by low levels of oxygen leading to the stabilization of HIF-1 α . Stabilization of HIF-1 α in the cell leads to transcriptional activation of several genes to compensate for reduced oxygen availability. Therefore, I wanted to perform PHD-2 loss-of-function experiments using antisense oligonucleotides to block PHD-2 translation and observe the formation of vascular network and expression of hematopoietic genes such as mpo, lmo-2 and β -globin.

To determine the specificity of the morpholino used, a plasmid construct containing only PHD-2 wild type (WT) sequence which is complementary to the morpholino was coupled to EGFP sequence as a reporter. Synthetic mRNA was produced *in vitro*. When this mRNA will be co-injected along with PHD-2 morpholino, PHD-2 morpholino binds to PHD-2 WT sequence present

in the synthetic PHD-2 mRNA thereby arresting the translation of EGFP sequence. In the other side of the embryo, only PHD-2 WT + EGFP mRNA will be injected. Because of the absence of PHD-2 morpholino, EGFP will be translated and signal will be observed in this side of the embryo (Fig.21A).

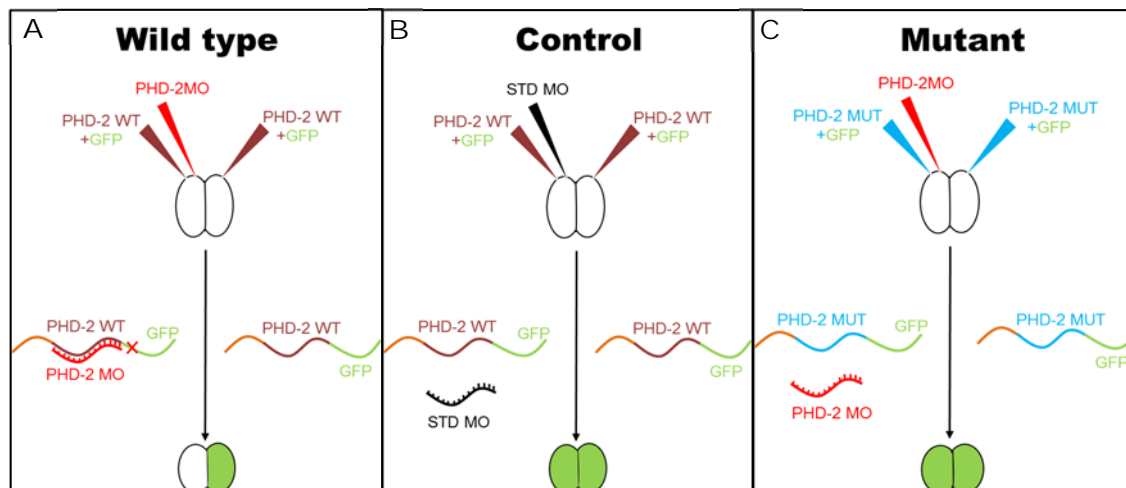


Figure 21: Schematics of PHD-2 MO specificity determination: Prior to *in vivo* experiments, two constructs were made. The first construct consists of PHD-2 WT (wild type) sequence complementary to the PHD-2 MO (morpholino) coupled to EGFP. In a second, construct, named PHD-2 MUT, the same PHD-2 WT sequence was mutated at multiple bases to reduce complementarity to PHD-2 MO. This was also coupled to EGFP coding sequence. **A)** PHD-2 WT-EGFP mRNA was co-injected with PHD-2 MO into one cell and PHD-2 WT-EGFP mRNA alone into the other cell of a two cell stage embryo. Sequence complementarity between PHD-2 WT sequence and PHD-2 MO blocks GFP translation therefore no green signal will be observed. On the other hand, in the other cell, PHD-2 WT + GFP will be translated into functional GFP thereby showing green signal when observed under UV light. **B)** Similar experimental procedures were followed as performed in the above experiment by substituting PHD-2 MO with STD/control MO. Having highly randomized sequence, STD MO cannot bind to PHD-2 WT sequence thereby allows formation of functional GFP protein. Hence, in this case, GFP signal is observed in both sides of the embryo. **C)** In one side, PHD-2 MUT (mutated version of PHD-2 sequence) + EGFP will co-injected with PHD-2 MO, in the other only PHD-2 MUT + GFP. Because of the dissimilarities between PHD-2 MUT and PHD-2 MO sequences, PHD-2 MO cannot bind to PHD-2 MUT thereby allowing translation of EGFP. Also in this case, GFP signal will be observed in both sides of the embryo.

As control, control/standard morpholino (random sequence morpholino) can be injected instead of PHD-2 morpholino. With the sequence being highly dissimilar, control morpholino could not bind to PHD-2 WT sequence leading to translation of EGFP and the fluorescent green signal will be observed (Fig.21B). To test the specificity of the morpholino, a construct with a PHD-2 sequence mutated at multiple sites (PHD-2 MUT) was made, which does not allow PHD-2 morpholino to bind. Injection of this construct also leads to the expression of GFP (Fig.21C). Microinjections were performed using the constructs described above. Statistics are shown in Table 4. Comparing the number of embryos showing signal in PHD-2 WT EGFP + PHD-2 MO against PHD-2 WT EGFP + Control MO and PHD-2 MUT EGFP + PHD-2 MO suggests that PHD-2 morpholino acts specifically as intended.

Table 4: PHD-2 MO specificity statistics: Microinjections were performed as stated in previous section and embryos expressing GFP signal on single side or both sides were calculated respectively. Boxes filled with green colour are the embryos of interest. Experiment was performed twice.

	PHD-2 WT EGFP + PHD-2 MO	PHD-2 WT EGFP + Control MO	PHD-2 MUT EGFP + PHD-2 MO
Signal on one side	168 (97.1%)	3 (8.4%)	37 (60.7%)
Signal on both sides	5 (2.9%)	33 (91.6%)	24 (39.3%)
Total	173	36	61

Embryos were injected with 500 pg PHD-2 WT EGFP synthetic mRNA + 0.5 pmol PHD-2 MO in one side and only 500 pg PHD-2 WT EGFP synthetic mRNA in the other side when embryos were at two cell stage. In the PHD-2 WT EGFP synthetic mRNA + PHD-2 MO injected side, no GFP signal was observed. This is because, PHD-2 MO binds to PHD-2 WT sequence and blocks the translation of EGFP. In the other side of the embryo, PHD-2 WT EGFP is translated showing green fluorescent signal when observed under UV light. See Fig.22A and B. As a control experiment, embryos were injected with 500 pg PHD-2 WT EGFP + 0.5 pmol Control MO in one side and only 500 pg PHD-2 WT EGFP synthetic mRNA in the other side. Control MO has a highly random sequence and cannot bind to PHD-2 WT sequence. This allows translation of EGFP sequence. Hence, GFP signal was observed in both sides of the embryo (Fig.22C and D). In addition to this control experiment, another control experiment was also performed by injecting the mutated PHD-2 sequence. 500 pg PHD-2 MUT EGFP + 0.5 pmol PHD-2 MO was injected in one side and only 500 pg PHD-2 MUT EGFP synthetic mRNA in the other side. As PHD-2 morpholino does not bind to mutated PHD-2 sequence, GFP signal was observed in both sides of the embryo (Fig.22E and F). All embryos were screened for GFP signal at NF st-24 and the results suggest that PHD-2 MO acts specifically.

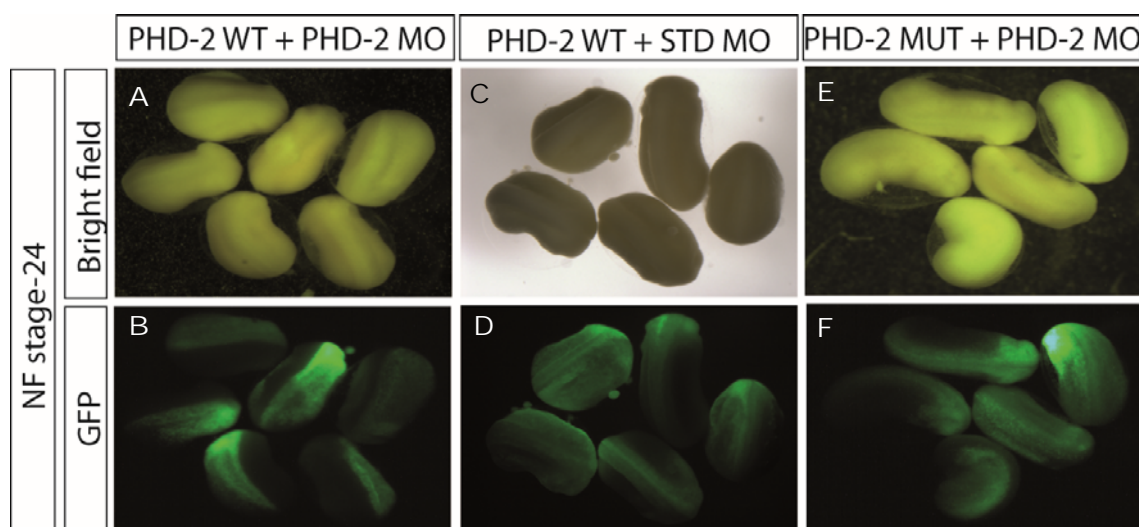


Figure 22: PHD-2 MO specificity: After microinjections, embryos were raised until NF st-24 and examined for GFP signal. Images in the top row show embryos captured in bright light and in the bottom using GFP filter. **A)** Embryos showed GFP signal in PHD-2 WT + EGFP injected side while no signal was observed in PHD-2 WT + EGFP and PHD-2 MO injected side. **B)** GFP signal was observed in both sides of the embryo, in PHD-2 WT + EGFP and STD MO injected side as well as PHD-2 WT + EGFP injected side. **C)** GFP signal was observed in both sides of the embryo i.e. PHD-2 MUT + EGFP and PHD-2 MO injected side as well as PHD-2 MUT + EGFP injected side.

4.10 PHD-2 loss-of-function reduces vascular network formation

During my master thesis, I have shown that PHD-2 loss-of-function reduces Ami expression in the injected side of the embryo. In the injected side, VVN was highly reduced. Fewer blood vessels were observed with irregular pattern and less number of branches. ISV could not be observed. However, PCV was observed in the un-injected side (Fig.23A). Quantifying vascular vitelline network (VVN) by counting the number of branching points showed significant difference between un-injected and injected sides. On average, un-injected side had 98 branching points whereas injected side showed less than 36 branching points, ~2.5 fold overall reduction. Five embryos were used for statistics and significance of the results were determined using t-test (Fig.23B). The total number of embryos showing the reduced vascular network phenotype is shown in Supplementary Table 10.

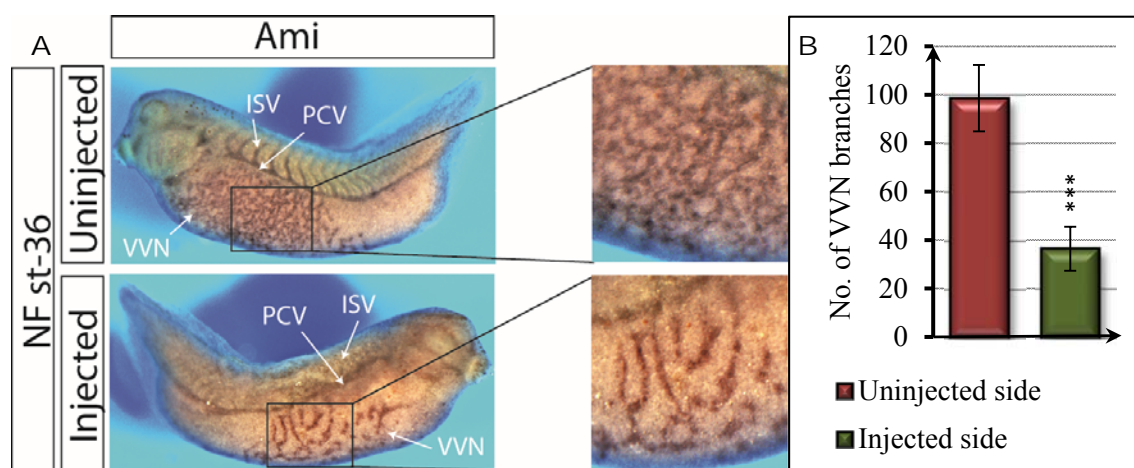


Figure 23: A) Spatial expression of *Ami* in PHD-2 loss-of-function embryos: PHD-2 MO was injected into one cell of a two celled embryo. Embryos were grown until NF st-36 and performed WMISH against vascular marker, *Ami*. Un-injected side showed compact, elaborate VVN with several branches. Presence of ISV and PCV was evident. In contrast, on the injected side, VVN was irregular with very few branches and blood vessels. Although PCV could be observed, ISV were completely absent. **B) PHD-2 MO loss-of-function VVN quantification:** Total number of branching points in the un-injected side were counted and compared to branching points in the injected side. PHD-2 knock-down showed significant loss in the formation of VVN. Un-injected side showed 98 branching points whereas injected side showed only 36. Five embryos were used in each case for VVN quantification. Averages were calculated and standard deviation was derived. The significance of the results when I compared un-injected side to injected side was determined using a t-test. * shows that the difference in the observations are significant. * corresponds to p-value between 0.05 - 0.005, ** corresponds to p-value between 0.005 - 0.0005 and *** corresponds to p-value <0.0005.

PHD-2 knock-down lead to a phenotype that was also observed in hypoxia embryos. In both hypoxia experiments and PHD-2 loss-of-function experiments, formation of VVN was affected in similar ways. Reduced branches and absence of ISV were prevalent. Further, I wanted to inhibit the function of PHD-2 using a chemical substance to confirm that reduction of vascular structures is due to the loss of PHD-2. Previous studies showed that Dimethylloxallyl Glycine (DMOG) is an effective PHD-2 inhibitor (Bruick *et al.*, 2001; Ivan *et al.*, 2001; Jaakkola *et al.*, 2001). Embryos were treated with 1.0 mM DMOG starting at NF st-12. DMOG was replaced twice a day from the stock until the embryos reached tadpole stages (NF st-35/36). Control embryos were treated with the same amount of ethanol that was used to dissolve 1 mM DMOG. Control embryos were harvested at NF st-36. However, after NF st-35/36, DMOG treated embryos did not develop further. Although further development was ceased, embryos were found to be alive even after 48 hours at the same stage. Interestingly, embryos developed normally, but the posterior end was shorter. This kind of phenotype was also observed in hypoxia grown embryos. Performing

WMISH using these embryos against vascular marker Ami revealed similar results as seen in hypoxia grown embryos as well as in PHD-2 loss-of-function experiments. Few blood vessels were observed in the lateral side of the embryo. Improper formation of blood vessels was also observed. ISV could not be seen completely. PCV was observed (Fig.24A). 20 embryos were treated with DMOG. Analysing embryonic vasculogenesis of all the embryos showed significant loss of VVN. Reduced VVN was reduced in all embryos (Fig.24B). Total number of embryos showed reduced VVN phenotype is showed in Supplementary Table 11.

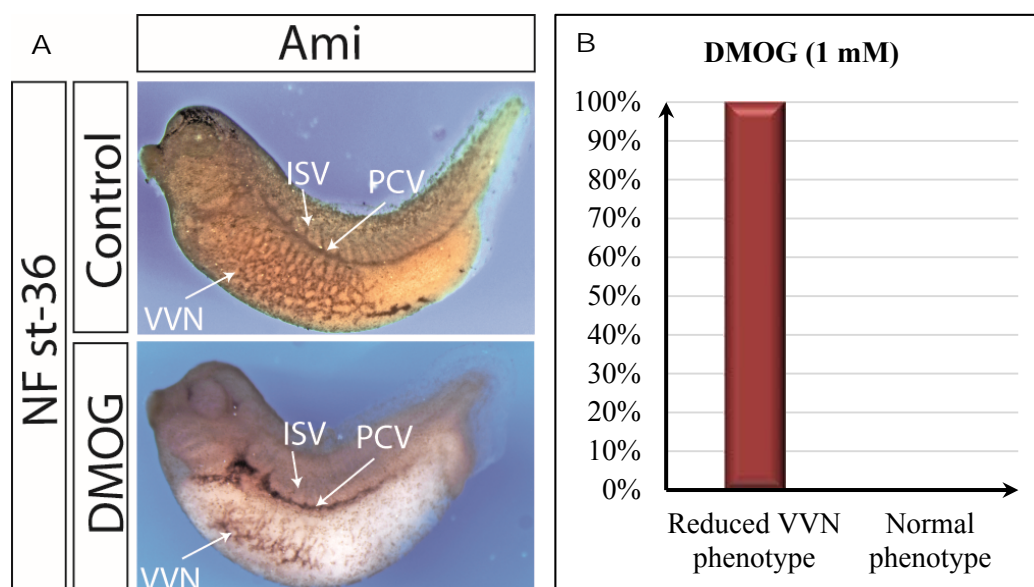


Figure 24: A) Spatial expression of Ami in DMOG treated embryos: Embryos were treated with 1.0 mM DMOG (Dimethylloxallyl Glycine) starting at NF st-12. Buffer containing freshly added DMOG was replaced twice a day until embryos reach NF st-36. After NF st-36, DMOG treated embryos did not develop further for 48 hours but were found alive. Embryos were collected at this point and the vascular network was analysed. Un-treated embryos showed normal VVN with several branches and also ISV and PCV. On the other hand, DMOG treated embryos showed significantly less formed VVN. Blood vessels did not form properly. Fewer branches were seen. ISV were completely absent though PCV presence was evident. **B) PHD-2 chemical inhibition statistics:** 20 embryos were treated with 1.0 mM DMOG. Analysis of VVN using WMISH revealed that all treated embryos had reduced VVN phenotype.

4.11 PHD-2 loss-of-function phenotype can be rescued

To check if the reduced vascular structures caused by PHD-2 loss-of-function can be rescued, functional PHD-2 mRNA, which could not bind to the morpholino, was co-injected together with PHD-2 morpholinos. Co-injecting functional mRNA with morpholino would recover the loss-of-function effects caused by the morpholino alone as the mRNA is translated into functional protein of the respective gene. If the PHD-2 loss-of-function phenotype will be rescued, then it can be suggested that the effects observed in PHD-2 loss-of-function experiments are not off-target

effects. Therefore, complete ORF of PHD-2 was cloned and transcribed *in vitro*. 0.5 pmol PHD-2 MO was co-injected with ~500 pg PHD-2 mRNA in one cell of a two cell stage embryo. Xurbo GFP was used as a lineage tracer. Embryos were sorted out according to the GFP signal, raised until NF st-37 and harvested. Performing WMISH against vascular marker Ami revealed normal vascular network formation in both injected as well as non-injected sides of the embryos. VVN was distributed to a greater extent in the lateral sides. Both sides showed blood vessels with several branches. Expression of Ami in the ISV and PCV were also seen normal (Fig.25). 80% of the total experimental embryos showed rescue of the VVN network as shown in Supplementary Table 12.

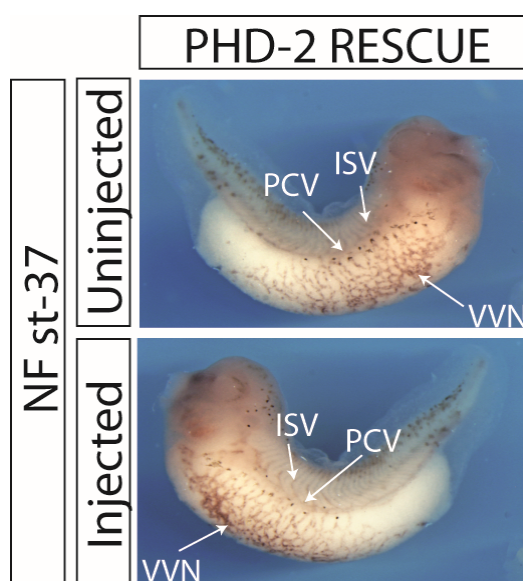


Figure 25: Spatial expression of Ami in PHD-2 rescued embryos: PHD-2 MO was co-injected with functional PHD-2 mRNA into one cell in a two celled embryo. Embryos were raised until NF st-37 and collected. Performing WMISH against Ami showed normal VVN formation in both sides of the embryo. Elaborated VVN was found along with ISV and PCV in the injected side as well. GFP was used to trace the injected side.

4.12 PHD-2 loss-of-function reduces myeloid progenitor formation

As the results of PHD-2 loss-of-function experiments were consistent with the results of the hypoxia experiments with respect to development of vascular network, it was of great interest to investigate the expression of marker genes that were examined in hypoxia grown embryos. First, WMISH was performed against myeloid precursor cells (mpo). Expression of mpo was observed in the injected side as well as in the non-injected side of the embryo. In the non-injected side, mpo cells were observed to be concentrated at the anterior-ventral side, which is called the ventral blood island (VBI) region. In the injected side, fewer cells were observed to be concentrated at the VBI region. However, general migration of mpo expressing cells was not affected, since mpo expressing cells were distributed along the embryo in the non-injected and the injected side

(Fig.26A). Quantifying mpo precursor cells showed less mpo expressing cells in the injected side compared to control side. Five embryos were used for quantification. On average, 700 mpo precursor cells were observed in the control side and 593 in the injected side. Although fewer cells were found in this case, the effect was not as strong as seen in hypoxia grown embryos (Fig.26B). Total number of embryos that showed reduced mpo expression are shown in Supplementary Table 13.

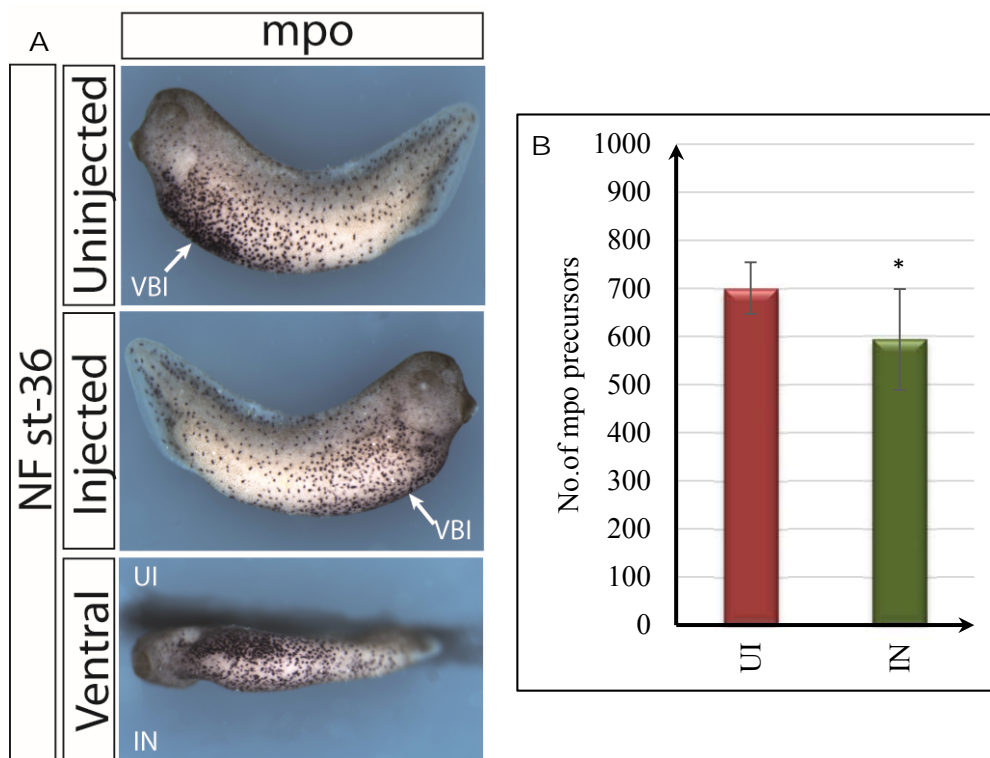


Figure 26: A) Spatial expression of mpo in PHD-2 loss-of-function embryos: PHD-2 MO was injected into one cell of a two cell embryo. Embryos were cultured until NF st-36 and WMISH was performed to detect myeloid precursor cells by analysing mpo expression. Un-injected side (UI) showed mpo expression all over the embryo. However, majority of the expression was observed in the ventral blood island (VBI) region. Although mpo expression was seen all over the embryo in the injected side (IN), VBI region showed fewer cells compared to un-injected side. **B) Quantification of mpo expressing cells in PHD-2 loss-of-function embryos:** Quantification of the total number of precursor cells showed that the injected side had fewer cells compared to control side. On average, 700 mpo expressing cells were found in the un-injected side and 593 cells were found in the injected side. Five embryos were used for quantification. Average and standard deviation were calculated and significance was determined using t-test.

4.13 PHD-2 loss-of-function does not affect erythroid precursor differentiation

WMISH was performed against two erythroid markers namely β -globin and lmo-2 as used in the hypoxia embryos. Careful examination showed no significant difference in the expression of either of these markers in the injected side compared to control side. Expression of lmo-2 is

restricted to the ventral blood island (VBI) region and branchial arches (BA) and expression of β -globin is restricted to the ventral blood island region (VBI). Expression could be observed clearly in the ventral view (Fig.27A and B). On both sides of the embryo, expression of β -globin and *lmo-2* markers was unaltered. Total number of embryos showing normal phenotype are showed in Supplementary Table 14 and 15 respectively.

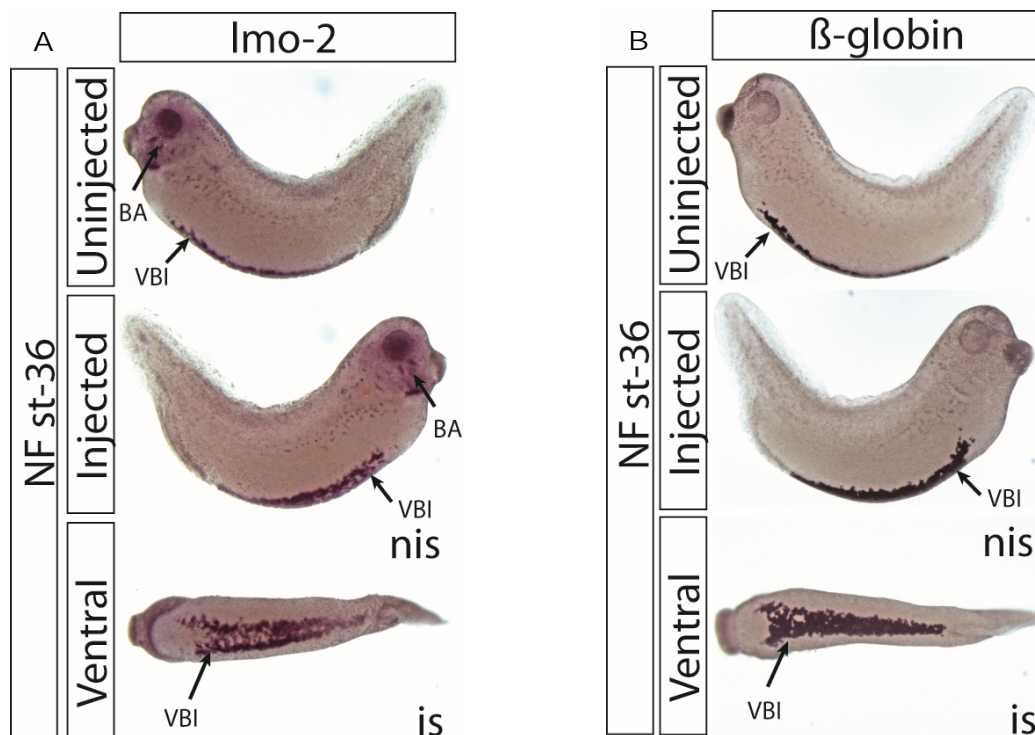


Figure 27: A) Spatial expression of *lmo-2* in PHD-2 loss-of-function embryos: PHD-2 MO was injected into one cell of a two cell embryo. Embryos were cultured until NF st-36 and performed WMISH against *lmo-2*. Careful examination showed that PHD-2 MO did not affect *lmo-2* expression. Similar expression was observed on both sides, the injected and the control side. **B) Spatial expression of β -globin in PHD-2 loss-of-function embryos:** PHD-2 loss-of-function also did not affect β -globin expression. No significant difference could be noted in the expression pattern between injected and un-injected side.

4.14 Loss of PHD-2 alone is sufficient to affect VVN formation

Several prolyl-4-hydroxylases (PHDs⁷) are discovered so far, but the roles of PHD-1, 2 and 3 are widely studied. Most studies suggest that PHD-2 is the major regulator of the HIF's during endothelial differentiation. Therefore, I investigated the role of PHD-2 in my experiments first. Results showed that its function is of high importance during embryonic vasculogenesis. Hence, I wanted to examine the importance of the other two PHD's, PHD-1 and 3. 1.25 pmol PHD-1 Mo and 1.25 pmol of PHD-3 MO were injected into one cell of a two cell stage embryo respectively. Xurbo GFP was co-injected to trace the injected side. Embryos were raised until tadpole stage (NF st-37) and harvested. Using these embryos, WHISH was carried out against vascular marker

Ami to visualize the vascular vitelline network (VVN). The images are shown in Fig.28A and B. In general, no significant loss of vascular structures was seen in either of the morpholino injected embryos. Hence, this study suggests that loss of PHD-2 alone is sufficient to affect embryonic vasculogenesis, PHD-1 and PHD-3 loss alone does not have significant effect on vascular vitelline network (VVN) formation. Number of embryos showing normal phenotype are shown in Supplementary Table 16 and 17 respectively.

000

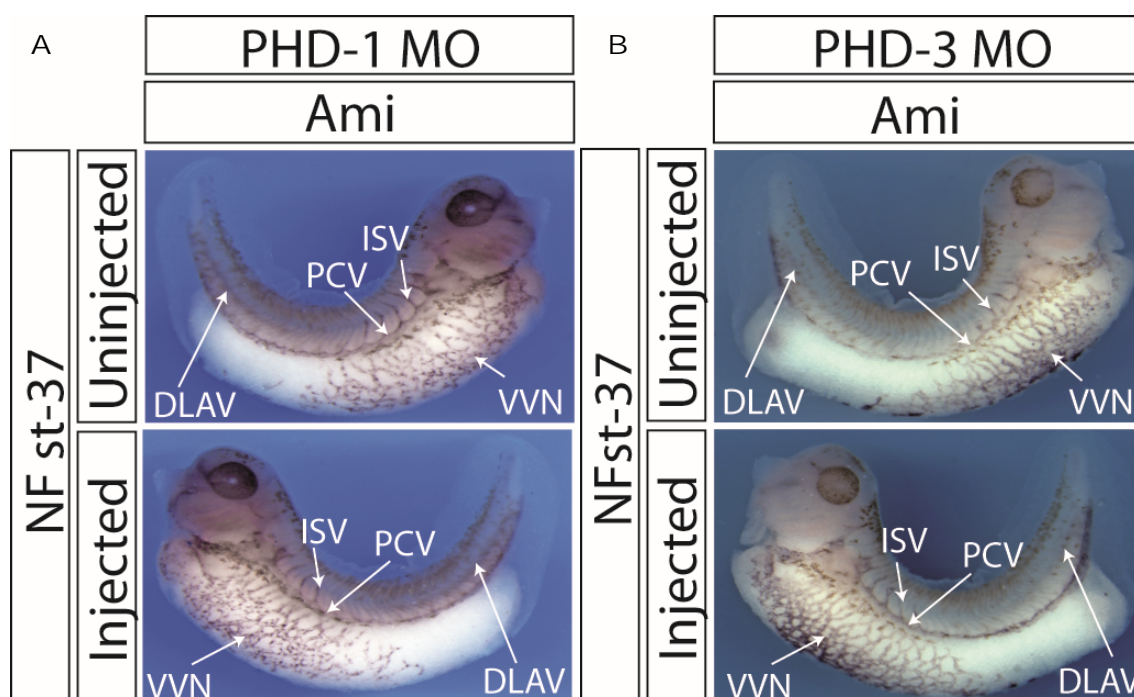


Figure 28: A) Spatial expression of Ami in PHD-1 loss-of-function embryos: PHD-1 MO was injected into one cell of a two cell stage embryo. Embryos were sorted according to GFP signal and collected at NF st-37 for vascular vitelline network (VVN) analysis. Expression of Ami was found to be normal in un-injected as well as injected side. Vascular vitelline network (VVN) was distributed in the major portion of lateral sides of the embryo. Several blood vessels were found highly branched. In addition, inter-somatic vessels (ISV), posterior cardinal vein (PCV) and dorsal longitudinal anastomosing vessel (DLAV) were also normally formed. **B) Spatial expression of Ami in PHD-3 loss-of-function embryos:** PHD-3 MO was injected into one cell of a two cell stage embryo. Embryos were sorted according to GFP signal and collected at NF st-37 for vascular vitelline network (VVN) analysis. Expression of Ami was found to be normal in un-injected as well as injected side. Vascular vitelline network (VVN) was distributed in the major portion of lateral sides of the embryo. Several blood vessels were found highly branched. In addition, inter-somatic vessels (ISV), posterior cardinal vein (PCV) and dorsal longitudinal anastomosing vessel (DLAV) were also normally formed.

4.15 HIF-1 α eoe1 MO acts specifically

To investigate the impact of HIF-1 α on embryonic vasculogenesis, HIF-1 α loss-of-function experiments were carried out. Initially, a morpholino was designed that should bind to the end sequence of the first exon and to the beginning of the following intron in HIF-1 α gene. The morpholino was named HIF-1 α eoe1 (end of exon 1) MO. It is a direct method to determine the specificity of a morpholino. Such a design is advantageous since it blocks the splicing of the gene itself thereby effectively blocking the gene function *in vivo*. Activity of the morpholino can be determined quantitatively by examining the mRNA levels of the corresponding gene against which the morpholino was employed. This can be achieved using semi-quantitative PCR. Whereas, in morpholinos targeting start codon, protein levels of the respective gene have to be determined in order to check the activity of the morpholino. Hence, morpholinos that block splicing aid in determining the specificity of the morpholino under investigation in a rather simple, cost-effective yet reliable way.

1.25 pmol control MO or HIF-1 α eoe-1 MO was injected in all cells of a four cell stage embryo. 10 embryos were collected at different stages of development such as NF st-5, 9, 11, 13, 15 and 19 and snap frozen in liquid nitrogen. Total mRNA was extracted and cDNA was synthesised. Analysis of temporal expression of HIF-1 α gave results that are shown in Fig.29A. In HIF-1 α eoe-1 MO injected embryos, expression of HIF-1 α mRNA was seen from NF st-5 and remained constant until NF st-11. After gastrulation, i.e., NF st-11, the amount of mRNA was gradually down regulated until the last stage examined, (NF st-19) (Fig.29B). This suggests that the morpholino employed could effectively target the intended region thereby reducing correct splicing during development. ODC-1 was used to control the amount of input RNA in both cases.

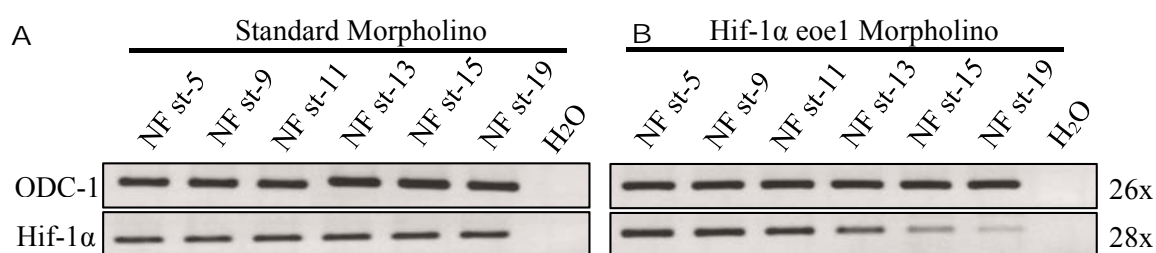


Figure 29: A) Examining HIF-1 α eoe1 MO specificity using standard morpholino: Standard morpholino was injected in four cells of a four cell embryo, total mRNA was extracted and cDNA was synthesized. Performing SQ-PCR against HIF-1 α showed constant expression throughout the developmental stages examined. **B) Examining HIF-1 α eoe1 MO specificity using HIF-1 α eoe1 morpholino:** HIF-1 α eoe1 MO was injected in all cells of a four cell embryo. Embryos were snap frozen at various developmental stages as mentioned. Total mRNA was extracted and cDNA was synthesized *in vitro*. Semi-quantitative PCR was performed against HIF-1 α and showed constant expression until NF st-11. During further development, mRNA level was reduced sequentially. ODC-1 was used to control input mRNA in both cases.

4.16 Suppression of HIF-1 α function led to reduced vascular structures

1.25 pmol HIF-1 α MO were microinjected into one cell of a two cell stage embryo. Embryos were raised until NF st-37, collected and analysed for the expression of vascular marker Ami via WMISH. EGFP was used as tracer. In the non-injected side, Ami expression could be seen displaying vascular vitelline network (VVN) which is highly branched, regular and distributed in major portion of the lateral side of the embryo. Inter-somatic vessels (ISV) and posterior cardinal vein (PCV) could be seen as well. In contrast, in the injected side of the embryo, fewer blood vessels were present and Inter-somatic vessels (ISV) could not be noted. Posterior cardinal vein (PCV) was seen on both sides of the embryo (Fig.30). Therefore, from the results above, it can be inferred that HIF-1 α plays a role in normal development of embryonic vasculature. Supplementary Table 18 shows the total number of embryos which showed reduced Ami expression.

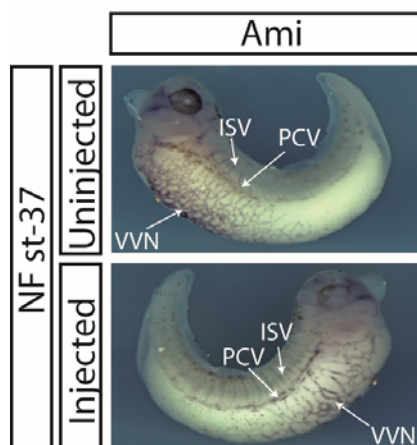


Figure 30: Spatial expression of Ami in HIF-1 α loss-of-function embryos: HIF-1 α eoe1 MO was injected and embryos were collected at NF st-37. WMISH was performed against Ami. Comparing both sides showed less blood vessel formation and branching on the injected side. Absence of inter-somatic vessels (ISV) was also noted. However, Ami expression in posterior cardinal vein (PCV) was seen.

4.17 VHL eoe2 MO acts specifically

To investigate the impact of VHL in the embryonic vasculogenesis, VHL loss-of-function experiments were carried out. Initially, morpholino was designed that should bind to the end sequence of the second exon and to the beginning of the following intron in VHL gene. This morpholino was named VHL eoe2 (end of exon 2) MO.

2.5 pmol control MO / VHL eoe-2 MO were injected in all cells of a four cell stage embryo. 10 embryos were collected at different stages of development such as NF st-5, 9, 11, 13, 15 and 19 and snap frozen in liquid nitrogen. Total mRNA was extracted and cDNA was synthesised. Analysis of temporal expression of VHL gave results that are shown in Fig.31A. In VHL eoe-2 MO injected embryos, expression of VHL mRNA was seen from NF st-5 and remained constant

until NF st-9. After gastrulation, i.e., NF st-11, the amount of mRNA was gradually down regulated until the last stage examined, (NF st-19) (Fig.31B). This suggests that the morpholino employed could effectively target the intended region thereby reducing its expression during development. ODC-1 was used to control the amount of input mRNA in both cases.

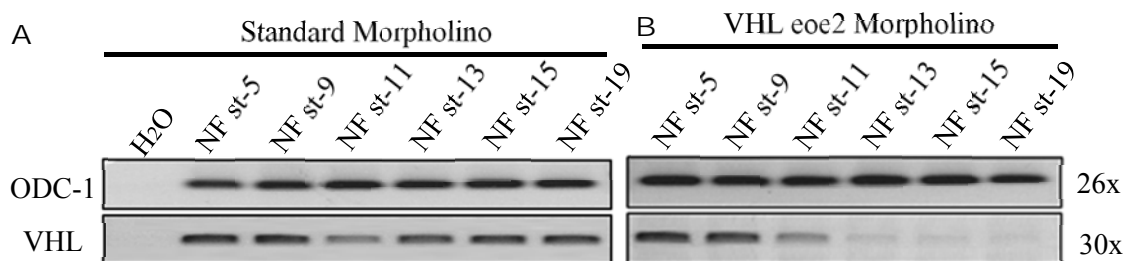


Figure 31: A) Examining VHL eoe2 MO specificity using standard morpholino: Standard morpholino was injected in four cells of a four celled embryo, extracted total mRNA and synthesized cDNA. Performing SQ-PCR against VHL showed constant expression throughout the developmental stages examined. **B) Examining VHL eoe2 MO specificity using VHL eoe2 morpholino:** VHL eoe2 MO was injected in all cells of a four celled embryo. Embryos were snap frozen at various developmental stages as mentioned. Total mRNA was extracted and cDNA was synthesized *in vitro*. Semi-quantitative PCR was performed against VHL showed constant expression until NF st-9. During further development, its expression became weaker. ODC-1 was used to control input mRNA in both cases.

4.18 Suppression of VHL function affects vascular structures

It is known that Von-Hippel-Lindau (VHL) complex targets the hydroxylated form of HIF-1 α to proteasomal degradation. Inhibiting the function of VHL complex should, in theory lead to increased levels of hydroxylated HIF-1 α . However, functionality of this hydroxylated protein is unknown. In current experiment, I wanted to investigate the effect of hydroxylated HIF-1 α on embryonic vasculogenesis. 2.5 pmol VHL eoe-2 MO was injected in one cell of a two cell stage embryo. Embryos were raised, sorted according to EGFP signal and harvested at NF st-37 for expression analysis of Ami using WMISH (Fig.32).

Images in Fig.32 show that the expression of vascular marker Ami is reduced on the injected side of the embryo compared to non-injected side. All vascular features could be observed on control side such as vascular vitelline network (VVN), inter-somitic vessels (ISV) and posterior cardinal vein (PCV) as well. However, on the morpholino injected side, reduced number of blood vessels were observed. Branches were irregular and inter-somitic vessels (ISV) were not seen. Ami expression in posterior cardinal vein (PCV) was reduced. Hence, from the present experiments, it can be demonstrated that VHL loss-of-function also affect embryonic vasculogenesis. Supplementary Table 19 shows the total number of embryos which showed reduced Ami expression.

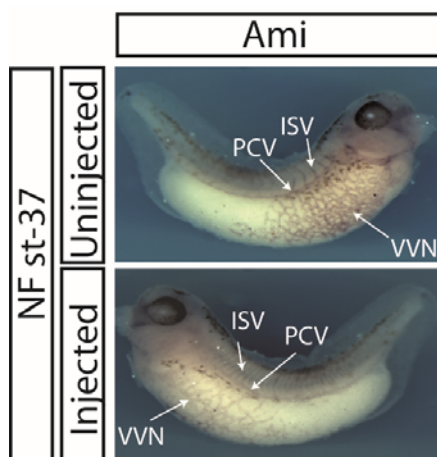


Figure 32: Spatial expression of Ami in VHL loss-of-function embryos: VHL eoe2 MO was injected and embryos were collected at NF st-37. WMISH was performed against Ami. Comparing both sides showed less blood vessel formation and branching in the injected side. Absence of inter-somitic vessels (ISV) was also noted. However, Ami expression in posterior cardinal vein (PCV) was seen.

4.19 Combined loss of HIF-1 α and VHL functions leads to reduced vasculature

In previous experiments, individual loss of HIF-1 α as well as VHL function showed reduced VVN. Performing combined knock-down experiments of both HIF-1 α and VHL (1.25 pmol each) also showed similar pattern of vascular network as seen in HIF-1 α and VHL knock-down experiments. Fewer blood vessels were observed in the injected side and inter-somitic vessels (ISV) were absent as well. Hence, it can be suggested that both HIF-1 α and VHL play a role in the development of vascular network during embryogenesis (Fig.33). Supplementary Table 20 shows the total number of embryos, which showed reduced Ami expression.

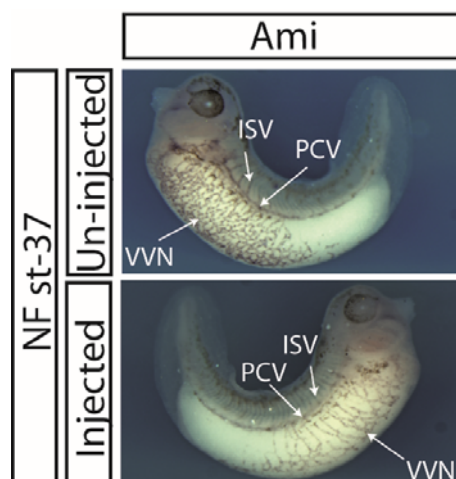


Figure 33: Spatial expression of Ami in HIF-1 α + VHL loss-of-function embryos: Both, HIF-1 α eoe1 MO and VHL eoe-2 MO were injected into one cell of a two cell embryo and collected at NF st-37. Performing WMISH against vascular marker Ami showed reduced expression in the vascular structures.

5 Discussion

During early embryonic development, one of the first functional systems formed in the embryo is the vascular system. Previous research in cancer cells cultured in hypoxia showed increased HIF-1 α levels. As HIF-1 α is a pro-angiogenic factor, it has been suggested that hypoxia increases blood vessel formation. However, no data is available that shows the importance of oxygen availability on the formation of the vascular network during embryogenesis. Hence, it is of great interest to investigate the effect of oxygen on vasculogenesis and early angiogenesis.

The current study was undertaken to investigate whether vasculogenesis, one of the important and early processes, is an independent genetic program or whether external factors such as oxygen can influence its genesis during vertebrate embryogenesis. To answer this fundamental question, *Xenopus* embryos were exposed to various strictly maintained low oxygen conditions (hypoxia) throughout embryonic development and assessed for the development of vascular network.

Embryos were exposed to hypoxic conditions right after the first cell division i.e. 2 cell stage to eliminate addition of non-fertilized embryos into hypoxia chambers. Embryos were later collected at various tadpole stages. Therefore, embryos grew under constant oxygen conditions throughout their development until harvesting. Hypoxia experiment was designed to cultivate embryos at decreasing dissolved oxygen levels. The oxygen concentrations at which embryonic development were analysed, were 35%, 25%, 15%, 8%, 6% and 4% O₂.

5.1 Oxygen is essential for proper embryonic morphogenesis and ontogenesis

Survival rates of embryos grown in 35%, 25% or 15% O₂ was indistinguishable from embryos raised under normoxic conditions. Developmental rate was also found to be similar compared to embryos grown under normoxic conditions. Decreased survival rates could be observed when embryos were grown in 8% O₂ or less. First effects could be seen already at gastrulation. Defects in the closure of blastopore were observed (images not shown). Highest death rates were recorded during tailbud stages of development. 3%, 12% and 13% embryos died at 8%, 6% and 4% O₂ respectively during tailbud stages. Hence, tailbud stages are more sensitive to external oxygen levels during development. This was confirmed by performing type-2 hypoxia experiments. But in type-2 hypoxia experiments wherein embryos were exposed to hypoxic conditions starting at different stages of their development such as gastrulation (NF st-12), neurulation (NF st-18) and tadpole stages (NF st-24 and 30), 99% embryos survived when exposed to 4% oxygen starting from NF st-30 until they reached NF st-37. This could be because when embryos were exposed to 4% oxygen starting from NF st-2, they are much longer time in hypoxic conditions than the embryos exposed to 4% oxygen starting from NF st-30.

Developmental rate was also notably affected at and below 8% O₂. Until embryos reached a critical stage i.e. NF st-30, at 8% O₂, embryos developed undistinguishable from control embryos. Embryos raised in both chambers reached NF st-30 in 44 hrs. Later, embryos grown in 8% oxygen

needed more time to reach NF st-37. Controls needed 18 hrs to develop from NF st-30 to NF st-37 whereas embryos raised in 8% O₂ needed 31 hrs. Lower oxygen concentrations such as 6% and 4% O₂ hindered development right after gastrulation. Increased hypoxic stress led to delayed development. Embryos raised in 4% O₂ needed 13 hrs more than embryos grown in normoxia to reach NF st-30. In addition, to develop from NF st-30 to NF st-37, control embryos needed 22 hrs whereas embryos grown in 4% O₂ needed 68 hrs. This unusually prolonged development could possibly be because of delayed cell division. In my studies, less number of proliferating cells were observed using proliferation (pH3) assay in embryos grown in hypoxia. On average, embryos grown in normoxia showed 802 dividing cells at NF st-30. Embryos raised in 8% O₂ showed 394, 6% O₂ grown embryos showed 374 and very few cells were found in 4% O₂ grown embryos (285). Hence it can be suggested that low oxygen availability affects mortality and could considerably slow down growth and development via delayed cell division during embryogenesis.

Furthermore, morphological defects were observed in embryos raised in very low oxygen levels (4% O₂). Although differences could be observed in embryos grown in 8% and 6% O₂, defects were more prominent in much lower oxygen conditions. Primary observation was reduced overall size of the embryo. Another notable difference was a shortened tail. This could be clearly observed in 4% O₂ grown embryos at NF st-37. Literature search suggests role of a possible candidate for the delayed development which is called mTOR (mammalian target of rapamycin). mTOR is a serine-threonine kinase which was shown to play an important role in the regulation of cell growth during embryonic development. mTOR consists of two complexes, mTORC1 and mTORC2 which controls cell protein synthesis, growth and proliferation, survival and metabolism (Semenza, 1999; Bruick, 2003; Guertin and Sabatin, 2005; Sarbassov *et al.*, 2005). Its orthologues have also been reported in *C. elegans* (Takeda *et al.*, 2006), *D. melanogaster* (Isaac and Andrew, 1996; Parmer *et al.*, 2006) and mammals (Tontonoz *et al.*, 1995; Simon *et al.*, 2002; Yun *et al.*, 2002; Liu and Simon, 2004). Inactivation of mTOR homologue or homologue of its substrate in *D. melanogaster* resulted in reduced cell size and embryonic lethality (Isaac and Andrew, 1996; Peng *et al.*, 2000; Parmer *et al.*, 2007). It has also been shown that flies with partial loss-of-function in these molecules displayed significantly smaller body sizes compared to wild type. In mouse, disruption of p70^{S6k1} which is a downstream target of mTOR also resulted in smaller size of the entire body (Mostafa *et al.*, 2000). Other evidence also shows that mTOR activity regulates G1 progression and overall body size (Manning and Krasnow, 1993; Samakovlis *et al.*, 1996). Previous studies showed that mTOR activity was clearly inhibited by oxygen deprivation (Arsham *et al.*, 2003). Because embryos in my study were raised in hypoxia, I speculate that the morphological differences and slower development could be due to altered mTOR activity. However, detailed studies have to be done to elucidate possible role of mTOR and its downstream targets.

5.2 Not all organs are affected by hypoxia during embryogenesis

To check if hypoxia specifically affects hematopoietic and vascular genes or hypoxia affects the formation of all organs during development, double whole mount *in situ* hybridizations were performed. Two markers were chosen to observe their expression simultaneously with the vascular marker Ami. One was the mesodermal marker muscle actin and the other was the neural marker n-tubulin.

Constant expression of muscle actin which is a mesodermal marker was detected in embryos grown in normoxia and 8%, 6% and 4% O₂. Expression of vascular marker Ami was found decreasing with decreasing available oxygen such as 8%, 6% and 4% O₂ respectively using double whole mount *in situ* hybridizations. Constant expression of the neural marker n-tubulin was detected in embryos grown in normoxia and 8%, 6% and 4% O₂ as shown in the embryo sections. Expression of vascular marker Ami was found decreasing with decreasing available oxygen such as 8%, 6% and 4% O₂ respectively using double whole mount *in situ* hybridizations. This suggests that hypoxia specifically affects the expression of vascular and hematopoietic genes but does not affect the formation of all organs during embryogenesis.

5.3 Embryonic vasculogenesis is not an independent pre-programmed process but requires oxygen

Experiments performed in hypoxic conditions using cancer cell lines showed increased HIF-1 α levels. HIF-1 α is a pro-angiogenic factor that drives the formation of new blood vessels. Performing functional analysis on the genes that are involved in HIF pathway have suggested the role of HIF-1 α as a pro-angiogenic factor. These studies include HIF-1 α loss-of-function experiments (; Ryan *et al.*, 1998; Weidemann and Johnson, 2008), VHL loss-of-function experiments (Gnarra *et al.*, 1997; Weidemann and Johnson, 2008), loss-of-function experiments on the targets of HIF-1 α such as angiopoietin-1. A hierarchy has been well established that HIF-1 α expression is regulated by oxygen availability. These experiments include experiments performed by introducing mutations in targets of HIF-1 α such as angiopoietin-1 or its receptors (Davis *et al.*, 1996; Suri *et al.*, 1996; Vikula *et al.*, 1996), VEGF receptors (e.g. Flt-1 receptor tyrosine kinase) (Fong *et al.*, 1995) and on other downstream targets of HIF-1 α also supported the role of HIF-1 α in embryonic vasculogenesis. Although these evidences do suggest significant roles of the individual candidates in cell culture experiments, direct evidence suggesting the importance of oxygen during embryogenesis is lacking. To know the importance of oxygen itself during embryogenesis, oxygen availability to the developing embryo has to be limited. Therefore, I performed experiments where developing embryos grow in limited oxygen concentrations. In organisms supporting internal fertilization and *in utero* development such as mouse, nutrients and oxygen are delivered through the placenta. In such model systems, creating a hypoxic environment is largely impractical. *Xenopus laevis* is an excellent model organism to study the

effects of oxygen during embryogenesis directly, as fertilization and development of these organisms is external. Thus, *Xenopus* embryos could be cultured in regulated oxygen chambers. In my experiments, loss of ER71 expression, which can be used as a marker for endothelial precursor cells, was seen in several areas such as posterior cardinal vein (PCV), posterior precursors (PP), branchial arches (BA), vitelline veins (VV) and ventral precursors (VP). Greatest loss was seen in branchial arches (BA), vitelline veins (VV) and ventral precursors (VP). Consequently, by checking the expression of Ami which is a vascular marker of differentiation, reduced number of mature blood vessels were observed. Significant loss of vascular vitelline network (VVN) and inter-somitic vessels (ISV) could be explained by the loss of their respective precursor cells. Because oxygen was the only parameter that was provided in a controlled and reduced manner, it can be suggested that these effects on vasculogenesis are due to low oxygen. Therefore, decreased expression of ER71 and Ami in embryos grown in hypoxia shows the necessity of oxygen to drive the differentiation of endothelial precursors from the mesoderm and their subsequent formation of a vascular network.

Previous reports suggest that hypoxia caused increased angiogenesis and vascularization via activation of the HIF pathway (Forsythe *et al.*, 1996; Gerber *et al.*, 1997; Kaelin and Ratcliffe, 2008). Increased or induced formation of blood vessels was also reported during neoangiogenesis, caused by hypoxia (Gerhardt *et al.*, 2003; Semenza, 2003). However, it is important to note that in my experiments, hypoxia did not increase the formation of blood vessels during embryogenesis. Lower numbers of blood vessels were observed in the embryos grown under hypoxic conditions.

PHD-2 has been suggested to function as the oxygen sensing enzyme in the cells (Edurma *et al.*, 2003). Therefore, reducing the expression of PHD-2 should mimic a hypoxic situation inside the developing embryo. In my PHD-2 loss-of-function experiments, to my surprise, I have seen significantly low expression of Ami. Suppression of PHD-2 function resulted in reduced blood vessel formation. Only few blood vessels were found in the injected side. This situation was not expected because, according to previous results in other systems, HIF levels were expected to rise, thereby increasing the total number of blood vessels. Recent results suggested increased angiogenesis in multiple organs in conditional PHD-2 knockout mice (Takeda *et al.*, 2007), improved vascular survival and arteriogenesis in ischemic hind limbs of PHD-2 knockout mice (Takeda *et al.*, 2014) and normal embryonic vascularization in PHD-2^{-/-} mouse embryos (Takeda *et al.*, 2006). In contrast, PHD-2^{-/-} mice embryos died at E12.5-14.5 due to defects in labyrinthine branching in placenta (Takeda *et al.*, 2006; Ozolins *et al.*, 2009). It is noteworthy that PHD-2 loss-of-function led to embryonic lethality due to defective placentation which is an extra embryonic tissue. Hence, I suggest that PHD-2, which is recognized as the oxygen sensor, might be regulated in a distinct manner *in vivo* in *Xenopus* embryos and that vasculogenesis require oxygen for proper formation of blood vessels.

Influence of hypoxia as well as loss of PHD-2 function was also assessed on the formation of myelogenic precursor cells (mpo) and erythrocytic precursor cells (lmo-2 and β -globin). In hypoxia experiments and PHD-2 loss-of-function experiments, fewer cells were found expressing mpo suggesting that hypoxia and PHD-2 loss-of-function affects the formation of mpo expressing cells during embryogenesis. In contrast, difference in erythropoietic precursor formation was not prominent in embryos grown in hypoxia as well as in PHD-2 KD experiments. However, structures expressing β -globin were less at late stages (NF st-37) in embryos grown in hypoxia. Further investigation on the effect of hypoxia and PHD-2 loss-of-function on the expression of lmo-2 and β -globin has not been performed. However, previous *in vivo* PHD-2 knock-down studies in one-cell murine zygotes reported increased erythropoiesis (Ozolins *et al.*, 2009). It has also been shown that PHD-2 deficient mice developed polycythemia (Minamashima *et al.*, 2008; Takeda *et al.*, 2008; Rankin *et al.*, 2012).

5.4 HIF pathway might not be the solo player during embryonic vasculogenesis

Extensive research in cancer field has focussed on the HIF pathway. Multiple studies show the effects of functional loss of individual components in this pathway. In my experiments, HIF-1 α loss-of-function experiments showed reduced vessel formation. These results are supported by previous experiments. Loss of HIF-1 α in endothelial cells led to impaired vascularization of xenografts (Tang *et al.*, 2004) and reduced tumour vessel density by 40% demonstrated by alterations in both vessel density and morphology (Ryan *et al.*, 1998). HIF-1 α null mouse embryos displayed disorganised vascularization compared to wild type and complete loss of neural vascularization and incomplete somitic vascularization (Ryan *et al.*, 1998). However, comparing injected side with the non-injected side in my HIF-1 α loss-of-function embryos, mild effects on vascularization were observed. Hence, I suggest that HIF plays a notable role in the embryonic vasculogenesis.

On the other hand, VHL loss-of-function should allow HIF-1 α to escape proteasomal degradation, thereby activating hypoxic response genes resulting in increased blood vessel formation. In contrast to this, VHL loss-of-function in embryos also displayed less blood vessels. Analysis of homozygous knock out of VHL in mice was difficult as the embryos died due to severe vascular defects in embryos. Granna *et al.*, 1997 and Haase *et al.*, 2001 demonstrated that homozygous VHL $^{-/-}$ mice died in utero at E10.5 to E12.5. They could show that embryonic death was due to failure in placental vasculogenesis. However, whether this phenotype was mediated by increased HIF has not been studied. Performing combined HIF-1 α and VHL knock down in my experiments also resulted in reduced vasculature. Because there was mild effect on the formation of vascular network in HIF-1 α and VHL loss-of-function embryos when compared to embryos raised in hypoxic conditions, it is possible that HIF-1 α and VHL are not the only factors that are involved in the formation of vascular system during embryogenesis. However, in my experiments, PHD-2

loss-of-function impaired the formation of vascular system similar to embryos grown in hypoxia. This might be due to the effect of PHD-2 on targets other than HIF-1 α . Therefore, it can be suggested that HIF pathway is not the only player during embryonic vasculogenesis. Further investigation is necessary to elucidate the importance of other potential candidates.

5.5 Conclusion

Hypoxia decreased the survival rate of embryos during development. Very low oxygen conditions such as 4% oxygen significantly slowed down the developmental rate. It also affected overall morphology of the embryos. Embryos grown in hypoxia were shorter compared to embryos grown in normoxia. Hypoxia had a strong effect on the formation of endothelial precursor cells as well as on the formation of vascular structures during embryogenesis. A significant effect was also observed on the formation of myelopoietic precursor cells. However, only a mild effect was noticed on the migration of erythropoietic precursor cells. I could show that hypoxia did not affect the formation of all organs during embryogenesis. It had a specific effect on the formation of vascular network and hematopoietic precursors. Therefore, it can be suggested that oxygen availability is important during embryonic vasculogenesis and is not an independent pre-programmed genetic process. Roles of genes involved in oxygen sensing mechanism were also analysed individually. Loss of PHD-2 also resulted in the formation of reduced vascular network which was observed in embryos grown in hypoxia. However, effect on the formation of myelopoietic and erythropoietic precursor cells was limited. Examining the effects of HIF-1 α and VHL loss-of-function showed mild effect on the formation of vascular network. Although it has been suggested by studies in cancer cell lines that hypoxia stabilizes HIF-1 α and increases the formation of vascular network, opposite effect was observed in my experiments. Formation of the vascular network was greatly hindered by hypoxia during embryogenesis. Because the effect of hypoxia and PHD-2 loss-of-function was strong on the formation of vascular network but mild effect was observed in the HIF-1 α loss-of-function studies, it is possible that PHD-2 has targets other than HIF-1 α .

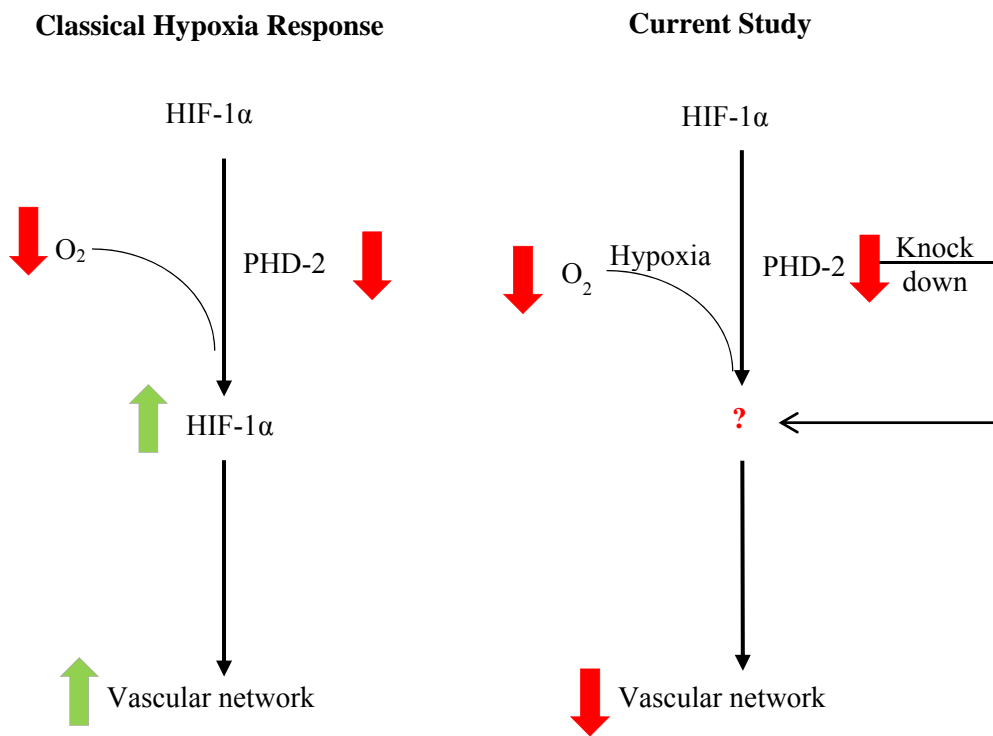


Fig.32: Comparison of classical hypoxia response pathway against current study.

6 Bibliography

- Adolfsson J, Mansson R, *et al.*, Jacobsen SE (2005) Identification of Flt3+ lympho-myeloid stem cells lacking erythro-megakaryocytic potential a revised road map for adult blood lineage commitment. *Cell* 121(2): 295-306.
- Aoyama M: Disvolvigo de sangvasoj de la mez kaj finintesto ce hynobius naevius. *Kaibogaku Zasshi*, 31, 1956, pp. 573-598.
- Appelhoff RJ, Tian YM, *et al.*, Gleadle JM (2004) Differential function of the prolyl hydroxylases PHD1, PHD2, and PHD3 in the regulation of hypoxia-inducible factor. *J Biol Chem* 279(37):38458-38465.
- Arsham AM, Howell JJ, & Simon MC (2003) A novel hypoxia-inducible factor-independent hypoxic response regulating mammalian target of rapamycin and its targets. *J Biol Chem* 278(32): 29655-29660.
- Baffert F, Le T, Sennino B, Thurston G, Kuo CJ, Hu-Lowe D & McDonald DM (2006) Cellular changes in normal blood capillaries undergoing regression after inhibition of VEGF signaling. *Am J Physiol Heart Circ Physiol* 290(2):H547-559.
- Berra E, Benizri E, Ginouves A, Volmat V, Roux D & Pouyssegur J (2003) HIF prolyl-hydroxylase 2 is the key oxygen sensor setting low steady-state levels of HIF-1alpha in normoxia. *EMBO J* 22(16):4082-4090.
- Bhattacharya S, Michels CL, Leung MK, Arany ZP, Kung AL & Livingston DM (1999) Functional role of p35srj, a novel p300/CBP binding protein, during transactivation by HIF-1. *Genes Dev* 13(1):64-75.
- Bruick RK (2000) Expression of the gene encoding the proapoptotic Nip3 protein is induced by hypoxia. *Proc Natl Acad Sci USA* 97(16):9082-9087.
- Bruick RK (2003) Oxygen sensing in the hypoxic response pathway: regulation of the hypoxia-inducible transcription factor. *Genes Dev* 17(21):2614-2623.
- Bruick RK & McKnight SL (2001) A conserved family of prolyl-4-hydroxylases that modify HIF. *Science* 294(5545):1337-1340.
- Caniggia I, Mostachfi H, Winter J, Gassmann M, Lye SJ, Kuliszewski M & Post M (2000) Hypoxia-inducible factor-1 mediates the biological effects of oxygen on human trophoblast differentiation through TGFbeta(3). *J Clin Invest* 105(5):577-587.
- Carmeliet P, Dor Y, *et al.*, Keshert E (1998) Role of HIF-1alpha in hypoxia-mediated apoptosis, cell proliferation and tumour angiogenesis. *Nature* 394(6692):485-490.
- Chen XD & Turpen JB (1995) Intraembryonic origin of hepatic hematopoiesis in *Xenopus laevis*. *J Immunol* 154(6):2557-2567.
- Choi K, Kennedy M, Kazarov A, Papadimitriou JC & Keller G (1998) A common precursor for hematopoietic and endothelial cells. *Development* 125(4):725-732.
- Chun YS, Kim MS & Park JW (2002) Oxygen-dependent and -independent regulation of HIF-1alpha. *J Korean Med Sci* 17(5):581-588.
- Claxton S & Fruttiger M (2004) Periodic Delta-like 4 expression in developing retinal arteries. *Gene Expr Patterns* 5(1):123-127.
- Cleaver O & Krieg PA (1999) Expression from DNA injected into *Xenopus* embryos. *Methods Mol Biol* 127:133-153.
- Cokic PV, Smith DR, Biancotto A, Noguchi TC, Puri KR & Schechter NA (2013) Globin gene expression in correlation with G protein-related genes during erythroid differentiation. *BMC Genomics* 14:116.
- Copenhaver WM (1926) Experiments on the development of the heart of *Amblystoma punctatum*. *Journal of Experimental Zoology* Volume 43(Issue 3):321-371.
- Cormier-Regard S, Nguyen SV & Claycomb WC (1998) Adrenomedullin gene expression is developmentally regulated and induced by hypoxia in rat ventricular cardiac myocytes. *J Biol Chem* 273(28):17787-17792.
- Davis S, Aldrich TH, *et al.*, Yancopoulos GD (1996) Isolation of angiopoietin-1, a ligand for the TIE2 receptor, by secretion-trap expression cloning. *Cell* 87(7):1161-1169.
- Eckhart AD, Yang N, Xin X & Faber JE (1997) Characterization of the alpha1B-adrenergic receptor gene promoter region and hypoxia regulatory elements in vascular smooth muscle. *Proc Natl Acad Sci USA* 94(17):9487-9492.

- Evans H: The development of the vascular system. Philadelphia, The Washington Square Press, 1912.
- Feldser D, Agani F, Iyer NV, Pak B, Ferreira G & Semenza GL (1999) Reciprocal positive regulation of hypoxia-inducible factor 1 α and insulin-like growth factor 2. *Cancer Res* 59(16):3915-3918.
- Ferrara N (2004) Vascular endothelial growth factor: basic science and clinical progress. *Endocr Rev* 25(4):581-611.
- Ferrara N, Carver-Moore K, *et al.*, Moore MW (1996) Heterozygous embryonic lethality induced by targeted inactivation of the VEGF gene. *Nature* 380(6573):439-442.
- Firth JD, Ebert BL, Pugh CW & Ratcliffe PJ (1994). Oxygen-regulated control elements in the phosphoglycerate kinase 1 and lactate dehydrogenase A genes: similarities with the erythropoietin 3' enhancer. *Proc Natl Acad Sci USA* 91(14):6496-6500.
- Flamme I, Frolich T & Risau W (1997) Molecular mechanisms of vasculogenesis and embryonic angiogenesis. *J Cell Physiol* 173(2):206-210.
- Fong GH, Rossant J, Gertsenstein M & Breitman ML (1995) Role of the Flt-1 receptor tyrosine kinase in regulating the assembly of vascular endothelium. *Nature* 376(6535):66-70.
- Forsythe JA, Jiang BH, Iyer NV, Agani F, Leung SW, Koos RD & Semenza GL (1996). Activation of vascular endothelial growth factor gene transcription by hypoxia-inducible factor 1. *Mol Cell Biol* 16(9):4604-4613.
- Gerber HP, Condorelli F, Park J & Ferrara N (1997) Differential transcriptional regulation of the two vascular endothelial growth factor receptor genes. Flt-1, but not Flk-1/KDR, is up-regulated by hypoxia. *J Biol Chem* 272(38):23659-23667.
- Gerhardt H, Golding M, *et al.*, Betsholtz C (2003) VEGF guides angiogenic sprouting utilizing endothelial tip cell filopodia. *J Cell Biol* 161(6): 1163-1177.
- Gilbert SF: Sinauer Associates, Inc.: Developmental Biology. (Sixth edition. ed.). Sunderland, Massachusetts, USA, 2000, pp. 471-501.
- Gilbert SF: Sinauer Associates, Inc.: Developmental Biology. (Eighth edition. ed.). Sunderland, Massachusetts, USA, 2006, pp. 471-504.
- Gleadle JM & Ratcliffe PJ (1997) Induction of hypoxia-inducible factor-1, erythropoietin, vascular endothelial growth factor, and glucose transporter-1 by hypoxia: evidence against a regulatory role for Src kinase. *Blood* 89(2):503-509.
- Gnarra JR, Ward JM, *et al.*, Linehan WM (1997) Defective placental vasculogenesis causes embryonic lethality in VHL-deficient mice. *Proc Natl Acad Sci USA* 94(17):9102-9107.
- Guertin DA & Sabatini DM (2005) An expanding role for mTOR in cancer. *Trends Mol Med* 11(8):353-361.
- Haase VH, Glickman JN, Socolovsky M & Jaenisch R (2001) Vascular tumors in livers with targeted inactivation of the von Hippel-Lindau tumor suppressor. *Proc Natl Acad Sci USA* 98(4):1583-1588.
- Heinke J, Patterson C & Moser M (2012) Life is a pattern: vascular assembly within the embryo. *Front Biosci (Elite Ed)* 4:2269-2288.
- Hellstrom M, Phng LK, *et al.*, Betsholtz C (2007) Dll4 signalling through Notch1 regulates formation of tip cells during angiogenesis. *Nature* 445(7129):776-780.
- Hewitson KS, McNeill LA, *et al.*, Schofield CJ (2002) Hypoxia-inducible factor (HIF) asparagine hydroxylase is identical to factor inhibiting HIF (FIH) and is related to the cupin structural family. *J Biol Chem* 277(29):26351-26355.
- Hock H & Orkin SH (2005) Stem cells: the road not taken. *Nature* 435(7042):573-575.
- Hofmann JJ & Iruela-Arispe ML (2007) Notch signaling in blood vessels: who is talking to whom about what? *Circ Res* 100(11):1556-1568.
- Hu J, Discher DJ, Bishopric NH & Webster KA (1998) Hypoxia regulates expression of the endothelin-1 gene through a proximal hypoxia-inducible factor-1 binding site on the antisense strand. *Biochem Biophys Res Commun* 245(3):894-899.
- Hughes S & Chang-Ling T (2000) Roles of endothelial cell migration and apoptosis in vascular remodeling during development of the central nervous system. *Microcirculation* 7(5):317-333.
- Inui M & Asashima M (2006) A novel gene, Ami is expressed in vascular tissue in *Xenopus laevis*. *Gene Expr Patterns* 6(6):613-619.

- Isaac DD & Andrew DJ (1996) Tubulogenesis in *Drosophila*: a requirement for the trachealless gene product. *Genes Dev* 10(1):103-117.
- Isogai S, Horiguchi M & Weinstein BM (2001) The vascular anatomy of the developing zebrafish: an atlas of embryonic and early larval development. *Dev Biol* 230(2):278-301.
- Ivan M, Kondo K, *et al.*, Kaelin WG Jr. (2001) HIF α targeted for VHL-mediated destruction by proline hydroxylation: implications for O₂ sensing. *Science* 292(5516):464-468.
- Iyer NV, Kotch LE, *et al.*, Semenza GL (1998) Cellular and developmental control of O₂ homeostasis by hypoxia-inducible factor 1 α . *Genes Dev* 12(2):149-162.
- Jaakkola P, Mole DR, *et al.*, Ratcliffe PJ (2001) Targeting of HIF- α to the von Hippel-Lindau ubiquitylation complex by O₂-regulated prolyl hydroxylation. *Science* 292(5516):468-472.
- Jiang BH, Rue E, Wang GL, Roe R & Semenza GL (1996) Dimerization, DNA binding, and transactivation properties of hypoxia-inducible factor 1. *J Biol Chem* 271(30):17771-17778.
- Kaelin WG (2005) Proline hydroxylation and gene expression. *Annu Rev Biochem* 74:115-128.
- Kaelin WG Jr. & Ratcliffe PJ (2008) Oxygen sensing by metazoans: the central role of the HIF hydroxylase pathway. *Mol Cell* 30(4):393-402.
- Kallio PJ, Okamoto K, O'Brien S, Carrero P, Makino Y, Tanaka H & Poellinger L (1998) Signal transduction in hypoxic cells: inducible nuclear translocation and recruitment of the CBP/p300 coactivator by the hypoxia-inducible factor-1 α . *EMBO J* 17(22):6573-6586.
- Kallio PJ, Wilson WJ, O'Brien S, Makino Y & Poellinger L (1999) Regulation of the hypoxia-inducible transcription factor 1 α by the ubiquitin-proteasome pathway. *J Biol Chem* 274(10):6519-6525.
- Kau CL & Turpen JB (1983) Dual contribution of embryonic ventral blood island and dorsal lateral plate mesoderm during ontogeny of hemopoietic cells in *Xenopus laevis*. *J Immunol* 131(5):2262-2266.
- Kietzmann T, Roth U & Jungermann K (1999) Induction of the plasminogen activator inhibitor-1 gene expression by mild hypoxia via a hypoxia response element binding the hypoxia-inducible factor-1 in rat hepatocytes. *Blood* 94(12):4177-4185.
- Kolker SJ, Tajchman U & Weeks DL (2000) Confocal imaging of early heart development in *Xenopus laevis*. *Dev Biol* 218(1):64-73.
- Leslie JD, Ariza-McNaughton L, Bermange AL, McAdow R, Johnson SL & Lewis J (2007) Endothelial signalling by the Notch ligand Delta-like 4 restricts angiogenesis. *Development* 134(5):839-844.
- Levine AJ, Munoz-Sanjuan I, Bell E, North AJ & Brivanlou AH (2003) Fluorescent labeling of endothelial cells allows in vivo, continuous characterization of the vascular development of *Xenopus laevis*. *Dev Biol* 254(1):50-67.
- Liao ECaLIZ: Conservation of themes in vertebrate blood development. Cell lineage and fate determination. San Diego, Academic press, 1999, pp. 569-582.
- Lieb ME, Menzies K, Moschella MC, Ni R & Taubman MB (2002) Mammalian EGLN genes have distinct patterns of mRNA expression and regulation. *Biochem Cell Biol* 80(4):421-426.
- Lindahl P, Johansson BR, Leveen P & Betsholtz C (1997) Pericyte loss and microaneurysm formation in PDGF-B-deficient mice. *Science* 277(5323):242-245.
- Lipscomb EA, Sarmiere PD & Freeman RS (2001) SM-20 is a novel mitochondrial protein that causes caspase-dependent cell death in nerve growth factor-dependent neurons. *J Biol Chem* 276(7):5085-5092.
- Liu L & Simon MC (2004) Regulation of transcription and translation by hypoxia. *Cancer Biol Ther* 3(6):492-497.
- Lok CN & Ponka P (1999) Identification of a hypoxia response element in the transferrin receptor gene. *J Biol Chem* 274(34):24147-24152.
- Lu S, Gu X, Hoestje S & Epner DE (2002) Identification of an additional hypoxia responsive element in the glyceraldehyde-3-phosphate dehydrogenase gene promoter. *Biochim Biophys Acta* 1574(2):152-156.
- Manning GaK,; Development of the *Drosophila* tracheal system. New York: Cold Spring Harbor Laboratory Press, 1993.
- Maxwell PH, Wiesener MS, *et al.*, Ratcliffe PJ (1999) The tumour suppressor protein VHL targets hypoxia-inducible factors for oxygen-dependent proteolysis. *Nature* 399(6733):271-275.

- McNeill LA, Hewitson KS, *et al.*, Schofield CJ (2002) The use of dioxygen by HIF prolyl hydroxylase (PHD1). *Bioorg Med Chem Lett* 12(12):1547-1550.
- Mead PE, Deconinck AE, Huber TL, Orkin SH and Zon LI (2001) Primitive erythropoiesis in the *Xenopus* embryo: The synergistic role of LMO-2, SCL and GATA-binding proteins. *Scopus: Development* 128(12):2301-2308.
- Melillo G, Musso T, Sica A, Taylor LS, Cox GW & Varesio L (1995) A hypoxia-responsive element mediates a novel pathway of activation of the inducible nitric oxide synthase promoter. *J Exp Med* 182(6): 1683-1693.
- Metzen E, Berchner-Pfannschmidt U, *et al.*, Fandrey J (2003) Intracellular localisation of human HIF-1 alpha hydroxylases: implications for oxygen sensing. *J Cell Sci* 116(Pt 7):1319-1326.
- Millard N: The development of venous system of "*Xenopus laevis*". *Trans. R. Soc. S. Africa*, 32, 1949, pp. 55-97.
- Millauer B, Wizigmann-Voos S, Schnurch H, Martinez R, Moller NP, Risau W & Ullrich A (1993) High affinity VEGF binding and developmental expression suggest Flk-1 as a major regulator of vasculogenesis and angiogenesis. *Cell* 72(6):835-846.
- Minamishima YA, Moslehi J, Bardeesy N, Cullen D, Bronson RT & Kaelin WG Jr. (2008) Somatic inactivation of the PHD2 prolyl hydroxylase causes polycythemia and congestive heart failure. *Blood* 111(6):3236-3244.
- Mohun TJ, Leong LM, Weninge, WJ & Sparrow D B (2000) The morphology of heart development in *Xenopus laevis*. *Dev Biol* 218(1):74-88.
- Moore MA & Metcalf D (1970) Ontogeny of the haemopoietic system: yolk sac origin of *in vivo* and *in vitro* colony forming cells in the developing mouse embryo. *Br J Haematol* 18(3):279-296.
- Mostafa SS, Miller WM & Papoutsakis ET (2000) Oxygen tension influences the differentiation, maturation and apoptosis of human megakaryocytes. *Br J Haematol* 111(3):879-889.
- Mukhopadhyay CK, Mazumder B & Fox PL (2000) Role of hypoxia-inducible factor-1 in transcriptional activation of ceruloplasmin by iron deficiency. *J Biol Chem* 275(28):21048-21054.
- Neuhaus H, Muller F & Hollemann T (2010) *Xenopus* er71 is involved in vascular development. *Dev Dyn* 239(12):3436-3445.
- Nieuwkoop PD & Faber J: *Normal Tables of Xenopus laevis* (Daudin). Amsterdam.: Elsevier/North-Holland Biomedical Press, 1967.
- Noguera-Troise I, Daly C, *et al.*, Thurston G (2006) Blockade of Dll4 inhibits tumour growth by promoting non-productive angiogenesis. *Nature* 444(7122):1032-1037.
- Norris ML & Millhorn DE (1995) Hypoxia-induced protein binding to O₂-responsive sequences on the tyrosine hydroxylase gene. *J Biol Chem* 270(40):23774-23779.
- O'Rourke JF, Pugh CW, Bartlett SM & Ratcliffe PJ (1996) Identification of hypoxically inducible mRNAs in HeLa cells using differential-display PCR. Role of hypoxia-inducible factor-1. *Eur J Biochem* 241(2):403-410.
- Olsson AK, Dimberg A, Kreuger J & Claesson-Welsh L (2006) VEGF receptor signalling - in control of vascular function. *Nat Rev Mol Cell Biol* 7(5):359-371.
- Ozolins TR, Fisher TS, *et al.*, Li B (2009) Defects in embryonic development of EGLN1/PHD2 knockdown transgenic mice are associated with induction of Igfbp in the placenta. *Biochem Biophys Res Commun* 390(3):372-376.
- Parmar K, Mauch P, Vergilio JA, Sackstein R & Down JD (2007) Distribution of hematopoietic stem cells in the bone marrow according to regional hypoxia. *Proc Natl Acad Sci USA* 104(13): 5431-5436.
- Patan S (2004) Vasculogenesis and angiogenesis. *Cancer Treat Res* 117:3-32.
- Peng J, Zhang L, Drysdale L & Fong GH (2000) The transcription factor EPAS-1/hypoxia-inducible factor 2alpha plays an important role in vascular remodeling. *Proc Natl Acad Sci USA* 97(15):8386-8391.
- Pfirrmann T, Lokapally A, Andreasson C, Ljungdahl P and Hollemann T (2013) SOMA: a single oligonucleotide mutagenesis and cloning approach. *PLoS One* Volume 8(6):e64870.
- Phng LK & Gerhardt H (2009) Angiogenesis: a team effort coordinated by notch. *Dev Cell* 16(2):196-208.

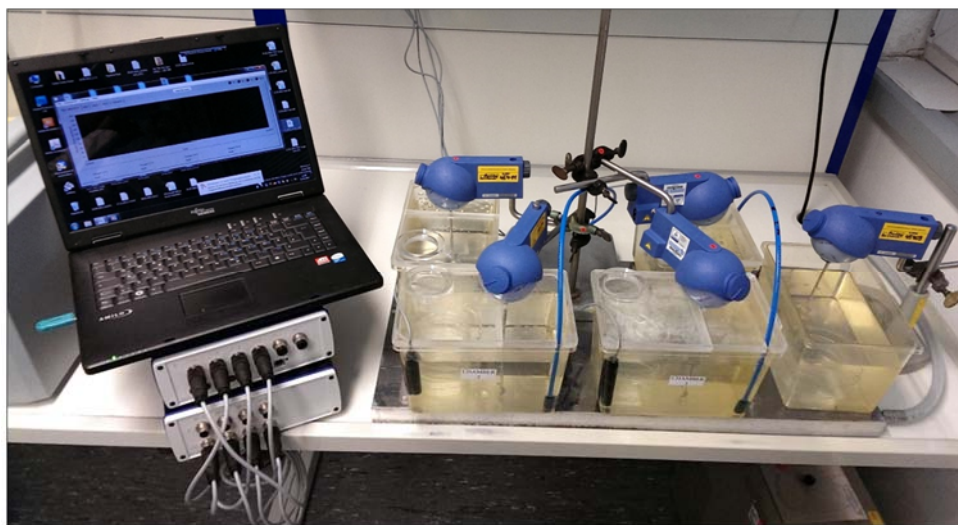
- Pugh CW, O'Rourke JF, Nagao M, Gleadle JM & Ratcliffe PJ (1997) Activation of hypoxia-inducible factor-1; definition of regulatory domains within the alpha subunit. *J Biol Chem* 272(17):11205-11214.
- Rampon C & Hube, P (2003) Multilineage hematopoietic progenitor activity generated autonomously in the mouse yolk sac: analysis using angiogenesis-defective embryos. *Int J Dev Biol*, 47(4), 273-280.
- Rankin E B, Wu C, *et al.*, Giaccia AJ (2012) The HIF signaling pathway in osteoblasts directly modulates erythropoiesis through the production of EPO. *Cell* 149(1):63-74.
- Rechsteiner M & Rogers SW (1996) PEST sequences and regulation by proteolysis. *Trends Biochem Sci* 21(7):267-271.
- Ridgway J, Zhang G, *et al.*, Yan M (2006) Inhibition of Dll4 signalling inhibits tumour growth by deregulating angiogenesis. *Nature* 444(7122):1083-1087.
- Rolfs A, Kvietikova I, Gassmann M & Wenger RH (1997) Oxygen-regulated transferrin expression is mediated by hypoxia-inducible factor-1. *J Biol Chem* 272(32):20055-20062.
- Rossant J & Hirashima M (2003) Vascular development and patterning: making the right choices. *Curr Opin Genet Dev* 13(4):408-412.
- Rouhi P, Jensen LD, *et al.*, Cao Y (2010) Hypoxia-induced metastasis model in embryonic zebrafish. *Nat Protoc* 5(12):1911-1918.
- Ryan HE, Lo J & Johnson RS (1998) HIF-1 alpha is required for solid tumor formation and embryonic vascularization. *EMBO J* 17(11):3005-3015.
- Sainson RC, Aoto J, Nakatsu MN, Holderfield M, Conn E, Koller E & Hughes CC (2005) Cell-autonomous notch signaling regulates endothelial cell branching and proliferation during vascular tubulogenesis. *FASEB J* 19(8):1027-1029.
- Samakovlis C, Hacohen N, Manning G, Sutherland DC, Guillemin K & Krasnow MA (1996). Development of the *Drosophila* tracheal system occurs by a series of morphologically distinct but genetically coupled branching events. *Development* 122(5):1395-1407.
- Sambrook J, Fritsch EF, Maniatis T: *Molecularcloning; a laboratory manual*, Edition 2, ColdSpring Harbor Laboratory Press, Cold Spring Harbor, NY 11724, 1989.
- Sarbassov DD, Guertin DA, Ali SM & Sabatini DM (2005) Phosphorylation and regulation of Akt/PKB by the rictor-mTOR complex. *Science* 307(5712):1098-1101.
- Schofield CJ & Ratcliffe PJ (2004) Oxygen sensing by HIF hydroxylases. *Nat Rev Mol Cell Biol* 5(5):343-354.
- Semenza GL (1999) Regulation of mammalian O₂ homeostasis by hypoxia-inducible factor 1. *Annu Rev Cell Dev Biol* 15:551-578.
- Semenza GL (2000) HIF-1: mediator of physiological and pathophysiological responses to hypoxia. *J Appl Physiol* 88(4):1474-1480.
- Semenza GL (2001) HIF-1, O₂, and the 3 PHDs: how animal cells signal hypoxia to the nucleus. *Cell* 107(1):1-3.
- Semenza GL (2003) Targeting HIF-1 for cancer therapy. *Nat Rev Cancer* 3(10):721-732.
- Semenza GL, Roth PH, Fang HM & Wang GL (1994) Transcriptional regulation of genes encoding glycolytic enzymes by hypoxia-inducible factor 1. *J Biol Chem* 269(38):23757-23763.
- Shalaby F, Ho J, *et al.*, Rossant J (1997) A requirement for Flk1 in primitive and definitive hematopoiesis and vasculogenesis. *Cell* 89(6):981-990.
- Siekmann AF & Lawson ND (2007) Notch signalling limits angiogenic cell behaviour in developing zebrafish arteries. *Nature* 445(7129):781-784.
- Simon MC, Ramirez-Bergeron D, Mack F, Hu CJ, Pan, Y & Mansfield K (2002) Hypoxia, HIFs, and cardiovascular development. *Cold Spring Harb Symp Quant Biol* 67:127-132.
- Sive H, Grainger RM, Harland RM: *Early Development of Xenopus laevis: A laboratory Manual*. New York: Cold Spring Harbor Laboratory Press, 2000.
- Smith JS, Kotecha S, Towers N, Latinkic VB & Mohun JT (2002) XPOX2-peroxidase expression and the XLURP-1 promoter reveal the site of embryonic myeloid cell development in *Xenopus*. *Mechanisms of Development* 117:173-186.
- Sowter HM, Ratcliffe PJ, Watson P, Greenberg AH & Harris AL (2001) HIF-1-dependent regulation of hypoxic induction of the cell death factors BNIP3 and NIX in human tumors. *Cancer Res* 61(18):6669-6673.

- Suchting S, Freitas C, le Noble F, Benedito R, Breant C, Duarte A & Eichmann A (2007) The Notch ligand Delta-like 4 negatively regulates endothelial tip cell formation and vessel branching. *Proc Natl Acad Sci USA* 104(9):3225-3230.
- Suri C, Jones PF, *et al.*, Yancopoulos GD (1996) Requisite role of angiopoietin-1, a ligand for the TIE2 receptor, during embryonic angiogenesis. *Cell* 87(7):1171-1180.
- Takahashi Y, Takahashi S, Shiga Y, Yoshimi T & Miura T (2000) Hypoxic induction of prolyl 4-hydroxylase alpha (I) in cultured cells. *J Biol Chem* 275(19):14139-14146.
- Takeda K, Aguila HL, *et al.*, Fong GH (2008) Regulation of adult erythropoiesis by prolyl hydroxylase domain proteins. *Blood* 111(6):3229-3235.
- Takeda K, Cowan A & Fong GH (2007) Essential role for prolyl hydroxylase domain protein 2 in oxygen homeostasis of the adult vascular system. *Circulation* 116(7):774-781.
- Takeda K, Duan LJ, Takeda H & Fong GH (2014) Improved vascular survival and growth in the mouse model of hindlimb ischemia by a remote signaling mechanism. *Am J Pathol* 184(3):686-696.
- Takeda K, Ho VC, Takeda H, Duan LJ, Nagy A & Fong GH (2006) Placental but not heart defects are associated with elevated hypoxia-inducible factor alpha levels in mice lacking prolyl hydroxylase domain protein 2. *Mol Cell Biol* 26(22):8336-8346.
- Tang N, Wang L, *et al.*, Johnson RS (2004) Loss of HIF-1alpha in endothelial cells disrupts a hypoxia-driven VEGF autocrine loop necessary for tumorigenesis. *Cancer Cell* 6(5):485-495.
- Tontonoz P, Hu E, Devine J, Beale EG & Spiegelman BM (1995) PPAR gamma 2 regulates adipose expression of the phosphoenolpyruvate carboxykinase gene. *Mol Cell Biol* 15(1):351-357.
- Vikkula M, Boon LM, *et al.*, Olsen BR (1996) Vascular dysmorphogenesis caused by an activating mutation in the receptor tyrosine kinase TIE2. *Cell* 87(7):1181-1190.
- Wang GL, Jiang BH, Rue EA & Semenza GL (1995) Hypoxia-inducible factor 1 is a basic-helix-loop-helix-PAS heterodimer regulated by cellular O₂ tension. *Proc Natl Acad Sci USA* 92(12):5510-5514.
- Wax SD, Rosenfield CL & Taubman MB (1994) Identification of a novel growth factor-responsive gene in vascular smooth muscle cells. *J Biol Chem* 269(17):13041-13047.
- Weidemann A & Johnson RS (2008) Biology of HIF-1alpha. *Cell Death Differ* 15(4):621-627.
- Wenger RH (2002) Cellular adaptation to hypoxia: O₂-sensing protein hydroxylases, hypoxia-inducible transcription factors, and O₂-regulated gene expression. *FASEB J* 16(10):1151-1162.
- Wood HB, May G, Healy L, Enver T & Morriss-Kay GM (1997) CD34 expression patterns during early mouse development are related to modes of blood vessel formation and reveal additional sites of hematopoiesis. *Blood* 90(6):2300-2311.
- Wykoff CC, Beasley NJ, *et al.*, Harris AL (2000) Hypoxia-inducible expression of tumor-associated carbonic anhydrases. *Cancer Res* 60(24):7075-7083.
- Yun Z, Maecker HL, Johnson RS & Giaccia AJ (2002) Inhibition of PPAR gamma 2 gene expression by the HIF-1-regulated gene DEC1/Stra13: a mechanism for regulation of adipogenesis by hypoxia. *Dev Cell* 2(3):331-341.

7 Thesen

1. Xenopusembryonen wurden unter unterschiedlichen Sauerstoffkonzentrationen gehalten. Sauerstoffkonzentrationen zwischen 35 und 15% hatten keinen Einfluss auf die Vitalität und die Entwicklungsgeschwindigkeit der Embryonen. Bei geringeren Sauerstoffkonzentrationen von 8, 6 oder 4% hingegen verringerte sich die Vitalität und die Entwicklungsgeschwindigkeit zunehmend.
2. Geringe Konzentrationen von 8% O₂, 6% O₂ oder 4% O₂ führten zu reduzierter Differenzierung von Angioblasten.
3. Embryonen, die bei 8% O₂, 6% O₂ oder 4% Sauerstoff gehalten wurden zeigten deutliche Defekte bei der Ausbildung des Blutgefäßsystems.
4. Verringerte Sauerstoffkonzentrationen zwischen 8 und 4% beeinträchtigten die Differenzierung myelogener Blutzelllinien. Die Zahl der mpo exprimierenden Zellen verringerte sich mit abnehmender Sauerstoffkonzentration.
5. Ebenso war die Differenzierung erythropoetischer Blutzellen unter diesen Bedingungen gestört.
6. In Embryonen, die sich bei 8% O₂, 6% O₂ oder 4% Sauerstoff entwickelten war die Zahl der proliferierenden Zellen deutlich reduziert.
7. Die generelle Entwicklung der Embryonen war unter hypoxischen Bedingungen nicht gestört.
8. Eine Verringerung der Expression von Prolylhydroxylase-2 (PHD2) führte zur Beeinträchtigung der Gefäßbildung sowie der Differenzierung myelogener Blutzelllinien. Die Entwicklung erythrogener Blutzellen war nicht gestört.
9. Eine Verringerung der Expression von Prolylhydroxylase-1 oder -3 (PHD1, -3) hatte keinen Einfluss auf die Gefäßbildung oder die Differenzierung von Blutzellen.
10. Sowohl der Funktionsverlust von Hypoxia induced factor 1 α (HIF 1 α) als auch der Verlust des von-Hippel-Lindau-Tumorsuppressors (VHL) führte zur Beeinträchtigung der Entwicklung des Blutgefäßsystems.

8 Supplementary data



Supplementary Figure 1: Hypoxia chamber setup: Figure shows the hypoxia chambers in operation. Four hypoxia chambers and one control chamber were operated simultaneously. Oxygen probes were placed in each hypoxia chamber and connected to the oxygen regulating device. The oxygen regulating device is in turn connected a computer. The entry of nitrogen gas is regulated according to the values chosen by the user. All the chambers were placed on a thermostat to maintain constant temperature throughout the experiment.

Supplementary Table 1: Developmental profile: Table shows the time required by embryos from various hypoxia chambers and embryos grown in normoxia embryos to reach comparable developmental stages.

Time(hrs)	Developmental stage (NF stage)						
	Controls	35% O ₂	25% O ₂	15% O ₂	8% O ₂	6% O ₂	4% O ₂
0	0	0	0	0	0	0	0
2	2	2	2	2	2	2	2
19	12	12	12	12	12	12	12
27	18	18	18	18	18	18	17
44	30	30	30	30	30	27	26
51	34	34	34	34	32	30	28
62	36	36	36	35	34	32	31
66	37	37	37	36	35	33	32
70				37	36	34	32.5
75					37	35	33
81						36	34
92						37	35
116							36
125							37

The following tables show the total number of embryos showing normal expression (nor. --- expr.) and reduced expression of a marker examined (red. --- expr.). Total number of experiments performed using each marker is also shown (No. of expts')

Supplementary Table 2: Expression of ER71 in embryos raised in hypoxia.

		Nor. ER71 expr.	Red. ER71 expr.	No. of expts'
Controls	St-30	40	0	N=2
	St-33	18	1	N=2
	St-37	18	2	N=2
8% O2	St-30	1	19	N=2
	St-33	0	18	N=2
	St-37	0	20	N=2
6% O2	St-30	0	9	N=1
	St-33	1	19	N=2
	St-37	0	20	N=2
4% O2	St-30	1	9	N=1
	St-33	1	7	N=1
	St-37	0	10	N=1

Supplementary Table 3: Expression of Ami in embryos raised in hypoxia.

		Nor. Ami expr.	Red. Ami expr.	No. of expts'
Controls	St-30	35	6	N=4
	St-33	18	1	N=3
	St-37	51	1	N=5
35% O2	St-30	27	1	N=2
	St-33	23	1	N=2
	St-37	44	0	N=2
25% O2	St-30	26	2	N=2
	St-33	28	0	N=2
	St-37	41	1	N=2
15% O2	St-30	29	4	N=2
	St-33	32	2	N=2
	St-37	27	1	N=2
8% O2	St-30	1	19	N=2
	St-33	2	18	N=2
	St-37	3	30	N=4
6% O2	St-30	1	16	N=2
	St-33	4	25	N=3
	St-37	2	23	N=3
4% O2	St-30	0	29	N=3
	St-33	2	39	N=5
	St-37	0	20	N=3

Supplementary Table 4: Expression of mpo in embryos raised in hypoxia.

		Nor mpo expr.	Red. mpo expr.	No. of expts'
Controls	St-30	19	1	N=2
	St-33	20	0	N=2
	St-37	19	1	N=2
8% O2	St-30	2	23	N=2
	St-33	1	15	N=2
	St-37	0	18	N=2
6% O2	St-30	0	19	N=2
	St-33	1	19	N=2
	St-37	1	18	N=2
4% O2	St-30	0	9	N=1
	St-33	1	9	N=1
	St-37	0	9	N=1

Supplementary Table 5: Expression of lmo-2 in embryos raised in hypoxia.

		Nor. lmo-2 expr.	Red. lmo-2 expr.	No. of expts'
Controls	St-30	19	0	N=2
	St-33	21	1	N=2
	St-37	21	1	N=2
8% O2	St-30	17	0	N=2
	St-33	18	0	N=2
	St-37	5	18	N=2
6% O2	St-30	10	0	N=1
	St-33	20	1	N=2
	St-37	2	18	N=2
4% O2	St-30	10	2	N=1
	St-33	12	0	N=1
	St-37	0	4	N=1

Supplementary Table 6: Expression of β -globin in embryos raised in hypoxia.

		Nor. β - globin expr.	Red. β - globin expr.	No. of expts'
Controls	St-30	20	0	N=2
	St-33	19	2	N=2
	St-37	20	1	N=2
8% O ₂	St-30	15	4	N=2
	St-33	20	0	N=2
	St-37	3	15	N=2
6% O ₂	St-30	9	3	N=1
	St-33	23	0	N=2
	St-37	3	15	N=2
4% O ₂	St-30	10	1	N=1
	St-33	15	0	N=1
	St-37	0	12	N=1

Supplementary Table 7: pH3 assay using embryos raised in hypoxia.

		Nor. prol.	Red. prol.	No. of expts'
Controls	St-30	10	0	N=1
	St-37	10	0	N=1
8% O ₂	St-30	0	10	N=1
	St-37	0	8	N=1
6% O ₂	St-30	0	11	N=1
	St-37	0	9	N=1
4% O ₂	St-30	0	10	N=1
	St-37	0	9	N=1

Supplementary Table 8: Expression of Muscle Actin in embryos raised in hypoxia.

		Nor. MA expr.	Red. MA expr.	No. of expts'
Controls	St-33	21	0	N=2
8% O ₂	St-33	20	0	N=2
6% O ₂	St-33	27	1	N=2
4% O ₂	St-33	19	4	N=2

Supplementary Table 9: Expression of n-tubulin in embryos raised in hypoxia.

		Nor. N-tub. expr.	Red. N-tub. expr.	No. of expts'
Controls	St-33	16	2	N=2
8% O ₂	St-33	19	3	N=2
6% O ₂	St-33	14	4	N=2
4% O ₂	St-33	9	3	N=2

Supplementary Table 10: Expression of Ami in PHD-2 knock-down embryos.

	Nor. Ami expr.	Red. Ami expr.	No. of expts'
Controls	67	3	N=2
PHD-2 MO injected	16	44	N=2

Supplementary Table 11: Expression of Ami in DMOG treated embryos.

	Nor. Ami expr.	Red. Ami expr.	No. of expts'
EtOH treated	30	0	N=2
DMOG treated	0	45	N=3

Supplementary Table 12: Expression of Ami in PHD-2 rescued embryos.

	Nor. Ami expr.	Red. Ami expr.	No. of expts'
Controls	73	3	N=3
PHD-2 Rescued	59	14	N=3

Supplementary Table 13: Expression of mpo in PHD-2 knock-down embryos.

	Nor. mpo expr.	Red. mpo expr.	No. of expts'
Controls	27	3	N=2
PHD-2 MO injected	31	10	N=2

Supplementary Table 14: Expression of lmo-2 in PHD-2 knock-down embryos.

	Nor. lmo-2 expr.	Red. lmo-2 expr.	No. of expts'
Controls	20	3	N=2
PHD-2 MO injected	25	4	N=2

Supplementary Table 16: Expression of Ami in PHD-1 knock-down embryos.

	Nor. Ami expr.	Red. Ami expr.	No. of expts'
Controls	65	2	N=2
PHD-1 MO injected	47	15	N=2

Supplementary Table 18: Expression of Ami in HIF-1 α knock-down embryos.

	Nor. Ami expr.	Red. Ami expr.	No. of expts'
Controls	85	0	N=4
HIF-1 α MO injected	30	69	N=4

Supplementary Table 20: Expression of Ami in HIF-1 α + VHL knock-down embryos.

	Nor. Ami expr.	Red. Ami expr.	No. of expts'
Controls	28	0	N=2
HIF-1 α + VHL MO injected	16	51	N=2

Supplementary Table 15: Expression of β -globin in PHD-2 knock-down embryos.

	Nor. β -globin expr.	Red. β -globin expr.	No. of expts'
Controls	23	2	N=2
PHD-2 MO injected	30	3	N=2

Supplementary Table 17: Expression of Ami in PHD-3 knock-down embryos.

	Nor. Ami expr.	Red. Ami expr.	No. of expts'
Controls	65	2	N=2
PHD-3 MO injected	50	21	N=2

Supplementary Table 19: Expression of Ami in VHL knock-down embryos.

	Nor. Ami expr.	Red. Ami expr.	No. of expts'
Controls	85	0	N=4
VHL MO injected	41	61	N=4

Lebenslauf

PERSÖNLICHE ANGABEN

Familienname	Metikala
Vorname	Sanjeeva Sudhakar
Geschlecht	männlich
Geburtsdatum	07.08.1988
Geburtsort	Banaganapalli, Indien
E-Mail	sanjeeva.metikala@medizin.uni-halle

SCHULDBILDUNG

07/1993 – 06/2003	Grundschule
06/2003 – 03/2005	Mittelschule und Gymnasium (Raos Junior college), Nandyal, Indien

UNIVERSITÄTSAUSBILDUNG

08/2005 – 09/2009	Bachelorstudium “Biotechnology” an der Vinayaka Missions Universität in Chennai, Indien Abschluss: Bachelor of Engineering (BEng) in Biotechnology
10/2010 – 09/2012	Masterstudium “Biomedical Engineering” an der Martin-Luther-Universität Halle-Wittenberg und Hochschule Anhalt Abschluss: Master of Engineering (MEng) in Biomedical Engineering
10/2012 - heute	Promotion Institut für Physiologische Chemie Martin-Luther-Universität Halle-Wittenberg

BERUFSTÄTIGKEIT

07/2009 – 06/2010	Lehrer für Zoologie an der Kankara Gurreddy Mittelschule in Banaganapalli, Indien
-------------------	---

Halle (Saale), 22.10.2014

Selbständigkeitserklärung

Gemäß §6 der Promotionsordnung der Universität Halle erkläre ich hiermit an Eides statt, dass ich vorliegende Arbeit ohne unzulässige Hilfe Dritter und ohne Benutzung anderer als der angegebenen Hilfsmittel angefertigt habe. Die aus anderen Quellen direkt oder indirekt übernommenen Daten und Konzepte sind unter Angabe der Quelle gekennzeichnet. Frühere Promotionsversuche bestehen nicht. Die vorliegende Arbeit wurde weder im Inland noch im Ausland in gleicher oder ähnlicher Form einer anderen Prüfungsbehörde vorgelegt.



Halle (Saale), October 2014

Sanjeeva Sudhakar Metikala

Erklärung über frühere Promotionsversuche

Hiermit erkläre ich, dass ich außer der vorliegenden Arbeit keine weiteren Promotionsversuche durchgeführt habe.



Halle (Saale), October 2014

Sanjeeva Sudhakar Metikala

Acknowledgements

I owe my deepest gratitude to Prof. Thomas Hollemann for having faith in me and giving me an opportunity to work in his lab and pursue my research interests. I would like to thank for the invaluable guidance provided by him throughout the thesis by new ideas and supporting in every possible manner.

I am deeply indebted to Dr. Herbert Neuhaus whose help, stimulating suggestions and encouragement helped me to be motivated during the time of research and for writing of this thesis. He has offered me his support in a number of ways from being patient in answering my questions, help find appropriate materials for setting up hypoxia chambers to making necessary corrections in the manuscript.

I am obliged to my colleagues Ashwin Lokapally, Aisha Argai, Rebecca Wagner Enrico Jandt and Thorsten Pfirrmann and Marlen Metzgi, who helped me to make things easier with their valuable ideas and experience. Special thanks to our technical assistant, Juliane Herfurth, for her helping hands, maintenance of a good laboratory environment and arranging things in an organized way.

I sincerely thank Dr. Glanz for keeping the nitrogen chambers available for me, maintaining and ordering them as required for the successful completion of the experiment. Without the contribution of all the people, this thesis would not have been possible.

I am thankful to my parents and friends for their love and continual support throughout the project. I thank the God Almighty for giving me strength and courage to face challenges during this project and it surely are His blessings that led to a successful completion of the thesis in such a short period of time.